INTELLIGENT DEMAND SIDE MANAGEMENT OF RESIDENTIAL BUILDING ENERGY SYSTEMS

by

Maruti N. Sinha

A dissertation submitted to the faculty of
The University of North Carolina at Charlotte
in partial fulfillment of the requirements
for the degree of Doctor of Philosophy in
Mechanical Engineering

Charlotte

2013

Approved by:

Dr. Robert Cox

Dr. Scott D. Kelly

Dr. Ahmed Soliman

Dr. Yogendra K. Kakad

ABSTRACT

MARUTI N. SINHA. Intelligent Demand Side Management of Residential Building Energy Systems. (Under the direction of DR. ROBERT W. COX)

Building energy performance has emerged as a major issue in recent years due to growing concerns over costs, resource limitations, and the potential impact on climate. According to the *2011 Buildings Energy Data Book* (prepared by D&R International, Ltd. for the US Department of Energy, March 2012), the built environment demands about 41% of primary energy in the United States [1]. Given the emergence of modern sensing technologies and low-cost data-processing capabilities, there is a growing interest in better managing and controlling consumption within buildings. Estimates suggest that the simple act of continuous monitoring can lead to improvements on the order of 20% [118].

To further reduce and better control energy consumption, one can turn to the use of real-time energy-performance modeling. This thesis adopts the view that smaller buildings (i.e. homes and smaller commercial facilities), which represent more than half of the sector's consumption, provide a rich opportunity for low-cost monitoring solutions. The real advantage lies in the growth of so-called smart meters for demand monitoring and advanced sensing for improved load control. In particular, this thesis considers the use of a small sensor package for the creation of autonomously developed, data-driven thermal models. Such models can be used to predict and control the consumption of space heating and cooling equipment, which currently represent about 50% of residential consumption in the United States.

The key contribution of this work is the real-time identification of thermal parameters in homes using only two temperature sensors, solar irradiance measurements, and a power meter with load-tracking capabilities. The proposed identification technique uses the Prediction Error Method (PEM) to find a Multiple Input Single Output (MISO) state-space model. Two different models have been devised, and both have been field tested. The first focuses on energy forecasting and enables various diagnostic features; the other is formulated for more advanced capacity controls in vapor-compression air conditioners. A Model Predictive Control (MPC) scheme has been implemented and shown in simulation to yield energy reductions on the order of 30% over typical thermostatic control schemes. Similarly, the diagnostic model has been used to detect capacity degradation in operational units.

DEDICATION

This dissertation is dedicated to my wife for her unconditional and endless support, to my mother for being inspirational stone and to my grandfather for instilling discipline in my life.

ACKNOWLEDGMENTS

I would like to express sincere thanks to my advisor, Professor Robert Cox. He is the one who introduced me problems related to building energy systems-HVAC and concept of smart meter. He provided thorough guidance in my entire research, trained me to challenge existing practices and prepared me to contribute in science. Professor Cox is highly energetic and dedicated person. I will be fortunate to extend my research career with him beyond PhD as well.

Interestingly, being Mechanical Engineer from background I got the opportunity to work in Electrical Engineering department of UNC Charlotte. Here, I have earned several friends. Laboratory for Energy Efficient Systems and Jason Anderson's tailor house have been my laboratories to accomplish the goal. I am really thankful to Jason by allowing me to use his house for experimentation purpose.

I would like to thank Professor Yogendra Kakad and Professor Scott Kelly for training me in Controls System-Dynamics, and being part of my committee as well. Time to time I have obtained valuable suggestions from them to accomplish this huge task. I am also thankful to Professor Ahmed Soliman for agreeing to be a part of my dissertation committee and taking out his valuable time for me. I would like to thank Ms. Tracy Beauregard for continuous support during my graduate study.

I cannot forget to name Dr. Stuart Smith who always encouraged me during my downtime. I consider his gift to me "Newton's Principia" as my most valuable souvenir. Although he is not part of my research committee, his passionate support is still there.

To accomplish this research, financial needs have been there. The financial support from Mechanical Engineering and Engineering Science and EPIC, UNC

Charlotte are very much appreciated. Without their support, I could never have been successful to pursue this work.

In anybody's life, family comes first and I am no exception. I would like to express my gratitude to my mother Madhuri Sinha. Last but not the least; I would like to show my appreciation for my beloved wife Puja Sinha for her encouragement, patience, and sacrifices. She has been there like a shadow. My success is their combined dream.

TABLE OF CONTENTS

LIST OF TABLES xi

LIST OF FIGURES xii

LIST OF ACRONYMS xv

CHAPTER: 1 INTRODUCTION. 1

1.1 Energy Challenges in Buildings: Motivation and a Proposed Solution 1

1.2 General Overview of Vapor-Compression Air Conditioners 5

1.3 The Non-Intrusive Load Monitor 8

1.3.1 Preprocessor 9

1.3.2 Load classification 11

1.4 Research Scope and Thesis Outline 14

1.5 Thesis Contributions 15

CHAPTER 2: RESEARCH BACKGROUND. 16

2.1 Thermal Modeling Approaches for Buildings 16

2.1.1 Analytical or White-Box Approach 17

2.1.2 Hybrid Modeling Approaches 20

2.2 Energy Usage Forecasting 22

2.3 Summary 23

CHAPTER 3: RESIDENTIAL ENERGY SYSTEM IDENTIFICATION. 24

3.1 Model Identification 25

3.1.1 White Box Approaches 25

3.1.2 Gray Box Approaches 25

3.1.3 Black Box Approaches 25

3.2 Smoothing 27

3.3 Prediction Error Method 33

3.4 State Estimation 35

3.5 Proposed method for system identification 38

3.5.1 Overview 38

3.5.2 Experimental Test set up and Procedure 40

3.5.3 Stability, Controllability and Observability 47

3.5.4 Control Oriented Model Identification and Validation 50

CHAPTER 4: DEVELOPMENT OF CONTROL SYSTEMS. 67

4.1 Residential Control System 68

4.2 Model Predictive Control 72

4.2.1 Introduction 72

4.2.2 Formulation 73

4.2.3 Implementation of MPC in Residential HVAC systems 79

CHAPTER 5: DEVELOPMENT OF ENERGY PERFORMANCE MODEL. 87

5.1 Energy Performance- Oriented System Identification 87

5.2 Energy Performance Model validation 90

5.3 Energy Performance Model as Diagnostic Tool 101

5.4 .Diagnostic Tool demonstration 106

CHAPTER 6: CONCLUSION AND FUTURE WORK. 115

6.1 Conclusions 115

6.2 Future Directions 117

REFERENCES 118

APPENDIX A: EXPERIMENTAL SITE DESCRIPTION 127

APPENDIX B: EXPERIMENTAL SET UP AND RESULTS 128

APPENDIX C: PROGRAMMING 140

LIST OF TABLES

TABLE 1: Sensor and datalogger placement for thermal model identification of a residential house. 41

TABLE 2:Performance comparison of On-Off Controller and MPC. 85

TABLE 3: Comparison of measured and simulated total thermal energy, % difference for (a) fully charged with refrigerant, (b) partially charged with refrigerant. 112

TABLE 4: Dimensions of (a) doors, (b) windows. 127

TABLE 5: Coefficients for Compressor Model H25B35QABC. 132

TABLE 6: Sensors specifications and placements for cooling capacity measurement. 132

TABLE 7: Air velocity measurement using Hotwire Anemometer (measurement range is 0 -4 volt for .15 m/sec to 10 m/sec). 135

TABLE 8: Temperature and air flow values. 135

TABLE 9: Sensors and Data loggers for house thermal model identification. 136

LIST OF FIGURES

FIGURE 1: Energy consumption by sector. 2

FIGURE 2: Residential energy consumption by end use. 3

FIGURE 3: A typical vapor-compression air-conditioning system. 6

FIGURE 4: P-H diagram showing the refrigeration cycle. 7

FIGURE 5: Diagram showing the fundamental signal flow path in a NILM. 10

FIGURE 6: Real-power signal recorded in a test home. 11

FIGURE 7: Power drawn during the start of an incandescent light bulb and a motor. 12

FIGURE 8: Measured current and computed power during the start of a 2hp motor. 13

FIGURE 9: A typical two-story house. 19

FIGURE 10: An R-C equivalent model for a small residence. 20

FIGURE 11: Block diagram for System Identification process. 26

FIGURE 12: Concept Diagram of Prediction, Filtering and Smoothing. 28

FIGURE 13: Savitzky-Golay smoothing compared to direct measurement. 31

FIGURE 14: Block diagram representation for Kalman Filtering. 36

FIGURE 15: Diagram showing all of the relevant system components. 39

FIGURE 16: Unit circle to test the stability of a system. 48

FIGURE 17: System dynamics plot to show controllability. 48

FIGURE 18: Control-oriented model formulation including random errors. 51

FIGURE 19: Measured (and smoothed) and simulated data recorded during training. 52

FIGURE 20: (a) to (g) Control Oriented Model Validation. 54

FIGURE 21: Measured raw data and simulated data recorded during training. 57

FIGURE 22: (a) to (g) Using recursive PEM approach for control-oriented model validation. 58

FIGURE 23: (a) to (g) Using the Kalman Filter for control-oriented model validation. 62

FIGURE 24: Showing temperature dynamics under on-off control. 69

FIGURE 25: Pictorial representation of an on-off control strategy. 70

FIGURE 26: Block diagram representation of a typical MPC system. 76

FIGURE 27: Description of MPC strategy. 78

FIGURE 28: Simulink model for model predictive controller in a residential house. 82

FIGURE 29: Day-1-Comparison of On-Off Controller vs. MPC with Prediction Horizon 4 hrs. 83

FIGURE 30: Day-2 Comparison of On-Off Controller vs. MPC with Prediction Horizon 4 hrs. 84

FIGURE 31: Comparison of on-off Controller with MPC taking Prediction horizon as 2 hrs. 86

FIGURE 32: Energy usage-model formulation including random errors e. 88

FIGURE 33: Measured (and smoothed) and simulated data recorded during the training period. 89

FIGURE 34: (a)-(g) show Energy Usage Model Validation. 90

FIGURE 35: (a) to (g) Using Prediction based on recursive PEM approach for Energy Usage Model Validation. 94

FIGURE 36: (a) to (g) Using Prediction based on Kalman filter approach for Energy Usage Model Validation. 97

FIGURE 37: General framework of a diagnostic system. 101

FIGURE 38: Diagnostic algorithm classification. 102

FIGURE 39: (a) Cooling capacity, (b) Measured vs. Estimated cumulative cooling energy to show system performance with no fault. 105

FIGURE 40: Measured vs. Estimated cumulative cooling energy to show system performance with fault. 106

FIGURE 41: (a) Simulated and measured values of ECOOL over a single day when the experimental system has normal refrigerant charge. (b) The corresponding cooling capacity as a function of time. 107

FIGURE 42: Measured and simulated values of ECOOL when the system is undercharged by about 25%. 109

FIGURE 43: Coefficient of Performance (COP) based analysis of the system. 110

FIGURE 44: Residuals calculated each day to judge the system performance. 111

FIGURE 45: System performance study through compressor running time. 114

FIGURE 46: Compressor details provided by manufacturer (a) Compressor specification datasheet, (b) Compressor map. 128

FIGURE 47: Compressor (used in experiment) details provided by manufacturer (a) Compressor specification datasheet, (b) Compressor map. 130

FIGURE 48: Sensor and data loggers used in measuring cooling capacity. 133

FIGURE 49: Air flow measurement in rectangular duct. 134

FIGURE 50: Sensors and data loggers for house thermal model identification. 136

FIGURE 51: Sensors and data loggers installations on experimental site for thermal model identification. 137

LIST OF ACRONYMS

NILM: Non-Intrusive Load Monitor

HVAC: Heating Ventilation and Air Conditioning

PEM: Prediction Error Method

OEM: Output Error Method

SID: Subspace Identification method

MLE: Maximum Likelihood Estimation

MISO: Multiple Inputs Single Output

MPC: Model Predictive Control

T_z : Zone Temperature (°F)

T_o : Ambient Temperature (°F)

S : Solar Irradiance (w/m^2)

E_{COOL}: Cooling Energy (kW-hr.)

$\dot{Q}$: Cooling Capacity (W)

$\dot{m}_{ref}$: Refrigerant mass flow rate

$\dot{m}$: Mass flow rate of air

P_s : Pressure at the suction of compressor

T_s : Temperature at suction of compressor

P_c : Pressure at the exit of compressor or at the entry of condenser

T_c : Temperature at the exit of compressor or at the entry of condenser

η_{vol}: Volumetric efficiency of compressor

ARI: Air conditioning and Refrigeration Institute

CRTF: Comprehensive Room Transfer Function

LTI: Linear Time Invariant

LMTD: Log Mean Temperature Difference

NTU: Number of Transfer Units

BEMS: Building Energy Management Systems

VAV: Variable Air Volume

VCC: Variable capacity control

LQR: Linear Quadratic Regulator

PID: Proportional Integrated and Derivative

HTS: Set heating hysteresis

CTS: Set cooling hysteresis

CHAPTER 1: INTRODUCTION

Energy is essential to life. To drive modern society, humans harvest various resources from their environment and extract the energy embodied within them. Balance is required, however, so that consumption does not surpass the available resource supply. Growing concerns over resource limitations and the potential negative impact of primary energy conversion has led society to turn its collective attention towards new means for energy production and smarter means for energy utilization.

This thesis focuses on exploiting the power of modern sensors and computing power to better monitor and control the consumption of energy in smaller buildings. Particular emphasis is given to the use of thermal energy for space heating and cooling. This chapter begins in Section 1.1 with a description of the problem and a formulation of the solution developed in this work. Section 1.2 describes vapor-compression air-conditioners, which are the primary source of heating and cooling energy in small buildings. Section 1.3 describes the non-intrusive load monitor, which is the experimental platform used to support this work. Section 1.4 provides an outline of the thesis, and Section1.5 summarizes the primary contributions.

1.1 Energy Challenges in Buildings: Motivation and a Proposed Solution

Energy consumption throughout the world continues to grow. Figure 1 shows the projected growth within the United States. Since this thesis focuses primarily on homes, we focus our attention on the residential sector, for which growth is projected to be about

0.2% or 1 quadrillion BTUs per year from 2010 to 2035 [1]. This growth comes despite the proliferation of more efficient loads. Even more significant growth is expected in other parts of the world, particularly in Asia.

A closer look at the residential sector reveals that Heating, Ventilation, and Air Conditioning (HVAC) are the primary consumers. Figure 2 shows the typical breakdown in the United States, with space heating and cooling accounting for approximately 50% of consumption [1]. Given the clear importance of this end use, there is good reason to examine it more closely to determine what can be done to make the conversion process more efficient.

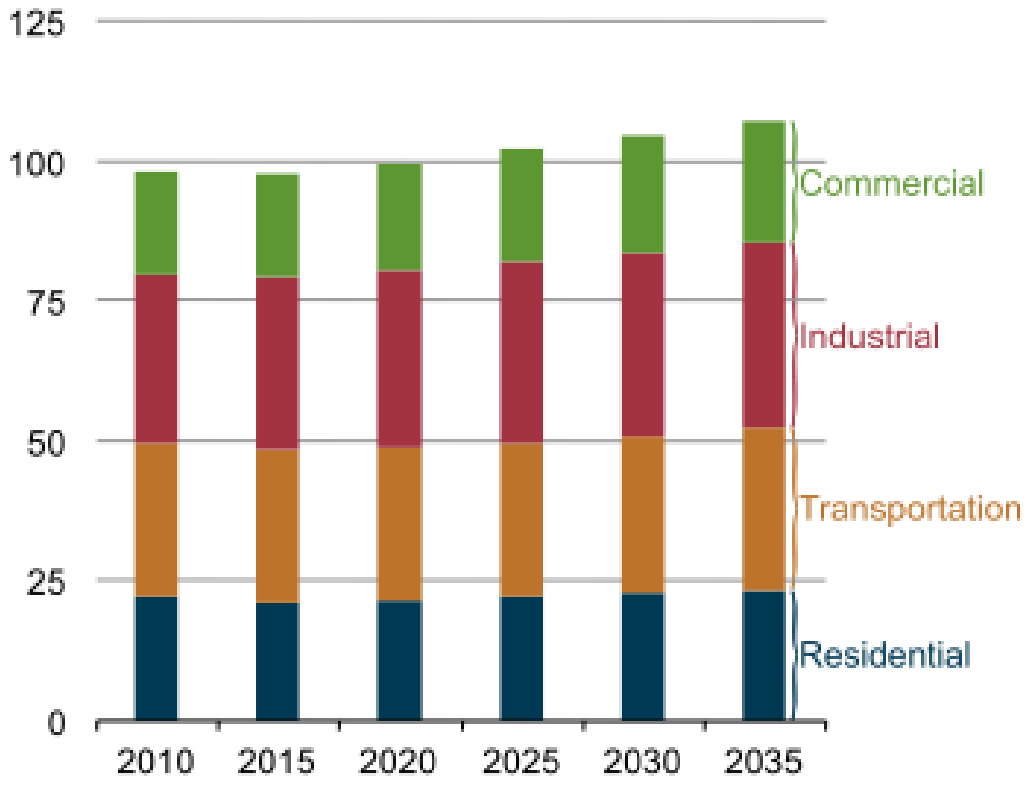

Figure 1: Energy consumption by sector, as projected to grow by 2035. Note that the y-axis is in units of quadrillions of BTUs (quads) (Adapted from [1]).

At present, most homeowners in the United States are unaware of the cost of energy, and thus efficiency is not a major concern. Consider for a moment, however, the following statistics. A recent field study of 4,168 in-service air conditioners found that 72% had refrigerant levels below manufacturer specifications [3]. The resulting loss of efficiency is estimated to waste some 17.6 TW-hrs of energy in homes each year [4]. At 10 cents per kW-hr, that represents a waste of $1.7 billion.

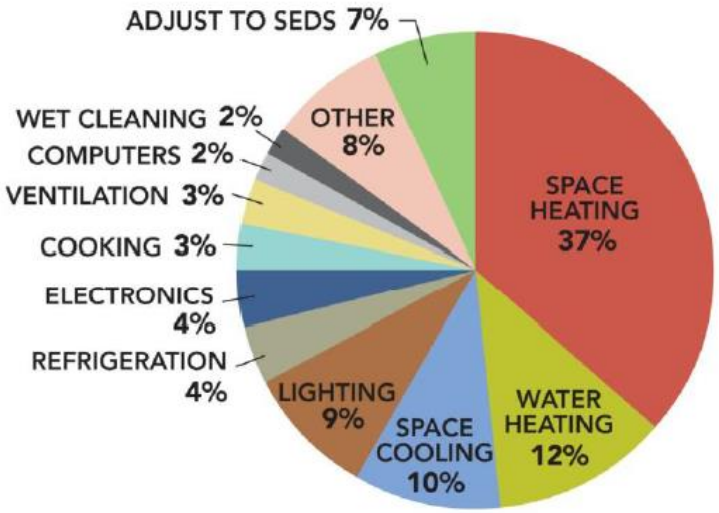

Figure 2: Residential energy consumption by end use (Adapted from [1]).

Inefficiencies such as the one described above are clearly rampant, but they can be easily detected by what are known as Building Energy Management Systems (BEMS). Such components use sensors and potentially some level of computation to monitor the conversion and consumption of energy within a building. Typically, the cost of these systems is prohibitive for smaller buildings such as homes. An interesting opportunity has recently arisen, however, in the form of what is known as “smart” meters. Utilities throughout the world are currently deploying these devices in homes and commercial

facilities. Smart meters are fundamentally electric meters with data acquisition and communication capabilities. They record electric power consumption and regularly communicate that information to the utility. If equipped with two-way communications and a gateway to various devices within the home, utilities can use smart meters to shut down certain loads during peak demand periods [1]. Although this framework provides a tremendous opportunity for innovative demand-response actions, it can also be used to monitor and control the performance of heating, ventilation and air-Conditioning (HVAC) systems within a home.

The primary objective of this research is to exploit the growing availability of smart meters and to use them as a platform for monitoring thermal performance in a home. Specifically, the goal is to use the data obtained by the smart meter and several additional sensors in order to develop a thermal model. This model can then be used for both diagnostics and improved control. The crucial step is the development of a reliable thermal model. Various approaches have been developed which can be classified in three broad categories, i.e. physics-based, data-driven and hybrid. Physics based model is popular as White box model. This model is solely based on fundamental principles of heat transfer whereas data driven model does not have any physics behind it. This is also called Black box approach. This type of model is purely developed on measured data. The hybrid model does not depend only on gathered data but also takes into account physics behind the process to a certain extent. This is also known as Grey box approach. All these methods have their own merits and limitations. Theoretically, physics based model is the best one to have.

The thermal model identification approach described in the research uses a smart

meter to find out compressor on-off schedule. This meter is known as Non-Intrusive Load Monitor (NILM) [5]. The detailed description of this meter has been given in section 1.3. It further describes how the NILM is used to detect several devices connected in home by just reading the current signatures. The research presents a discussion of the thermal-modeling procedure used for refrigerant-charge diagnostics, and it also describes a similar procedure that could be used with next-generation control systems. Experimental results are presented, and future work is described.

1.2 General Overview of Vapor-Compression Air Conditioners

Most homes and small buildings in the United States are cooled using what are known as vapor-compression air conditioners. These are typically coupled with a heating system such as a gas furnace, or potentially, the air conditioner is used as a heat pump to remove cold air during the winter months. Together, these components form the heating, ventilation, and air conditioning (HVAC) system. In general, any such system should regulate the following four quantities: air temperature, humidity, air circulation, and air quality.

The work in this thesis focuses heavily on vapor-compression air conditioners and heat pump systems. Since the performance of this equipment is so critical to the overall work, it is wise to first review their operation. Figure 3 shows the primary components, namely the compressor, the condenser, the expansion valve, and the evaporator. The function of each can be described through the pressure-enthalpy (P-H) diagram shown in Figure 4. This plot represents operation between 0ºC-40ºC, which is the typical range for a residential or light commercial air conditioner. The operation of each component can be seen as follows:

1. Compressor – This component compresses the refrigerant flowing through the fluid circuit shown in Figure 3. Scroll compressors are the most popular type in homes. Line 1-2 in Figure 4 shows the compression process.
2. Condenser - Compressed refrigerant passes through the condenser, where it cools at the same pressure. This is represented by the line labeled 2-3 in Figure 4.
3. Expansion Valve – This component, which is also referred to as a metering device, changes the pressure of the refrigerant at constant enthalpy. This is shown by line 3-4 in Figure 4. The expansion performed controls the amount of refrigerant flowing into the evaporator, which is the next component in the circuit.
4. Evaporator – Inside the evaporator the enthalpy of the refrigerant is changed at constant pressure. The path labeled 4-1 represents the action of the evaporator.

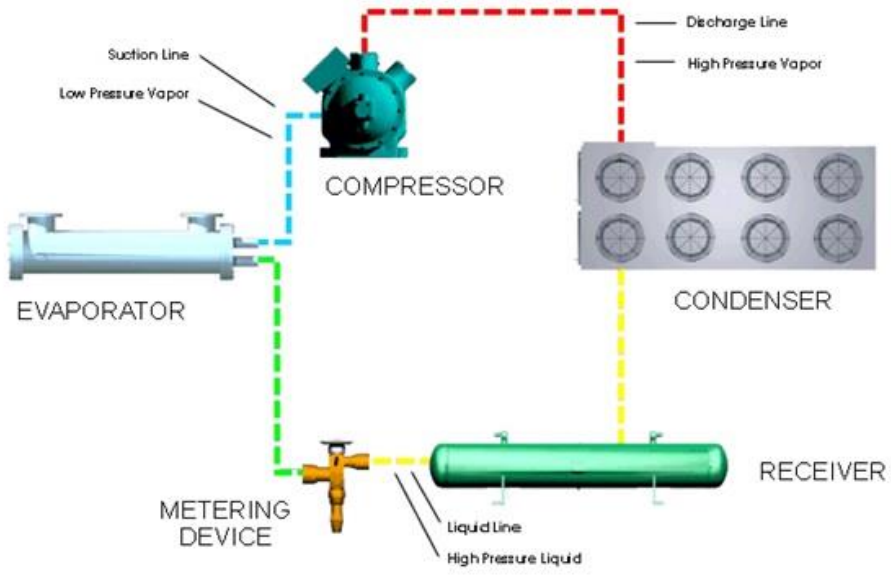

Figure 3: A typical vapor-compression air-conditioning system (HVAC system design by PES Institute of Technology, PACE).

As discussed before, working principles of all the components have been shown through P-H diagram. The system operates between two different pressures, evaporator and condenser pressures respectively. In fact these are the intake and exit pressures of compressor.

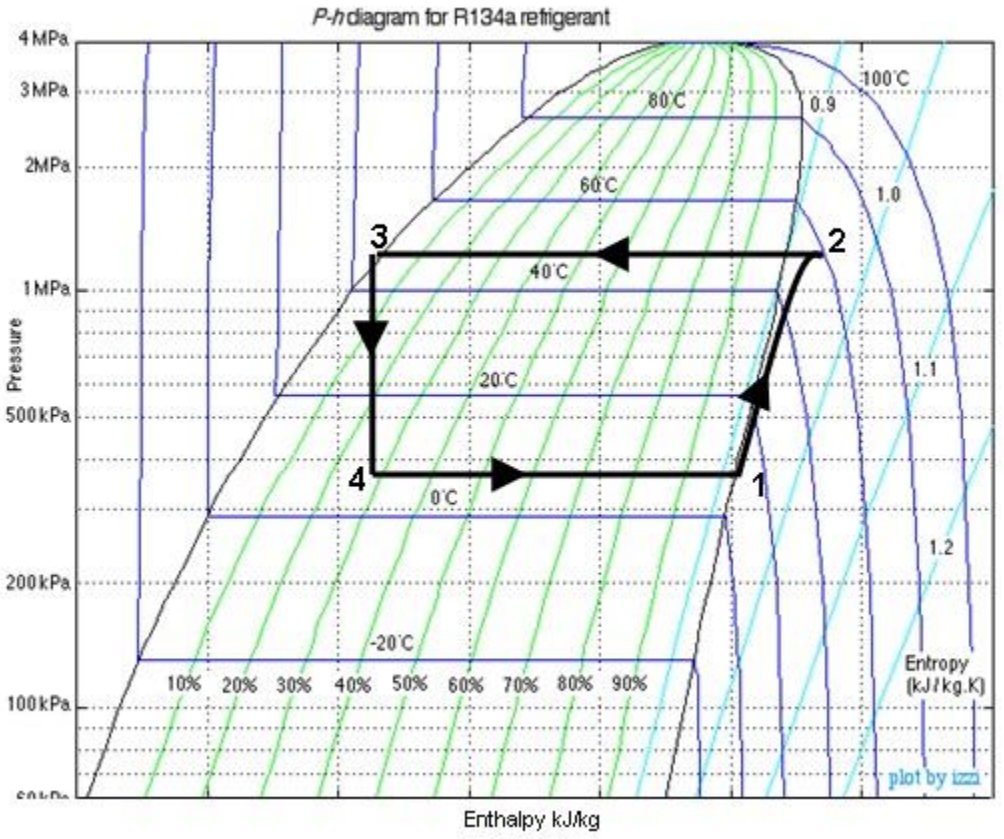

Figure 4: P-H diagram showing the refrigeration cycle for an air conditioner with R-134a refrigerant.

A fan passing air over the evaporator coils transfers heat from inside the space into the refrigerant circuit. The system is typically operated based on measurements of the air temperature within the occupied space. Typically, homes are divided into different zones, with each zone temperature controlled by a single dedicated thermostat. For heating and cooling applications, most residences are equipped with On-Off controllers. This goes by several names such as Bang-Bang Control or Hysteretic control. The

operating principle is quite simple and straight forward. The thermostat has the temperature setting and whenever the measured temperature is above/below the setting, the compressor turns on to supply thermal cooling/heating capacity [24], [25]. This type of controller runs between two states which is not preferred for any kind of mechanical device. The method is, however, inexpensive and simple to operate so it is preferred in most current and legacy systems.

To avoid frequent on-off operation and to improve efficiency, efforts are underway to build better control systems for buildings. Fuzz logic based controllers, i.e. fuzzy proportional, fuzzy proportional-plus integral etc. have been developed and compared [26]. Recent developments have also led to more straightforward feedback systems based on linear systems analysis (i.e. proportional-plus-integral compensators). [24], [25]

It is important to note that the thermal modeling procedures described in this thesis can be applied to other means of heating and cooling (i.e. gas furnaces, etc.). Given the fact that the refrigerant circuit in an air conditioner is so prone to leakage, this system was given significance in this work. All of the methods applied here could, however, be generalized to other systems.

1.3 The Non-Intrusive Load Monitor

As described in Section 1.1, the goal of this thesis is to leverage the growing availability of smart meters to help direct the monitoring and control of thermal performance. In particular, we have considered the use of a Non-Intrusive Load Monitor (NILM), which is a particular smart meter that can disaggregate the operation of individual loads from a single set of aggregate current measurements. Figure 5 shows a

block diagram of this smart meter. Note that the NILM is installed at the breaker cabinet, where it measures the aggregate current flowing in both phases of a typical split-phase residential utility connection. The NILM uses these signals to disaggregate the operating schedule of individual loads within the home. The NILM thus determines when the HVAC system is operating and when various heat sources (i.e. lights and appliances) are energized. Although the use of the NILM is not critical to the thermal-modeling procedure adopted in this thesis, it does assist in sensor-count reduction and its software can be easily installed in most commercially available smart meters.

This section describes the two main components of the NILM, namely the preprocessor and the event detector and classifier.

1.3.1 Preprocessor

Using measurements of the line voltage and aggregate current, a software-based preprocessor computes time-varying estimates of the frequency content of the measured line current [5]. Formally, these time-varying estimates, or spectral envelopes, are defined as

$$a_m(t) = \frac{2}{T}\int_{t-T}^{t} i(\tau)\sin(m\omega\tau)\,d\tau \quad (1)$$

and

$$b_m(t) = \frac{2}{T}\int_{t-T}^{t} i(\tau)\cos(m\omega\tau)\,d\tau. \quad (2)$$

These relationships are Fourier series analysis equations evaluated over a moving window of length T [6].

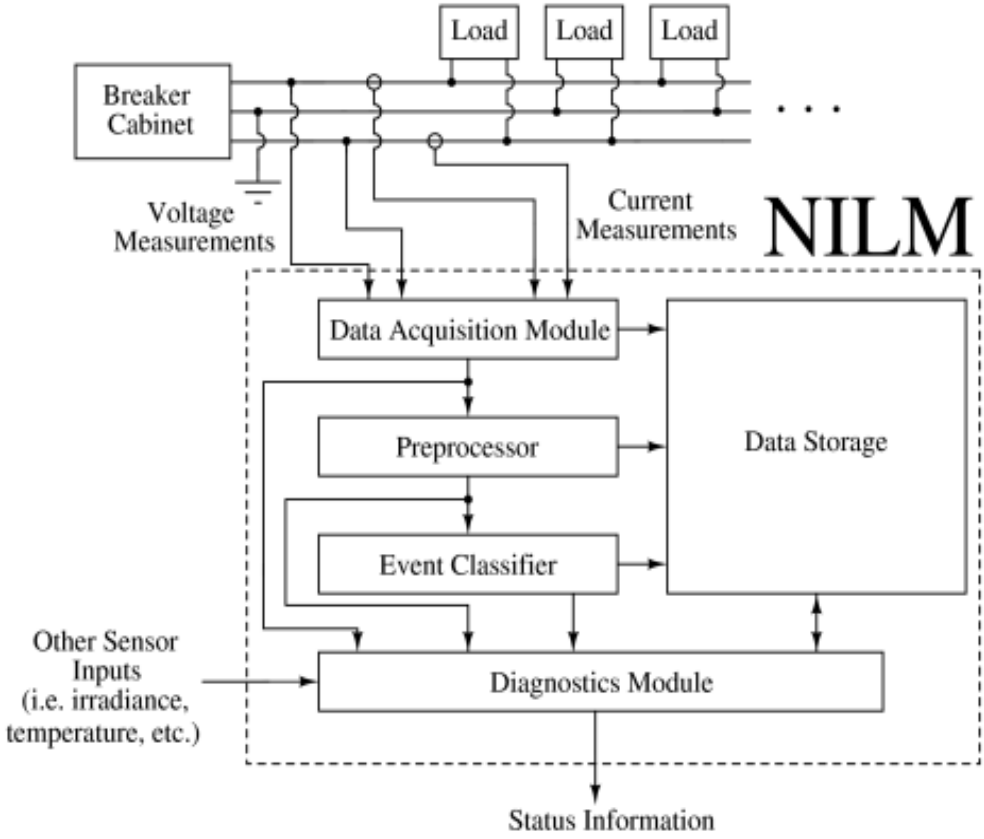

Figure 5: Diagram showing the fundamental signal flow path in a NILM connected in a residential home with a split-phase utility connection.

The coefficients $a_m(t)$ and $b_m(t)$ contain time-local information about the frequency content of $i(t)$. Provided that the basis terms $\sin(m\omega\tau)$ and $\cos(m\omega\tau)$ are synchronized to the line voltage, the spectral-envelope coefficients have a useful physical interpretation as real, reactive, and harmonic power [7]. For this reason, first spectral components of Fourier series a1 and b1 are often scaled by the magnitude of the line voltage and termed P_1 and Q_1, respectively. P_1 and Q_1 correspond to the conventional definitions of real and reactive powers. In general, $P_m = a_m$, $Q_m = b_m$. Figure 6 shows a typical real-power signal recorded over several minutes in a test home. It is noted that several different on/off events are labeled. The details have been described in section 1.3.2 about how these classifications were made.

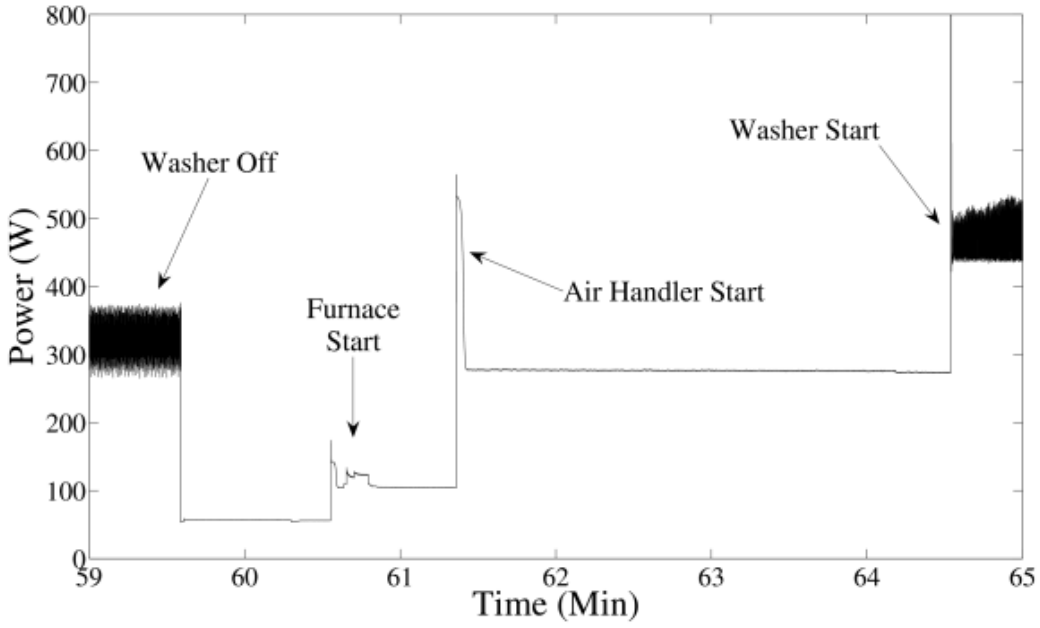

Figure 6: Real-power signal recorded in a test home. Several on/off events are shown.

1.3.2 Load Classification

The spectral envelopes computed by the preprocessor are sent to an event detector that identifies the operation of each of the major loads on the monitored electrical service. Identification is performed using both transient and steady-state information [8]. Field studies have demonstrated that transient details are particularly powerful because the transient electrical behavior of a particular load is strongly influenced by the physical task it performs [7]. As shown in Figure 7, for example, the physical differences between an incandescent lamp and an induction machine result in vastly different transient patterns.

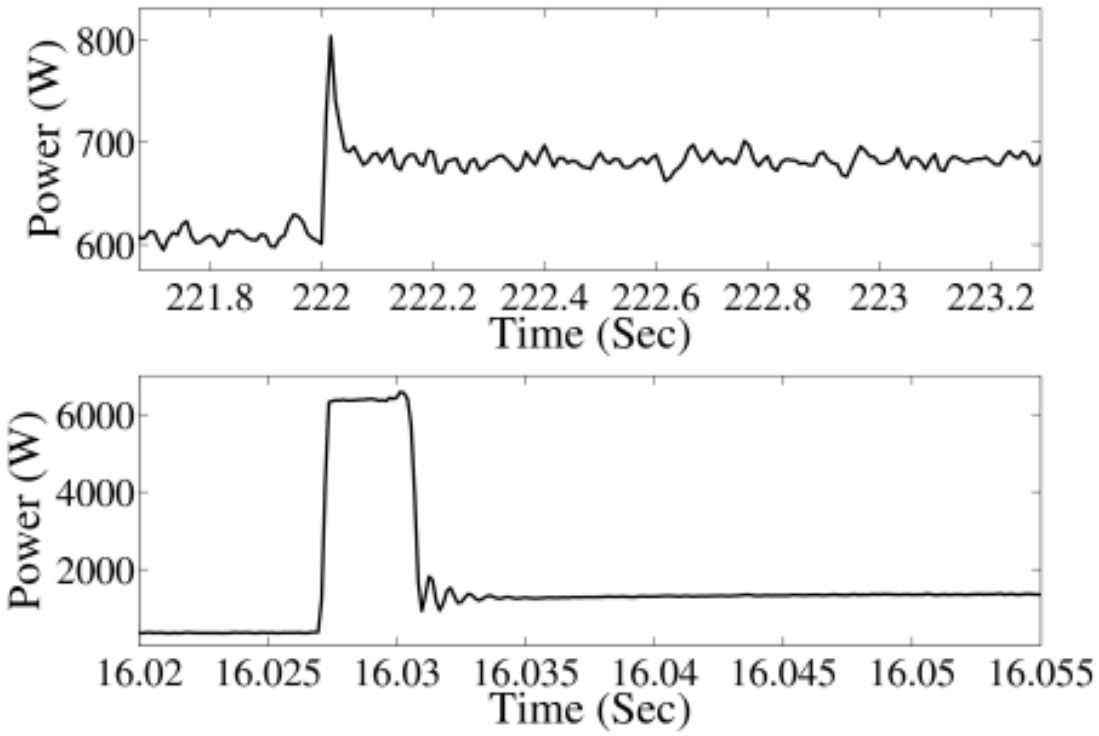

Figure 7: Top trace: The power drawn during the start of an incandescent light bulb. Lower trace: The power drawn during the start of an air conditioner.

Load identification relies on the ability to detect certain specific power changes and to match them to particular load events. The overall approach proceeds in two steps. First, an edge-detection algorithm locates abrupt changes in the real or reactive power signal. Subsequently, data around each edge is passed to a classifier that uses both transient and steady-state information to identify specific on/off events. Steady-state data includes information about the differences in real power, reactive power, and other spectral envelopes recorded before and after the event. Individual loads tend to have characteristic steady-state signatures learned during a one-time training process [5], [7], [8]. Transient shape information is also used to assist in load recognition. Most loads observed in the field have repeatable transient profiles or at least sections of their transient profile that are repeatable [5], [7], [8].

Transients are identified by matching events in the incoming aggregate power stream to previously defined transient shapes known as exemplars. As in the case of the state-state signatures noted above, these exemplars are determined during a one-time training process. When events occur, the resulting transient is fit to each exemplar using a least-squares process, and a best-fit metric (i.e. the 2-norm of the residuals) is used to determine the appropriate exemplar [7], [8]. The successful match of an exemplar to a motor transient is shown in Figure 8.

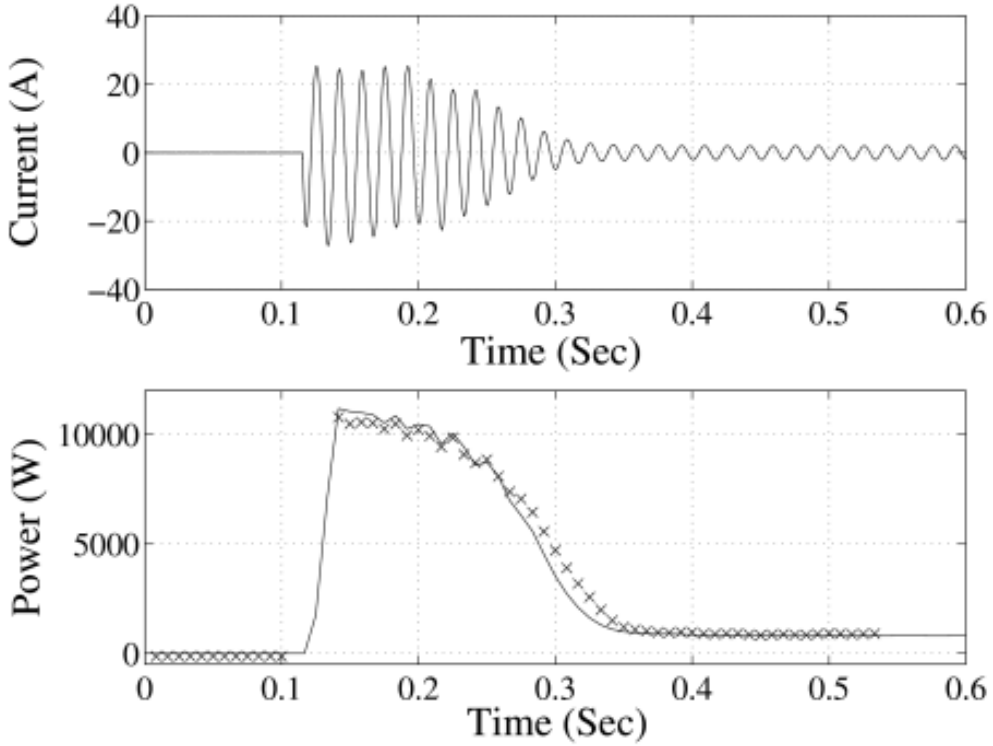

Figure 8: Measured current and computed power during the start of a 2hp motor.

Also shown in the power plot is the exemplar that has been successfully matched to the observed transient behavior by the transient classifier. The ultimate classification of any load is based on a combination of the best-fit metrics used by the steady-state classifier and its transient-based counterpart. Complete details are presented in [8]. After

a load has been properly classified, the NILM records this in a time-stamped data file. While a load remains energized, the NILM tracks its power consumption using a combination of the techniques described in [8] and [9].

Again, it is important to note that it the NILM is not essential to the work of this thesis, but it was the platform used for field studies. Given that most homes will have smart meters that measure only aggregate current, it makes sense to consider the use of the NILM's load disaggregation capabilities to determine when appropriate heat loads are operating. In this thesis, information about load operation is passed to the modeling software without having to separately monitor the operation of individual loads. Since the preprocessor and event-detection software could be installed on any smart meter, it thus makes sense to consider the use of the NILM.

1.4 Research Scope and Thesis Outline

As noted, the goal of this thesis is to develop thermal-performance models for small buildings using data measured by a small set of sensors. The thesis begins in Chapter 2 with a review of relevant background related to thermal modeling. It then proceeds to describe the data-driven modeling procedure used in this work. The next two chapters then consider specific applications of the proposed scheme. The first, which is found in Chapter 4, involves the use of the model for advanced model-based controls. Currently, homes do not use plant models and there is no notion of using weather forecast information. Chapter 4 considers both in an application of model-predictive control. The second application, which is described in Chapter 5, is the application of thermal models for diagnostics. The specific example considered is the loss of refrigerant, which was

noted to occur in over 70% of American homes without notice. Finally, the chapter presents conclusions and directions for future work.

1.5 Thesis Contribution

The primary contribution of this work is to present an on-line thermal modeling approach that is entirely sensor driven. This scheme can be made autonomous so that costly human intervention in the modeling process is not required. Through the development of such a process, one can monitor energy performance and find energy-wasting faults. Two specific applications are proposed, one is an optimal control strategy which that minimizes the energy consumed by space heating and cooling equipment. The other is a process that monitors energy consumption and detects the presence of energy-wasting faults. Field measurements are presented to justify the performance of the thermal models and to demonstrate the effectiveness of the proposed fault detection and diagnosis. Simulation results are used to validate the performance of the proposed control scheme.

CHAPTER 2: RESEARCH BACKGROUND

The fundamental challenge in this work is to construct a reliable model for the thermal performance of single-family residential buildings. To pursue this objective, a data-driven, scheme has been used in order to avoid excessive work in developing a complex physical model. Such schemes have been applied in numerous fields, including the life sciences, social sciences, economics, and aerospace. The first and most critical step is to identify an appropriate model. From an application standpoint, the selected model should be accurate, stable, and as simple as the physical situation will allow. Adaptability of the model is also important. It gives the opportunity to capture the changing behavior of the system itself. Once the model is identified, it can be used to predict system behavior and control load operation. The capability of the model can be exploited to develop diagnostic scheme as well. This is extremely important application area where plenty of works are needed.

This chapter provides relevant background information on detailed thermal modeling and an alternative approach, energy-usage forecasting using aggregated data. Note that the goal is to present typical approaches as a motivation for adopting the data-driven approach described in the next chapter.

2.1 Thermal Modeling Approaches for Buildings

Various schemes have been proposed for modeling thermal performance in buildings. This section considers both detailed analytical models and hybrid approaches

that rely on fewer direct physical considerations and more on field data. In general, analytical models have always been preferred tool for thermal modeling.

2.1.1 Analytical or White-Box Approach

Pure physics-based principles can be exploited to construct a thermal model. One common approach is to begin with an energy balance. This approach is used by EnergyPlus [10] and other modeling programs. A fundamental assumption is that the building exists in a steady thermal condition. This is a reasonable assumption in large commercial buildings, but it is not necessarily true in homes where heating and cooling equipment is operated cyclically. Using physical principles and direct information about the materiality of the building, an accurate model can be constructed. In practice, however, it can be extremely difficult to accurately capture all of the important material aspects.

Figure 13 shows a typical two-story home. In general, a home may have multiple zones to be heated or cooled. An energy-balance equation for this site must include all of the relevant heat sources, which include occupants, appliances, solar irradiance, and heating and cooling equipment. In addition, the equation must reflect the thermal energy stored in each zone as well as the amount of heat transferred between zones. The rate of thermal energy storage in a single zone is dependent upon what is known as the zonal thermal capacitance, C_Z. The rate of energy storage is proportional to both C_Z and the rate of change of the zone temperature, i.e. dT_Z/dt. This storage rate equals the rate at which energy which energy is provided or consumed by particular sources and transferred to other adjoining zones. Thus, the energy balance relationship for a single zone Z is

$$C_z \frac{dT_z}{dt} = \dot{Q}_{internal} + \dot{Q}_{surfaces} + \dot{Q}_{mixing} + \dot{Q}_{infiltration} + \dot{Q}_{sys} \quad (3)$$

The first term on the right-hand side is the sum of all internal heat loads, each of which provides energy at a rate $\dot{Q}_i$. Assuming N_{sl} heat loads, this is.

$$\sum_{i=1}^{N_{sl}} \dot{Q}_i = \dot{Q}_{internal}.$$

Assuming that each surface bounding the zone has a convective heat transfer coefficient h_i and an area A_i the sum of the convective heat transfer from all of the surfaces is

$$\sum_{i=1}^{N_{surfaces}} h_i A_i (T_{si} - T_z) = \dot{Q}_{surfaces}.$$

Furthermore, if air transfers from the $i-th$ adjoining zone at a mass flow rate $\dot{m}_i$ with a specific heat C_p and a temperature T_{zi}, the effect is represented as

$$\sum_{i=1}^{N_{zones}} \dot{m}_i C_i (T_{zi} - T_z) = \dot{Q}_{mixing}.$$

If any outside air at a temperature T_{inf} infiltrates from outside the building at a rate $\dot{m}_{inf}$, the result is to add or remove energy at rate

$$\dot{m}_{inf} C_p (T_{inf} - T_z) = \dot{Q}_{infiltration}$$

Finally, air may be supplied into the space by space conditioning equipment at a rate $\dot{m}_{sys}$ with a temperature T_{supply}. The effect of such space conditioning is

$$\dot{m}_{sys} C_p (T_{supply} - T_z) = \dot{Q}_{sys}$$

Many of the aforementioned terms can be exceptionally difficult to measure, especially under true ambient conditions. For instance, the effect of infiltration is difficult to quantify since it depends on thermal gradients and changing wind patterns. Furthermore, the heat transfer coefficients and areas are often not known by a modeler

and need to be carefully measured in the field. The use of a model is thus relatively limited for small buildings where the cost of model development can be excessive.

Figure 9: A typical two-story house.

Another major challenge in the process of model development is the identification of the appropriate number of zones. A two-story home such as the one shown in Figure 9 might have many such zones. In general, however, the number of zones is practically accepted to be equal to the number of thermostats and thus the number of temperatures that can be directly controlled. This is clearly a limited approach, and thus a true limitation of the effective use of physical-based models.

In the same vein, electrical circuit analogues can be used to develop thermal models. Figure 10 shows one candidate design for a small residence [11]. Using the R-C electrical circuit, a set of differential equation can be written and solved. This approach,

which is physics-based has similar problems, i.e. one must carefully measure and determine each of the relevant model parameters.

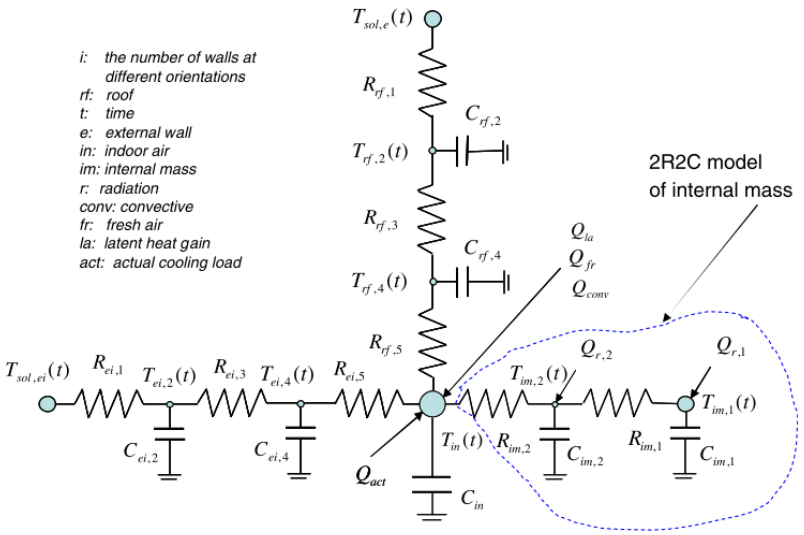

Figure 10: R-C equivalent model for a small residence.

2.1.2 Hybrid Modeling Approaches

As the name itself defines the methodology to a certain extent, it is the amalgamation of physics and some measured data relationship. To elaborate further some background research has been done to bring forth the techniques that have been known so far. The most typical approaches use data to develop transfer functions. These approaches relate the output of a linear system to a time series of current inputs and outputs to past inputs and outputs. It saves significant computation time over other schemes. Under this category there are numerous approaches such as Conduction Transfer Function (CTF) [12] and Comprehensive Room Transfer Function (CRTF) [13].

The Comprehensive Room Transfer Function (CRTF) proposed by J. Seem [14] and further refined by P. Armstrong [13] uses a function

$$Q_z = B^{1:n}(\phi_z, Q_z) + B^{0:n}(\theta_w, T_w) - B^{0:n}(\theta_z, T_z) \quad (4)$$

Equation $Q_z = B^{1:n}(\phi_z, Q_z) + B^{0:n}(\theta_w, T_w) - B^{0:n}(\theta_z, T_z)$ (5)

relates Q_z, which is the net heat input (or extraction) to a zone temperature and its past values. Here Q_z is considered to be the output of the system, and the subscripts *z* refer to zonal parameters and the subscripts *w* refer to wall parameters. The vectors ϕ and θ represent model parameters corresponding to either the walls or the various zones, respectively. B is the back-shift operator and is defined as

For zero lag term $B^{0:n}(x, y) = \sum_{k=0}^{n} x_k\, y(t-k)$ (6)

And for general form $B^{i:n}(x, y) = \sum_{k=i}^{n} x_k\, y(t-k)$ (7)

The inverse CRTF or iCRTF is defined as

$$\theta_{z,0} T_z = B^{0:n}(\emptyset_z, Q_z) + B^{0:n}(\theta_w, T_w) - B^{1:n}(\theta_z, T_z) \quad (10)$$

This equation treats zone temperature as an output in order to estimate the system parameters. It has been shown that parameter estimation through iCRTF is challenging but feasible [13].

Another modeling approach is the response factor method, which relates the output of a linear system to a time series of current and past inputs. To cite an example of thermal response factor formulation, calculation of response factor for a wall is

$$Q_A = T_A * X - T_B * Y$$

$$Q_B = T_A * Y - T_B * Z$$

Where Q_A and Q_B are the time-series for the influx in to surface A and out of surface B, respectively. T_A and T_B are the time-series for the temperatures at surfaces A and B respectively. X, Y are the time-series for the flux at surfaces A, B respectively due to a unit time series of temperatures at surface A. Similarly, Y and Z are the time-series for

the flux at surfaces A, B respectively due to a unit time series of temperatures at surface B. The same method has been extended to develop a thermal model for room called Room Thermal Response Factor [15].

There are many other works available in this area, almost all of which focus on large commercial buildings which are operating in stead-state conditions. Some of them start from general first order equation or equivalent thermal parameters equations and use regressive methods to estimate the parameters [16],[17],[18],[19],[20],[21]. All of the approaches considered here require significant data collection (i.e. wall temperatures, zone temperatures, etc.). Given that the focus of this thesis was placed on low-cost modeling for homes and small buildings, a simpler method was sought.

2.2 Energy Usage Forecasting

The present work revolves around the idea of using energy smartly. One way to develop a model could be to base it on prior data. A recent detailed study by the World Bank Development Research Group [22], [23] elaborates on such approaches. Reference [23] has a very thorough analysis of such demand-forecasting methods. Given the emphasis on low-cost approaches, this method was considered.

Generally, previous data can be used in one of three ways. The first involves time-series models of aggregate billing data. In this approach forecasting is based on known past events and patterns. This is very easy in implementation. As this is a bulk approach, it is very difficult to explain or arrest any kind of source of error. One way to refine such a model is to obtain detailed information about individual loads (i.e. appliances, etc). This method is known as end-used modeling and it is based on historical demand records for different appliances. This approach requires lot of

information to process, and it becomes exhaustive to implement. A third approach is to use econometric models, which determines energy demand by considering the influence of population, employment, income, weather etc. This is the most complex form of energy forecasting. It takes into account the demography and geography. It needs very high level of survey or study to develop a model.

The aforementioned forecasting models have potential for use in modeling the performance of thermal comfort systems, but they are very difficult to implement and would require numerous field-collection efforts over time to determine model updates. Such aggregate approaches would not be feasible in practice.

2.3 Summary

This chapter reviewed some relevant background on thermal-energy modeling. What is important to note is that the models presented here, while effective for their given purpose, are not useful for the purposes of this work. The goal is to determine an effective, adaptive model for small buildings. The models presented in Section 2.1 are effective for modeling, but they are either difficult to implement or require significant data. By comparison, the models presented in Section 2.2 require significant survey data and do not necessarily provide any indication about the source of model error. Chapter 3 now begins to look at approaches that can adaptively and easily model individual homes.

CHAPTER 3: RESIDENTIAL ENERGY SYSTEM IDENTIFICATION

“Essentially, all models are wrong, but some are useful" by George E. P. Box.

The simplest definition of a model would be it is a mathematical relationship between inputs and outputs which represents physical behavior of the system and can replace the real physical system for behavioral analysis. Models are broadly classified as Linear/Nonlinear and Discrete/Continuous. The focus of this research is towards residential building energy systems and therefore the models will be dealt with in that perspective only. The assumption has been made that mathematical model which represents a residential energy system is a Linear Time Invariant System. This kind of model doesn’t change over time i.e. same output can be produced by a given input irrespective of time. As discussed before, Armstrong [13] and Seem [14] have presented discretized state space model of a thermal model of a building energy system. For system identification purpose which is typically a reverse method, i.e. to find out the system parameters, various methods have been explored.

Every method has its own merit. Here it is being realized that a method should require little or ideally no human interactions during its operation and use. At the same time, it should be adaptive so that it could match up with actual physical system if it undergoes through changing behavior. In practice, it is extremely difficult to represent a system by a model. The model cannot capture the dynamics if the real system deviates in behavior due to changes in parameters. To accommodate the changing parameters of the

system, model continuously monitors its performance. Therefore, measurement based or data driven model seems to be the path to pursue. Also for the sake of clarity, it is worth mentioning here that model based approach has been preferred over other methods such as genetic algorithm or rule based approaches. This particular approach has wide applications e.g. in Control design, Forecasting, Fault detections.

3.1 Model Identification

Model identification is the process of investigation to represent a physical system through mathematical formulations using experimental data. The problem formulation for identification is also sometimes referred as inverse problem. This technique is widely used in automotive, aerospace, industrial process control. There are three established methods [27] to represent a physical model.

3.1.1 White Box Approaches

Laws of physics are used to build a model that represents the physical system. Here maximum time is devoted to build up the model. The typical example can be given of an aircraft flight model.

3.1.2 Gray Box Approaches

Empirical relations are used to represent the system. This is a balance approach where optimum time goes in building up and perfecting the model.

3.1.3 Black Box Approaches

This is purely a measurement data based model and also referred as data driven approach. This approach takes the least time in building up model. The technique is preferred over other methods especially when it is extremely difficult or complex to come

out with a formulation by well-established principles. In financial institutions, this is the most favored method for stock price forecast, investment return estimation etc.

Figure 11 shows a typical process of model identification where measured output Y_p of plant is compared to the model output $\hat{Y}_p$ with the same input U. The error in the observation helps in getting those system parameters to build up the model. For the model identification measured field data were divided into 2 different groups, one has been used for parameters estimation and the other for model validation.

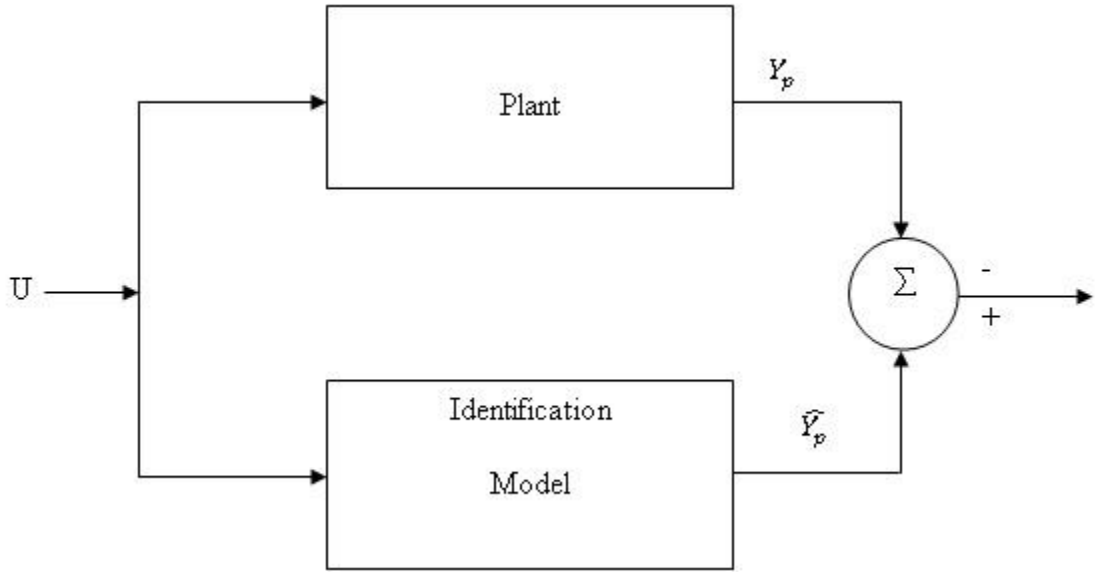

Figure 11: Block diagram for System Identification process.

In the model identification process, it is very important what kind of data is being fed for processing. Generally raw data, collected through sensors without any processing, can have noise. At the same time, sampling rate does create unwanted pattern which is not suitable for identification process. Therefore, preprocessing of the data is unavoidable and so smoothing has been considered to make data usable for the identification process.

3.2 Smoothing

In any measurement process, it is quite likely that data would be exposed to noise. Usage of the concerned model and noise level in it throw questions to what degree removal of noise is needed. For example, if measurement of temperature in an Intensive Care Unit (ICU) of a hospital is compared to temperature measurement in a blast furnace of Iron melt, precise measurement in the former is very much expected in comparison to later. Therefore, one has to take into account the application of the model too. Elimination of noise can cost some important information in the signal and so it is extremely important to understand how to control it without affecting the real information. Smoothing is used to suppress undesired data. This works as a low pass filter which eliminates noise present in the measured data.

There are various popular techniques of smoothing such as moving average, exponential moving average, local regression and Savitzky-Golay method. Before going further, it is worth to revisit concepts of Filtering, Smoothing and Prediction as these tools will be used later. The present work involves all three concepts at different levels and has been addressed adequately in different sections.

Fundamentals of Prediction, Filtering and Smoothing were explored by Norbert Wiener, Rudolf E. Kalman and Rchard S. Bucy. These three techniques are estimation problems. Optimal estimator processes measurements and minimizes error to estimate states using knowledge of the system and initial states. The concepts of prediction, filtering and smoothing [28] are closely related. This can be explained through an example of a moving vehicle. Filtering process refers to the vehicle position at a particular instant, say t_k. In prediction, the position of vehicle is computed at t_k knowing

position measurements up to t_{k-1}. If all measurements and post processing are done up to t_{k+1}, the estimation of where the vehicle was at time t_k, is called smoothing. Figure 12 describes the concept aptly. The concepts behind Prediction, Filtering and Smoothing have been explained in [29].

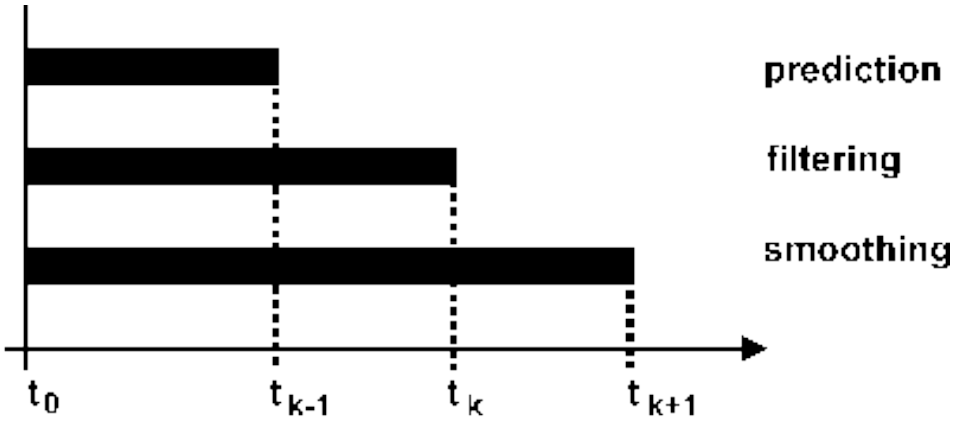

Figure 12: Concept diagram of Prediction, Filtering and Smoothing.

Coming back to the discussion of smoothing, it is extremely important to prepare data set for model identification out of collected data. There are various known methods and therefore choice should be judicious as each of the methods has its own merits and limitations.

Among all available smoothing techniques, moving average method is the most simple to use.

(a) Simple Moving average technique

It takes average of all the numbers in a window centered about a point recursively and assign the value to the center point [30], [31]. Although it does remove noise effectively but at the same time introduces some distortions. It is unable to maintain

peaks and valleys. In many applications this is undesirable because data characteristics have to be maintained. Apart from this problem, moving average method has lag also. This formulation is for symmetric window around a data point.

$$S_i = \sum_{i=-\frac{(n-1)}{2}}^{\frac{(n-1)}{2}} y_{(i+j)}/n \tag{11}$$

Symmetric window formulation is used in engineering mostly. One important point to notice the performance of this technique is compromised at the boundary.

(b) Exponential moving average technique

To overcome the inability in maintaining the data characteristics, exponential moving average method can be used which solves the problem to a certain degree. Lag is still there. This is the modification on simple moving average method. Exponential weights are applied in the window to find out the smoothen data and eliminate noise. The weights decrease exponentially before or after the central data point inside a given window [30], [31]. This is a very popular and widely used method in the class of moving average smoothing.

$$S_i = \alpha S_{i-1} + (1-\alpha) y_i \tag{12}$$

Where S_n is the smooth and y_n measured raw data. A series can be generated by doing backward substitution in the above equation. α is the time constant of the exponential trend or is the weight.

(c) Local regression

To overcome all these inherent problems, local regression method has been used for quite some time. Cleveland was the one who invented this local regression analysis [32], [33], [34], [35]. This approach does curve fitting locally i.e. in a given window of the selected order. This keeps the shape of data intact and also doesn't introduce lag.

Savitzky-Golay is based on least square curve fitting of any order in a given window. Generally higher order curve fitting allows higher order of smoothing without attenuating the data [36], [37], [38], [39], [40], [41].

Savitzky-Golay Smoothing

$$S_i = \sum_{n=-n_R}^{n_L} C_n y_{i+n} \tag{13}$$

To fit a polynomial $a_0 + a_1 i + a_2 i^2 + \cdots . + a_M i^M$ Least square method is applied to find the coefficients a's.

Here $a = (A^T A)^{-1} A^T y$

Here to find C_n instead of FIR (Finite Impulse Response) is chosen [42].

$$C_n = \{(A^T A)^{-1} A^T e_n\}_0$$

Local regression technique has been pursued and realized that it has tremendous merits over others. Local regression fits the data locally i.e. in the neighborhood. It adapts well at boundaries and in the high curvature zones. Smoothing has been applied on all the collected data, i.e. ambient temperature, solar irradiance and zone temperature. Initially moving average method was considered but discarded later. It does do smoothing but fails to retain the shape of signal. There is lag between the observed and smoothen signal but can be nullified by shifting the data set back in time series. Local regression method does not have these faults and do smoothing without any issue. Figure 13 (a), (b), (c) and (d) show Savitzky-Golay smoothing of zone, ambient and solar measurement data.

To explain and show the strength of Savitzky-Golay method, Figure 13 (b) has been produced from Figure 13 (a).

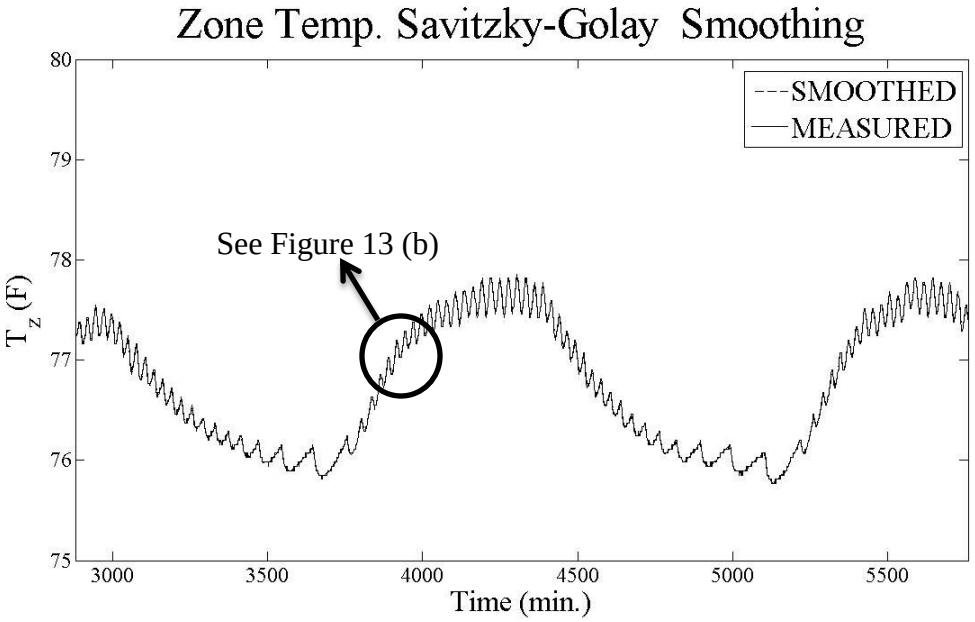
Zone Temp. Savitzky-Golay Smoothing
SMOOTHED
MEASURED
See Figure 13 (b)
T_Z (F)
Time (min.)
80
79
78
77
76
75
3000
3500
4000
4500
5000
5500

(a)

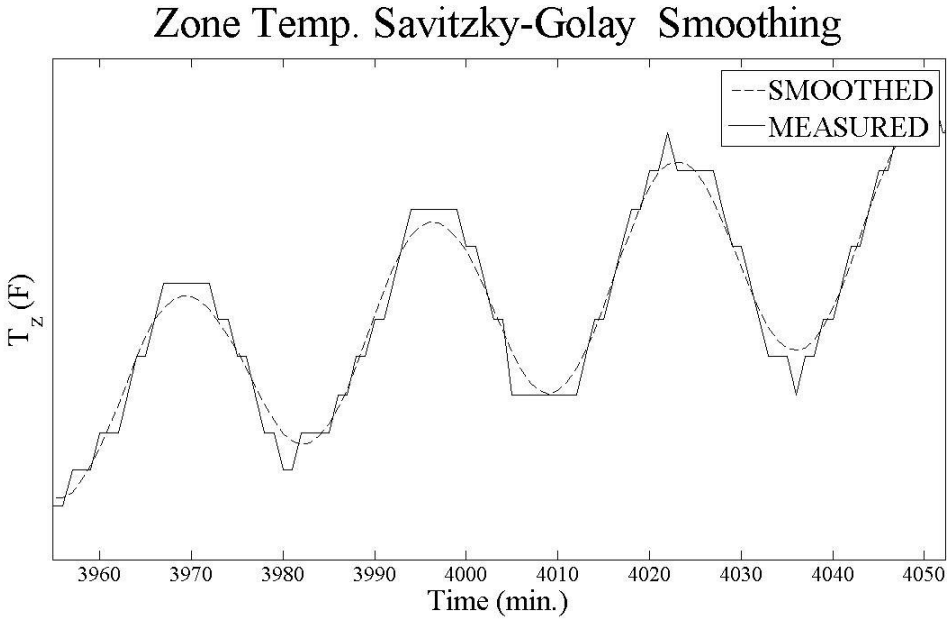
Zone Temp. Savitzky-Golay Smoothing
SMOOTHED
MEASURED
T_Z (F)
Time (min.)
3960
3970
3980
3990
4000
4010
4020
4030
4040
4050

(b)

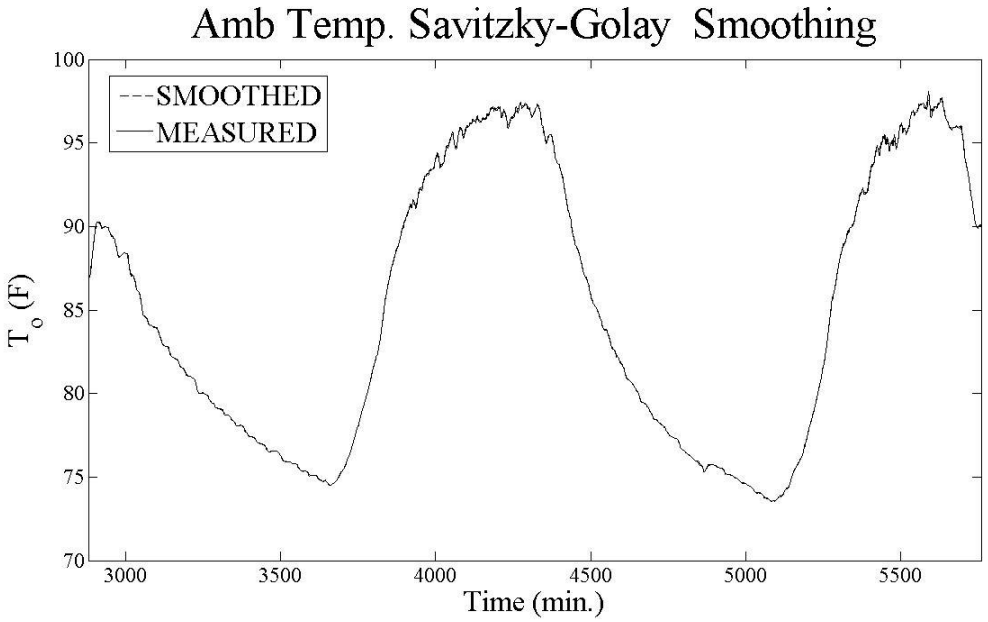

(c)

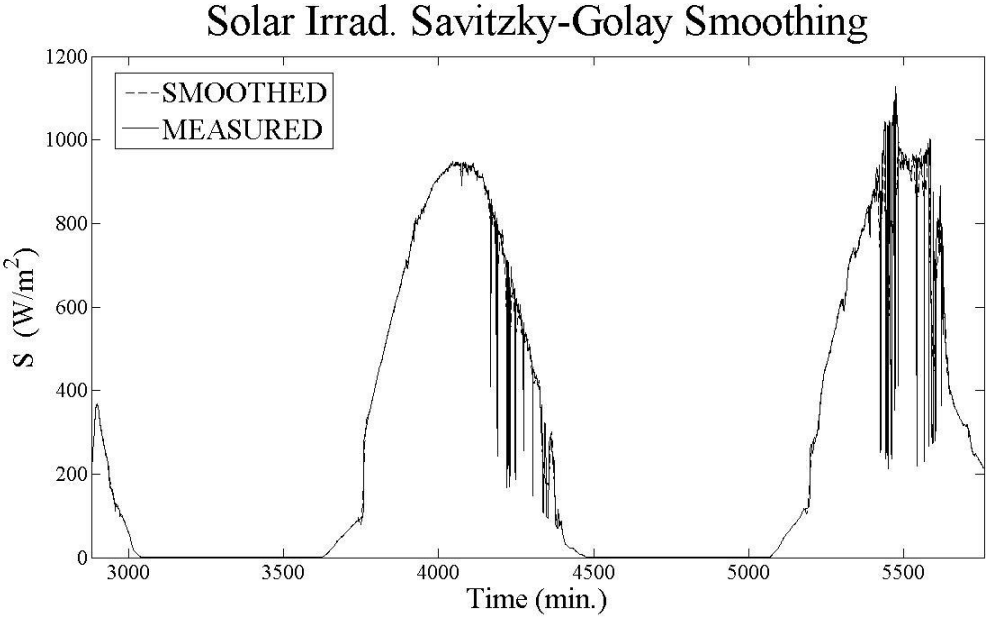

(d)

Figure 13: Smoothed data using Savitzky-Golay compared to direct measurement of (a) Zone temperature, (b) A snapshot of zone temperature, (c) Ambient temperature and (d) Solar Irradiance.

To implement this smoothing technique, MATLAB command ‘sgolay’ has been used. The order of polynomial is chosen as 4 which capture the individual cyclical dynamics of zone temperature in compressor on-off schedule.

3.3 Prediction Error Method

As discussed before, there are various ways to represent a physical system, analytical and empirical. Formulation can be in a form of state space or time series, or response surface [43]. The key question remains how to identify system parameters. This section will focus solely on the proposed parameter identification or estimation method [44] [45][46].

There are several established methods for parameter estimation. Some of them popular methods are Prediction Error Method (PEM) [47][48][49], Output Error Method (OEM) [50][51], and Subspace Identification Method (SID) [52][53].

PEM has been chosen over others because of its known merits. This method can deal with any kind of linear and nonlinear problem robustly. It is also used to improve the model determined by other techniques.

The models are trained in the field using sensor data and load operating schedules recorded over the course of several days. During this training period, N sample of each of the input and output variables are recorded at a rate T. At the k-th sampling instant t_k, these input and output variables are expressed in vector form as $\underline{u}_k$ and $\underline{y}_k$, respectively. Using the notation presented in [47][20] and [48], the dynamics of the system are represented in state-space form as

$$\underline{x}_{k+1} = \underline{\underline{A}}(\theta)\,\underline{x}_k + \underline{\underline{B}}(\theta)\underline{u}_k + \underline{\underline{K}}(\theta)\underline{e}_k \tag{14}$$

Where $\underline{e}_k$ is measurement white noise, $\underline{\underline{K}}(\theta)\underline{e}_k$ is process noise. Matrices $\underline{\underline{A}}(\theta)$, $\underline{\underline{B}}(\theta)$, and $\underline{\underline{K}}(\theta)$ are defined in terms of an initially unknown parameter set θ. This vector equation is coupled with an observation equation that relates the measurements to the state variables, i.e.

$$\underline{y}_k = \underline{\underline{C}}(\theta)\,\underline{x}_k + \underline{e}_k \tag{15}$$

Where $\underline{\underline{C}}(\theta)$ consists of another set of initially unknown parameters.

The challenge during the training phase is to determine the elements of the parameter set θ. Estimation is performed using the prediction error method [54]. In this approach, the parameters estimates solve the equation

$$\hat{\theta} = \arg\min V_N(\theta) \tag{16}$$

Where the objective function $V_N(\theta)$ is defined over the entire data set as

$$V_N(\theta) = \sum_{k=1}^{N} \underline{r}_k^T \underline{r}_k \tag{17}$$

The vector $\underline{r}_k$ is the set of residuals recorded at time t_k. These residuals are defined as the difference between the measured outputs at time t_k and the predicted outputs at the previous time step. Using the notation from [20],

$$\underline{r}_k = \underline{y}_k - \underline{\hat{y}}_k(-) \tag{18}$$

Where the prediction $\underline{\hat{y}}_k(-)$ can be written as

$$\underline{\hat{y}}_k(-) = \underline{\underline{C}}(\theta)\left[\left\{\underline{\underline{A}}(\theta) - \underline{\underline{K}}(\theta)\underline{\underline{C}}(\theta)\right\}\underline{\hat{x}}_{k-1} + \underline{\underline{K}}(\theta)\underline{y}_{k-1} + \underline{\underline{B}}(\theta)\underline{u}_{k-1}\right] \tag{19}$$

It is obvious that $\underline{\hat{y}}_k(-)$ is obtained from all the previous measurements i.e. outputs, inputs and states. If the states are not measureable quantities then they are estimated.

The search for the minimizing argument $\hat{\theta}$ is performed using the damped Gauss-Newton method [54]. $\underline{x}_0$ is the initial state which is obtained by PEM. For Gaussian disturbances, it coincides with the Maximum Likelihood Estimation (MLE).

3.4 State Estimation

State estimation is an integral part of problem formulation. Typically, states are estimated when they are not measureable quantities or simply not available for measurement due to various other reasons. In general, measurements are costly affairs because of sensors and data acquisition, and then also states are estimated.

In this section two methods of state estimations have been proposed, Kalman filtering and PEM based recursive state estimation.

- Kalman Filtering

Kalman filter [55], [56] was developed by Rudolf E. Kalman in 1960. It was initially investigated for spacecraft application but now days it is gaining its popularity in several areas. It has been a matter of interest for both theoreticians and practitioners. Currently this tool is widely used in numerous areas such as flight control, communication engineering, vehicle navigation, power systems and others. Kalman filter estimates the current states from measured data which are corrupted. Therefore, role of the filter becomes crucial. Kalman filter is potentially a state estimator which is mainly done for two important purposes, supervision and control. In the supervision application, states of the process variables are estimated to understand the system dynamics such as feed rate in a reactor, flow variations in chemical process plant, position in vehicle navigation. On the other hand in controls, states are used to track a trajectory so that corrective actions would take place to follow the trajectory or reference signal. It is

extremely important for Kalman filter implementation that all states are available, i.e. the system is observable.

From the above equation (14) and (15)

$$\underline{x}_{k+1} = \underline{\underline{A}}(\theta)\,\underline{x}_k + \underline{\underline{B}}(\theta)\underline{u}_k + \underline{\underline{K}}(\theta)\underline{e}_k \tag{20}$$

$$\underline{y}_k = \underline{\underline{C}}(\theta)\,\underline{x}_k + \underline{e}_k \tag{21}$$

Here process noise covariance is defined as $Q = E\{\,\underline{e}_k\,\underline{e}_k{}^T\}$

Kalman estimator for a discrete system [57], [58] will be written as

$$\underline{\hat{x}}_{k+1/k} = \underline{\underline{A}}\,\underline{\hat{x}}_{k/k-1} + \underline{\underline{B}}\,\underline{u}_k + \underline{\underline{L}}(\underline{y}_k - \underline{\underline{C}}\,\underline{\hat{x}}_{k/k-1}) \tag{22}$$

$\underline{\underline{L}}$ is obtained by solving Ricatti equation.

$$\underline{\underline{L}} = \left(\underline{\underline{P}}\,\underline{\underline{C}}^T + \underline{\underline{\breve{N}}}\right)\underline{\underline{\breve{R}}}^{-1} \tag{23}$$

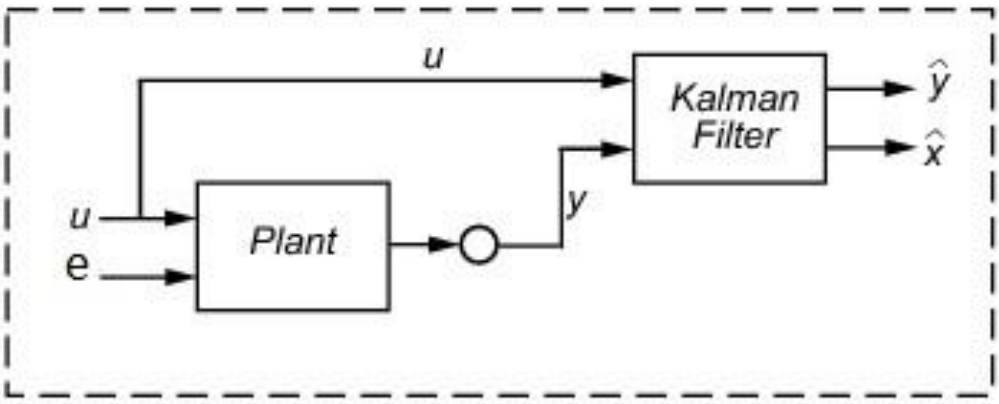

Figure 14: Block diagram representation for Kalman Filtering.

Where, $\underline{\underline{\breve{N}}} = \underline{\underline{G}}(\underline{\underline{Q}}\,\underline{\underline{H}}^T + \underline{\underline{N}})$

And $\underline{\underline{\breve{R}}} = \underline{\underline{R}} + \underline{\underline{H}}\,\underline{\underline{N}} + \underline{\underline{N}}^T\underline{\underline{H}}^T + \underline{\underline{H}}\,\underline{\underline{Q}}\,\underline{\underline{H}}^T$

$\underline{\underline{P}}$ is the steady state error covariance and is defined by

$$\underline{\underline{P}} = E\{(\underline{x} - \underline{\hat{x}})(\underline{x} - \underline{\hat{x}})^T\} \tag{24}$$

$$E(\underline{e}) = 0 \tag{25}$$

$$\underline{\underline{Q}} = \underline{\underline{R}} = \underline{\underline{N}} = E\{\underline{e}_k \, \underline{e}_k{}^T\} \tag{26}$$

For simplicity, it has been assumed that process noise is built upon the white noise and measurement noise is potentially a white noise.

Above Kalman filter formulation has been implemented in the present work and discussed in the section 3.5. Also recursive initial state estimation based on prediction error method has been proposed. The results of both compared and produced for detail analysis.

- Prediction Error Method based recursive state estimation.

The basic philosophy of this approach appreciates the fact that simulation in long time window is affected by measurement and process noise in the system. The errors caused by noise creep into the model. Due to this fact, the model observes deviation in the behavior compared to the real system. To control this error propagation, one has to recursively estimate states in a given interval of time once all the measurement become available. This is basically correction in states based on measurements. One sharp difference with Kalman filter approach can be drawn out that the time window of prediction can be long. In case of Kalman filter approach, the prediction is done just one data point ahead in time.

It goes with the same approach of PEM based parameters estimation. Since all the parameters of the systems are known and therefore from equation (17),

$$V_N(\theta) = \sum_{k=1}^{N} \underline{r}_k^T \underline{r}_k \quad (27)$$

$V_N(\theta)$ is minimized to get $\underline{x}_0$. The simulation is run based on the identified system and new estimated initial condition. This process is repeated with a selected operating window and renewed initial states.

3.5 Proposed method for system identification

So far all the discussions have been devoted towards building up fundamentals to formulate the present problem. Here onward, focus would be on developing the model and model validation.

3.5.1 Overview

To model thermal performance, load information obtained by the NILM is combined with data from various environmental sensors. Figure 15 shows the current setup, which includes the NILM, a thermostat, an outdoor temperature sensor, and a solar irradiance sensor. These remote sensors and NILM can be enabled to communicate via wireless links. The NILM would use all of the data to build a thermal model that relate the various inputs (i.e. solar irradiance, indoor heat gains, etc.) to the indoor temperature. After building up the model, it can be used for either control system design or energy performance and diagnostics.

The model formulation for control design takes indoor temperature as an output whereas for energy performance takes thermal energy. The underlying methodology, however, is similar in both cases.

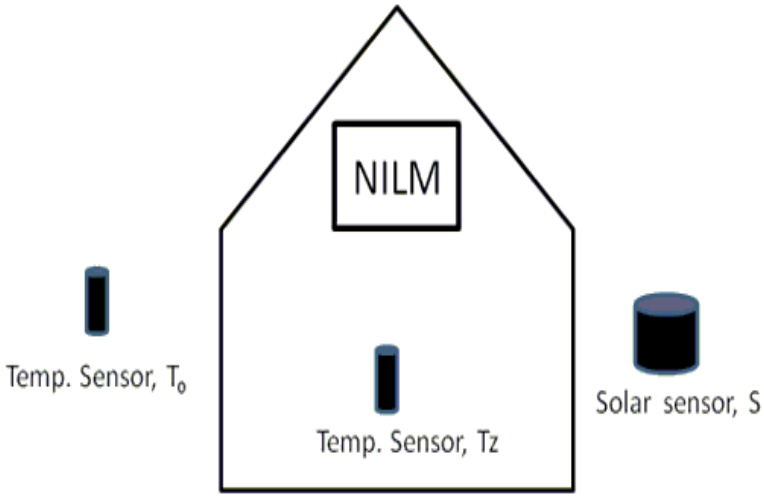

Figure 15: Diagram of a home showing all of the relevant system components. The remote sensors can relay their data to the NILM via wireless links.

To make a control system or energy performance model cost effective, it is important to build a thermal model with little or no human interaction. Physics-based models, as mentioned before, are not helpful as they require the user to provide extensive information about the properties of furniture, walls, and windows. Furthermore, these methods are not particularly adept at dealing with dynamic effects, such as changes in heat transfer caused by wind conditions along the building envelope. Similarly, grey-box models, which use some combination of user-generated parameters and input-output correlation modeling, are also undesirable as they still require relatively large amounts of user-provided information. Black-box approaches, which rely wholly on mathematical input-output relationships, are thus the most attractive option. Various black-box approaches have been proposed for modeling the thermal behavior of large-scale commercial facilities 0, [18]. There are several key differences between the operation of large and small buildings, however, that render these methods ineffective in homes and small commercial facilities. Most importantly, the HVAC systems in large buildings typically operate in steady-state for long periods of time; by comparison, the HVAC

equipment in smaller settings operates cyclically, meaning that the thermal variables are often in a transient condition.

A new robust modeling approach was developed to handle the unique thermal behavior of homes and small buildings without having to obtain information from users. In this setup, the distributed thermal system is modeled as Linear Time Invariant (LTI) system with a number of states. The exact number of these states is determined using field data, meaning that the number can be automatically modified as needed. The input and output variables used by the model differ depending upon its ultimate application, i.e. whether it is to be used energy performance and diagnostics or controls. The remainder of this chapter thus proceeds in a generalized manner, describing only generic inputs and outputs. The specific formulations of the model are analyzed in detail in the following section.

In practice, the model order is unknown and the training process is repeated on the same data set with a higher order formulation until the model predictions suitably match the measurements. Once the training process is complete, the parameter estimates are used to predict thermal behavior.

3.5.2 Experimental Test Setup and Procedure

In the previous section, overview of set up and process plan were given. Now, attention will be given to detailed procedure and experiments. Figure 15 has described the sensors and data loggers placements in a residential house. To develop a thermal model based on measurements, experimental site has been identified in Kings Mountain, NC. This is a trailer house. The detailed description of above mentioned house has been given in Appendix A.

Sensors installations have been described in Table 1. Detailed specifications have been given in Appendix B, Table 9 and Figure 50.

The specifications have been taken from [59]. For thermal model identification of house different temperature sensors have been identified and shown above. Here, temperature sensors inside the house will take reading of the zone. To tap the outside condition, two sensors are there for temperature and solar radiation reading. Sampling rate for temperature sensors have been set as 1 data per minute and unit is °F. Solar irradiance is recorded through same sampling rate. NILM records current data which gives the on-off schedule for compressor. The present scheme is based on sampling rate of 1 data per minute.

Table 1: Sensor and Data loggers placement for thermal model identification of a residential house

Sl no.	Sensors	Numbers	Location	Purpose
1	Temp.	1	Inside the House	House temp. observation
2	Temp.	1	Outside the House	Ambient temp. measurement
3	Solar	1	Outside the House	Solar irradiance measurement
4	NILM	1	Inside the House	On-Off cycle data logging

Having developed the plan for thermal model formulations, heat input/extraction needs to be found out. Heat input/extraction is superimposed on NILM on-off cycle to get the desired input signal in time. This study was done during summer and so cooling capacity has been taken into account. Here is the little introduction of cooling capacity and later experiments will be discussed to investigate that.

Cooling capacity

It is one of the most important and challenging variable in the modeling of energy systems. In general, cooling capacity value is written in the product specification supplied by manufacturer. There are already several established methods available and will be developing too in future to find it. Cooling capacity is defined as the rate at which heat is removed from a space. Generally, cooling capacities is expressed British Thermal Units (BTUs) per hour, or in tons. A ton of cooling capacity is equal to 12,000 BTUs per hour. Historically, tonnage of refrigeration has been defined as amount of heat extraction required to freeze one ton water in 24 hrs.

$$\text{In general, Cooling capacity (J/sec)} = \dot{m}_{air} * (h_{Eb} - h_{Ea}) \quad (28)$$

Where, $$\text{Air flow rate, } \dot{m}_{air} = \mu * A * V \quad (29)$$

$$\text{Change in enthalpy of air, } (h_{Eb} - h_{Ea}) = C_p * (T_{Eb} - T_{Ea}) \quad (30)$$

and μ is the air density $(kg/m\text{^}3)$, A cross-section through air flows $(m\text{^}2)$, V air velocity (m/sec), C_p sp. heat capacitance $(1.005KJ/Kg - K)$, T_{Eb} temperature before evaporator (°C) and T_{Ea} temperature after evaporator (°C).

Cooling capacity in BTU can be expressed as

$$\text{Cooling capacity (BTU)} = 4.5 * \text{CFM} * \text{Change in enthalpy} \quad (31)$$

Where, CFM is velocity of airflow in cubic feet per minute. "4.5" comes from .075 $(air\ density\ in\ LB/FT\text{^}3)\ X\ 60$.

Enthalpy tables or psychometric chart is used for enthalpy determination [60]. To find out cooling capacity of an existing system, there are potentially two ways to do it i.e. using analytical calculation and by measurements. This section has described the methods

in detail. Analytical method needs more information than available and therefore the present work has preferred the measurement method. This is more relevant and reliable.

Experimental procedures

1. Determine cooling capacity
    a. Based on analytical calculation
    b. Based on measurement
2. Placement of temperature sensors for zone and ambient, solar sensors for irradiance measurement.
3. NILM is deployed to find compressor ON-OFF schedule.
4. Thermal model identification.

As discussed before, cooling capacity is determined mainly in two ways i.e. through measurement or analytical approach. Both the methods have been discussed below.

a. Based on analytical calculation

Analytical approach goes with the parameters and detailed specification of compressor supplied by the manufacturer.

Refrigerant mass flow rate calculation

i) Compressor parameters: $RPM(N)$, $Stroke(L)$, $Bore(d)$, $Number\ of\ Cylinders(n)$

ii) Find swept volume $V_{disp} = n * (pi/4) * d\text{^}2 * L$

iii) Find clearance volume V_{cl}

iv) Calculate $V = (V_{disp}) * RPM * n$

v) Volumetric Efficiency calculation

- From the performance chart get $P_c(T_c)$ and $P_e(T_e)$
- Take ratio (Compression ratio) $r = P_c/P_e$
- Get the density for the refrigerant in vapor phase at T_e (or at superheat).
- Calculate the mass flow rate, $m\_\dot{c}alc_{ref} = V/density$
- Find $\eta_{vol} = 1 - \frac{V_{cl}}{V_{disp}} * \{r^{1/p} - 1\}$, where p is a polytropic exponent.

vi) Find $\dot{m_{ref}} = \eta_{vol} * m\_\dot{c}alc_{ref}$

Sometimes, actual flow rate is given in the performance chart too. It should always be verified first before going into details of analytical calculation.

Cooling Capacity Calculation

Refrigerant mass flow rate is known from previous shown calculation. It is used in the next step to yield cooling capacity [61].

i) Change in enthalpy, Δh is obtained from psychometric chart. Here sub cooled and superheated should be taken into account.

ii) Cooling capacity $\dot{Q} = \dot{m}_{ref} * C * \Delta h$

Here $\dot{m}_{ref}$ can be obtained directly through metering device [62], [63] and [64].

b. Based on measurements

I. ARI coefficient based on manufacturer's compressor map.

II. Based on mean temperature and effective conductance. [62]

III. Temperature across evaporator and air velocity measurement.

Cooling capacity determination through measurements has been explained in detail. This method is always preferred over getting information from manufacturers and

doe analytical calculations. The reason is that analytical equations are over simplified and do not represent exactly the system. Therefore later is always given due considerations.

I. ARI coefficient based on manufacturer's compressor map

To explain it better it is worth to understand compressor performance map first. Compressor map is provided by a manufacturer. Performance map shows mass flow rate, refrigeration capacity, the input power, input current as a function of evaporating and condensing temperatures.

Using this data, AIR recommends developed a curve fit to get 10 coefficients [65], [66]. The Air-Conditioning and Refrigeration Institute's (ARI) standard provides a method on how to present compressor performance data for all positive displacement refrigerant compressors and compressor units. This method uses compressor performance data to curve fit coefficients of polynomial equations. The equations are of the form

$$X = C_1 + C_2 \cdot T_{evap} + C_3 \cdot T_{cond} + C_4 \cdot T_{evap}^2 + C_5 \cdot T_{evap} \cdot T_{cond} + C_6 \cdot T_{cond}^2 + C_7 \cdot T_{evap}^3 + C_8 \cdot T_{cond} \cdot T_{evap}^2 + C_9 \cdot T_{evap} \cdot T_{cond}^2 + C_{10} \cdot T_{cond}^3 \quad (32)$$

Where X can represent refrigeration capacity, power input, mass flow rate or motor current.

$T_{evp}evp$ – saturated evaporating temperature,

$T_{evp}\ cond$ – saturated condensing temperature.

C1 to C10 - curve fit parameters.

To determine the 10 coefficients in each equation at least 10 measurements of the entity represented by X have to be made. This is based purely on mathematical ground however widely accepted as standard for refrigeration. All the coefficients have been

shown in Table no. 6. Each variable of interest has its own set of coefficients i.e. cooling capacity, electrical power, current and refrigerant mass flow rate.

A typical manufacturer's data sheet for compressors has been added. These have been taken for Bristol and Copeland compressor [67], [68]. In Appendix B, Figure 46 and Figure 47 represent the compressor performance map.

As discussed before, this formulation can be used to find cooling capacity if T_{evp} and T_{cond} are known. Temperature Sensors are employed to measure these values. They can also be found out by having Saturation pressures of condenser and evaporator values and looking in p-h diagram.

II. Based on mean temperature and effective conductance

This method comes out from a bulk approach towards air system and evaporator interaction and heat transfer between them [69]. Popular methods are Log Mean Temperature Difference (LMTD) and Number of Transfer Units (NTU).

III. Temperature across evaporator and air velocity measurement.

Test plan and placement of sensors: HOBO Sensors have been used for all the measurement and data acquisition [59].

Air velocity measurement: As per ASHRAE standard air flow measurement in a duct should be at least 25point for a rectangular shape [70]. The duct in the study has rectangular in shape. Hot wire anemometer is being used for velocity measurement. In Appendix B, Figure 1 shows the duct and recommended measurement points. Also, in Appendix B, Table 7 and Table 8 are showing air velocity measurements and cooling capacity calculations.

3.5.3 Stability, Controllability and Observability

Once the model is identified, it becomes extremely crucial to analyze the performance of the model of system. There are three most important tests laid out i.e. Stability, Controllability and Observability. These concepts have been dealt extensively in [71], [72], [73] and [74].These are vital for any system as they set standard for selection.

As discussed before, any LTI discrete system in state space representation will be

$$\mathrm{X(k+1) = AX(k) + BU(k)} \tag{33}$$

$$\mathrm{Y(k) = CX(k)} \tag{34}$$

Where X, U and Y are states, input and output respectively. A, B, and C are plant matrices or simply model parameters.

Where n=number of states. In the present case number of states is 4.

(a) Stability

Ideally, a system is called stable when the outputs do not go to infinity irrespective of the inputs.

To understand the stability, z-transform of the plant is taken and by doing mathematical rearrangement, (33) and (34) can be written as that the transfer function

$$G(z) = C(zI - A)^{-1}B = C\frac{adj(zI-A)}{\det(zI-A)}B \tag{35}$$

Here roots of $det(zI - A)$ or eigenvalues of A decides the stability of the system. This is equated to zero. It is also called characteristics equation. If absolute value of z i.e. |z| lie inside a unit circle, system is called stable else unstable.

Hence eigenvalues of characteristics equation is defined as follows. In the formulation, I is the identity matrix.

$$|zI - A| = 0 \tag{36}$$

The proposed model has all the roots are inside the unit circle and system is stable.

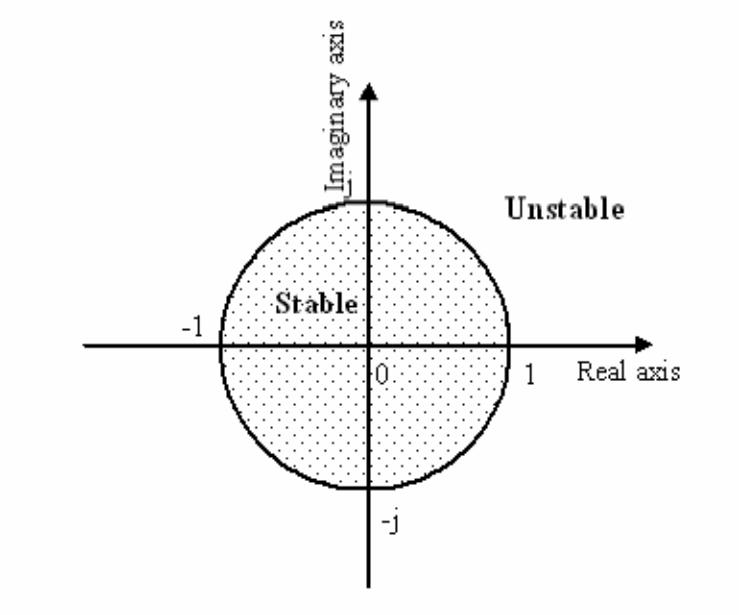

Figure 16: Unit circle to test the stability of a system.

(b) Controllability

A state of system is controllable if a control input can transfer it from initial state $X(0)$ to $X(T_s) = 0$ in finite time T_s. The entire system is controllable if all the states X are controllable. It has been shown in Figure 17.

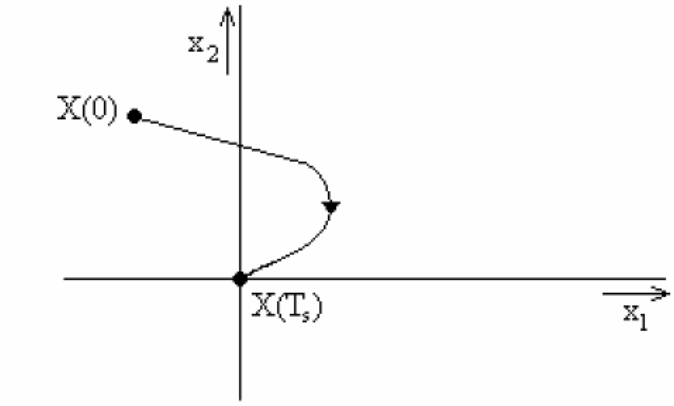

Figure 17: System dynamics plot to show controllability.

For a LTI discrete system, states are written as below,

$$X(k) = A^k X(0) + \sum_{j=0}^{k-1} A^{k-j-1} BU(j) \tag{37}$$

Expanding equation (36) would yield,

$$X(k) = A^k X(0) + A^{k-1} BU(0) + A^{k-2} BU(1) + A^{k-3} BU(2) + \cdots + BU(k-1) \tag{38}$$

Equation (37) can be re-written as equation (38) by shifting the first term on the left hand side. The whole purpose of this rearrangement is to make sure that only input terms associated with inputs only kept on one side.

$$X(k) - A^k X(0) = A^{k-1} BU(0) + A^{k-2} BU(1) + A^{k-3} BU(2) + \cdots + BU(k-1) \tag{39}$$

Right hand terms of equation (38) can be further re-arranged to represent in a row and column vectors.

$$X(k) - A^k X(0) = [B\ AB\ A^2B \ldots A^{k-1}B] \begin{bmatrix} U(k-1) \\ U(k-2) \\ U(k-3) \\ . \\ . \\ . \\ U(0) \end{bmatrix} \tag{40}$$

Now to get Controllability matrix one has to make no. of samples k equal to no. of states n in equation (39), i.e. replacing k with n.

$$\alpha = [B\ AB\ A^2B\ A^3B \ldots \ldots A^{n-1}B] \tag{41}$$

α should be full of rank for a system to be controllable. As discussed before, by choosing input U, a controllable system can be transferred from X (0) to X.

The proposed model of 4-states has rank 4 and therefore the system is entirely controllable.

(c) Observability

A system is called observable if initial states X (0) of all the states can be determined by knowing inputs and output. Any change in states affect output if the system is observable.

From above, inserting equation (36) in (33) yields

$$Y(k) = CX(k) = CA^k X(0) + \sum_{j=0}^{j=k-1} CA^{k-j-1} BU(j) \tag{42}$$

Now for k=0, 1, 2… n-1 and writing equation (42) in matrix form

$$\begin{bmatrix} Y(0) \\ Y(1) \\ Y(2) \\ . \\ . \\ Y(n-1) \end{bmatrix} = \begin{bmatrix} C \\ CA \\ CA^2 \\ . \\ . \\ CA^{n-1} \end{bmatrix} X(0) + \begin{bmatrix} 0 & 0 & . & . & 0 \\ 0 & 0 & . & . & CB \\ . & . & . & . & . \\ . & . & . & . & . \\ 0 & CB & . & . & CA^{n-2}B \end{bmatrix} \begin{bmatrix} U(n-1) \\ U(n-2) \\ U(n-3) \\ . \\ . \\ U(0) \end{bmatrix} \tag{43}$$

Here Observability matrix is written from equation (43)

$$\beta = \begin{Bmatrix} C \\ CA \\ CA^2 \\ CA^3 \\ . \\ . \\ . \\ CA^{n-1} \end{Bmatrix} \tag{44}$$

For system to be observable, β should be full of rank. The present system has full rank of 4 and therefore it is observable.

3.5.4 Control Oriented Model Identification and Validation

There is growing motivation to be able to better control HVAC systems in homes and small buildings. For instance, utilities are exploring the concept of shedding residential HVAC load as an effective means for reducing peak loads and dealing with the intermittency of renewable resources. A smart meter is able to predict internal zone

temperatures could be used to improve this activity because it could determine how long it would take for the zone temperature to reach a certain preset limit. Furthermore, zone temperature predictions could be coupled with variable-capacity systems. In future homes with appropriate thermal mass and variable-speed motors, this could lead to significant energy savings.

Figure 18 shows the control-oriented model formulation. The model output in this case is the internal zone temperature, T_Z, which is the variable one would likely seek to control. Once again, a fourth-order model is used, and training occurs over a three-day period.

Figure 19 shows representative training data, and Figure 20 (a)-(g) show measured and simulated zone temperatures recorded over a single day during the validation period. These results are there for validation and suggest that the thermal modeling procedure could be used to form the basis of a robust optimal control system in homes. Here the measurement data have been pre-processed using smoothing technique which has been discussed already.

Figure 21 shows the system identification based on just raw data.

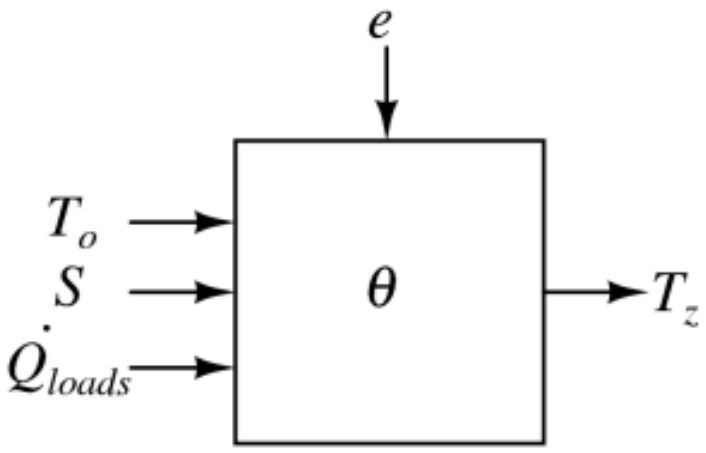

Figure 18: Control-oriented model formulation including random errors e.

It can be concluded that for training purposes data should be pre-processed to get rid of noise. Although, enough care should be taken as it might suppress some important signature. Matlab file has been added in Appendix C. The proposed state space equation of house would be

$$\underline{x}_{k+1} = \underline{\underline{A}}(\theta)\underline{x}_k + \underline{\underline{B}}(\theta)\left[\dot{Q}_k \; T_{o,k} \; S_k\right] + \underline{\underline{K}}(\theta)\underline{e}_k \tag{45}$$

$$\underline{T}_{z,k} = \underline{\underline{C}}(\theta)\underline{x}_k + \underline{e}_k \tag{46}$$

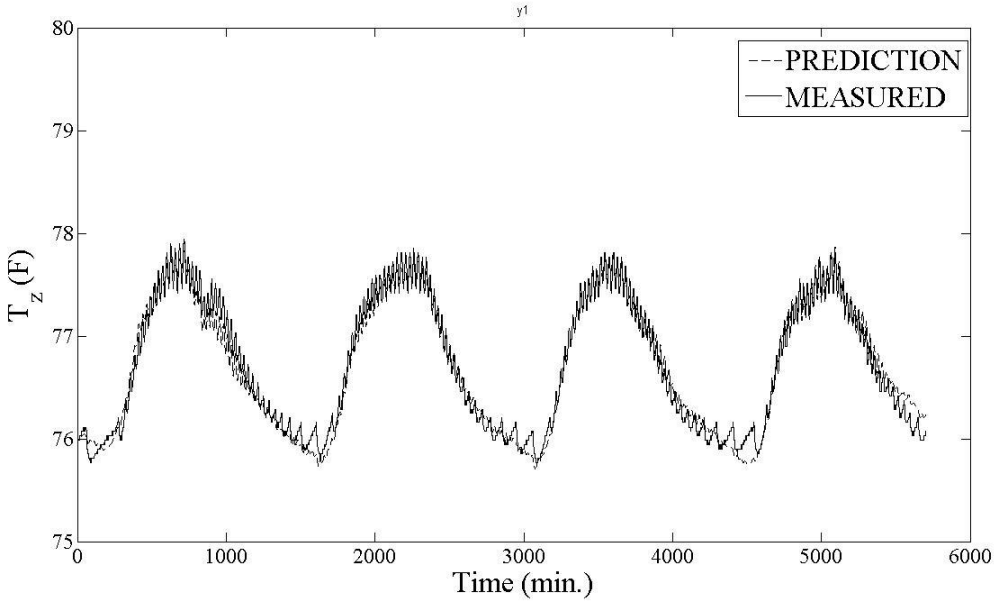

Figure 19: Measured (and smoothed) and simulated data recorded during the training period.

Based on the discussion before, poles of the identified system are

z = 0.9606 + 0.24151*j, 0.9606 - 0.2415*j, 0.9998, 0.9519

Since all the points are inside unit circle, it shows a stable system. Further, to check controllability, observability α - matrix and β - matrix respectively above mentioned formulations have been followed.

α- matrix has rank 4 and therefore the system is fully controllable.

β- matrix has rank 4 and therefore the system is fully observable.

To validate the identified model, consecutive days have been selected. To control the error propagation and disturbance, simulation is run for each full day independently. Also, simulation start and end time has been selected the same for consistency.

The model clearly tracks all the variations in the zone temperature. It does have tendency to deviate from actual as time progresses. Later in this work, two methods have been proposed to track the zone temperature more precisely, i.e. recursive state estimation based on Prediction Error method and Kalman filter [75].

Control model validation results have been shown in Figure 20. After the model identification through training, 7 consecutive days have been selected and the zone temperature is calculated using the identified model. Later, the calculated zone temperature is compared with the measured one. Figure 20 (a) to (g) clearly shows the capability of the identified model. Several months of data were recorded and compared with the calculated data which are obtained from the identified mode. The author can be contacted in this regard.

Control model validation

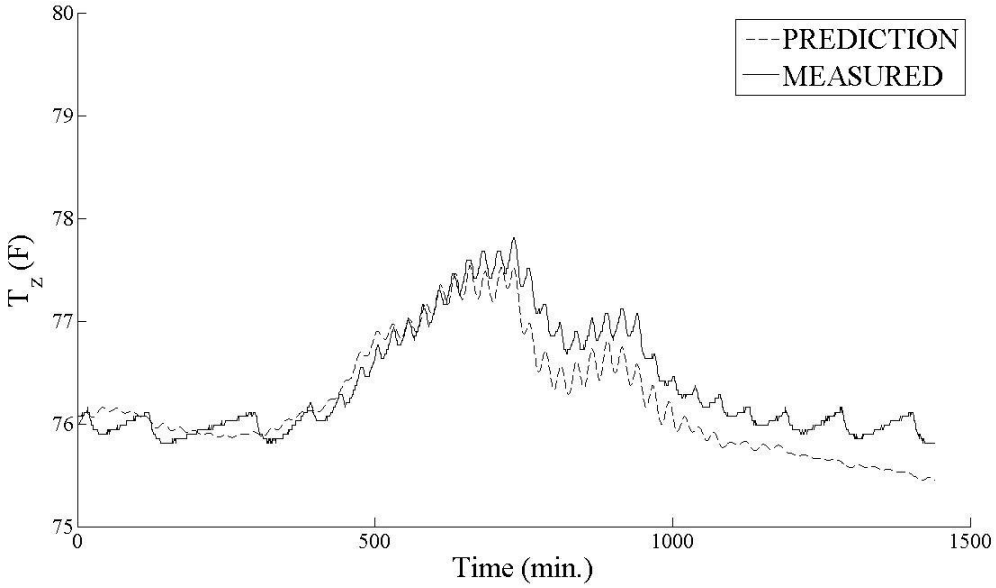

(a)

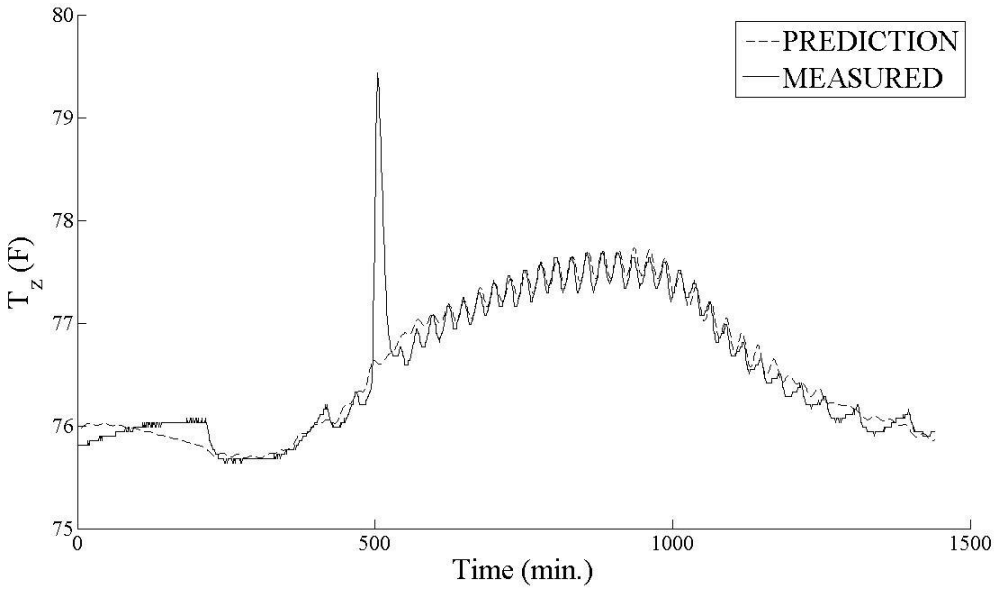

(b)

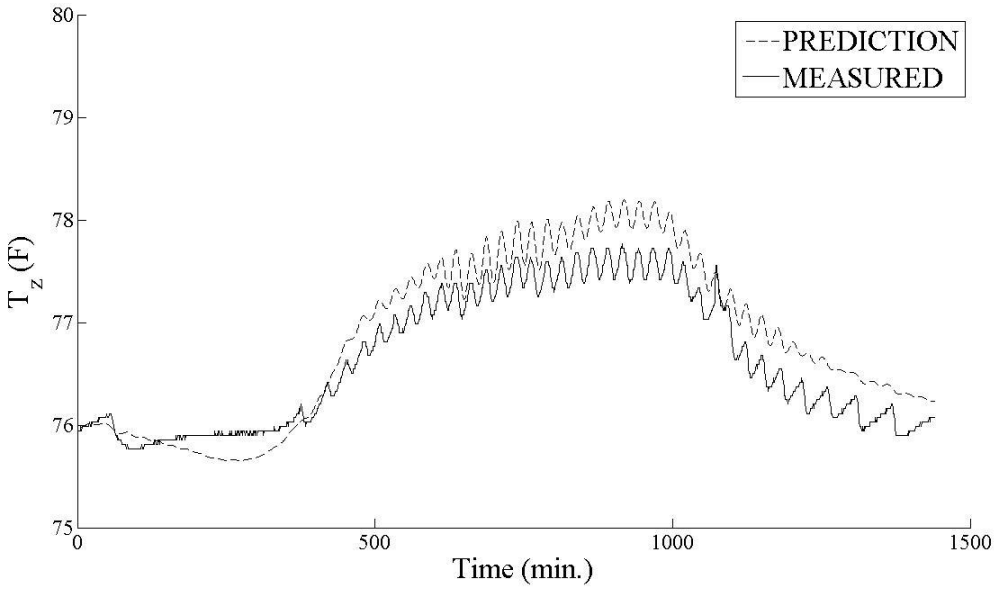
---PREDICTION
—MEASURED
80
79
78
77
76
75
T_z (F)
0
500
1000
1500
Time (min.)

(c)

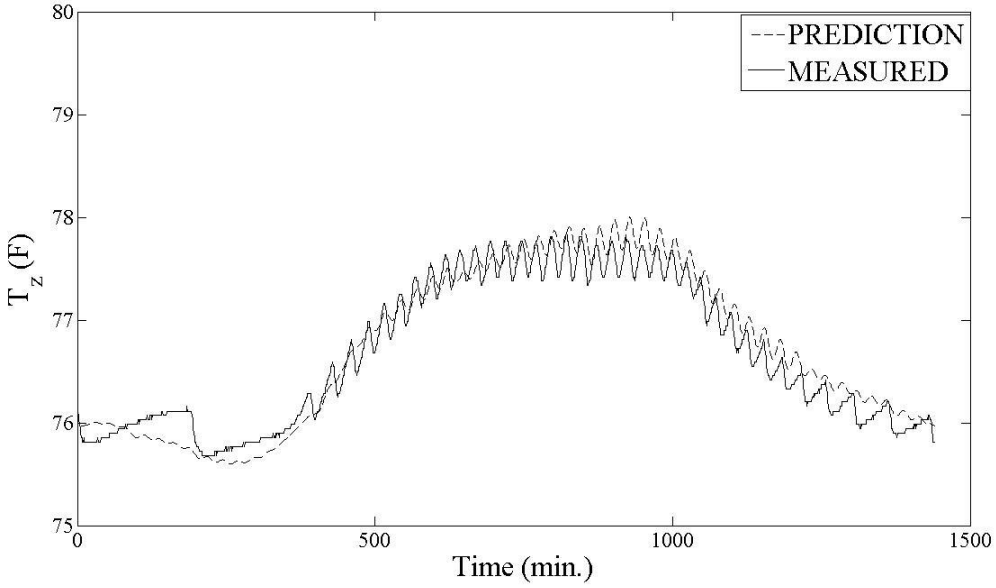
---PREDICTION
—MEASURED
80
79
78
77
76
75
T_z (F)
0
500
1000
1500
Time (min.)

(d)

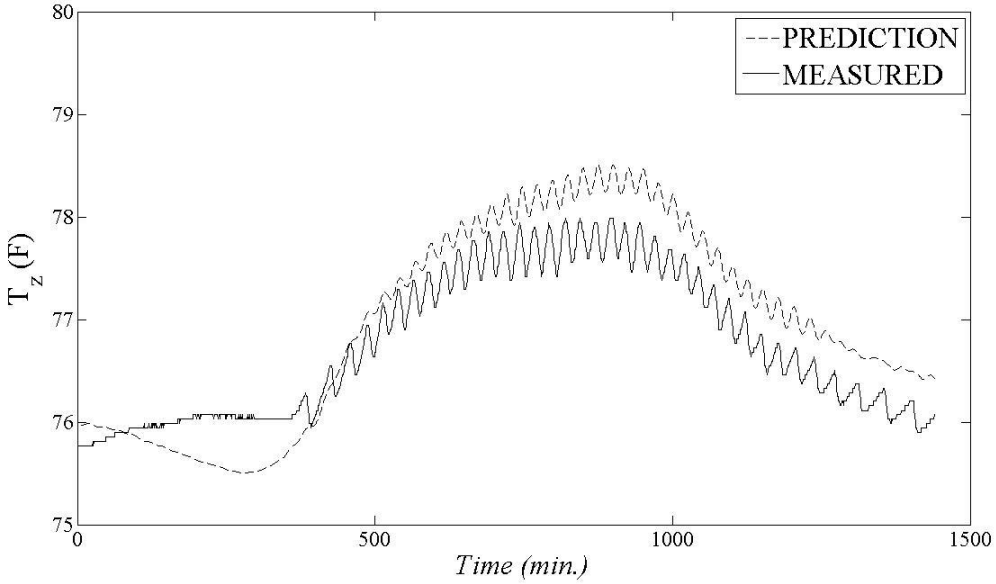
---PREDICTION
—MEASURED
80
79
78
77
76
75
T_z (F)
0
500
1000
1500
Time (min.)

(e)

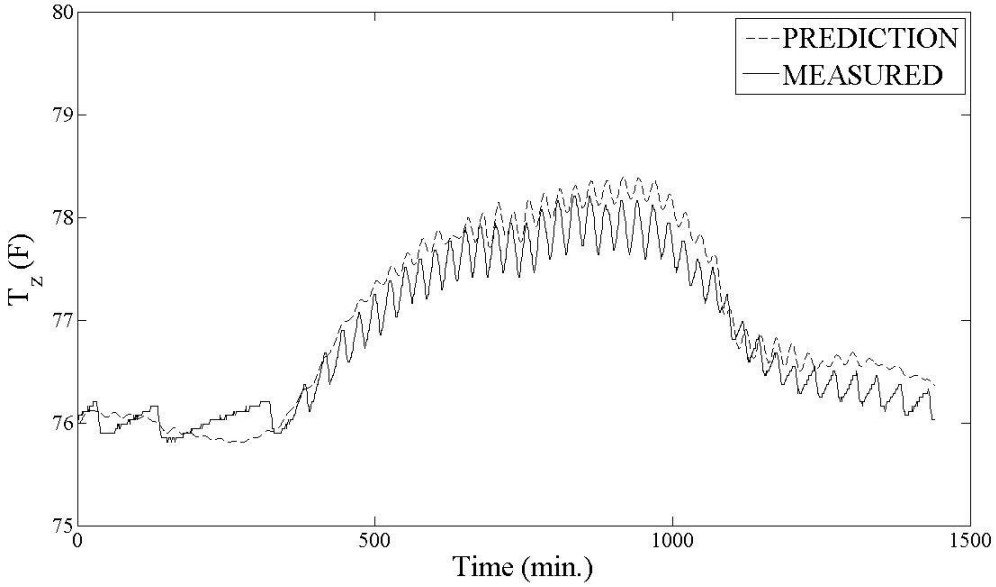
---PREDICTION
—MEASURED
80
79
78
77
76
75
T_z (F)
0
500
1000
1500
Time (min.)

(f)

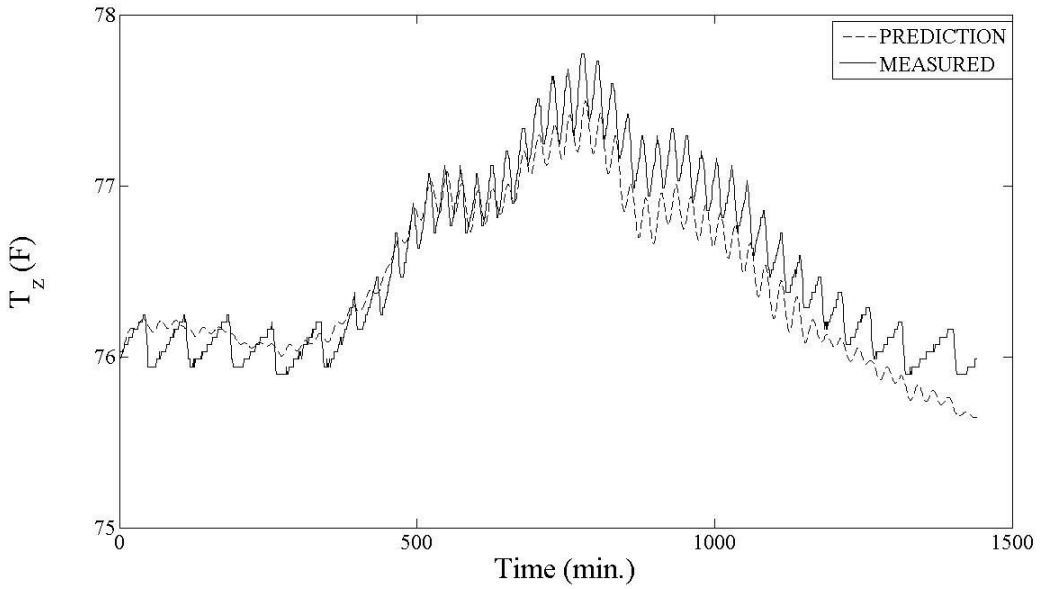

(g)

Figure 20: (a) to (g) Control Oriented Model Validation.

System identification based on purely raw (measured data without smoothing) data, it clearly shows how important role smoothing plays in the data preprocessing.

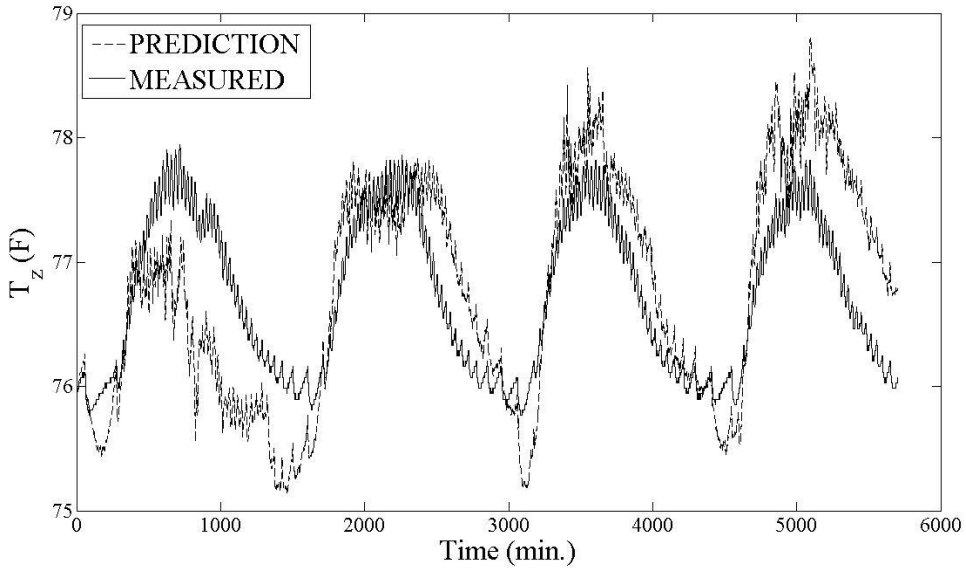

Figure 21: Measured (raw data, without Smoothing) and simulated data recorded during the training period.

As discussed previously, to take into account variations in the system two methods have been proposed.

1. Temperature prediction based on recursive state estimation using PEM.

This method recursively does initial state estimation based on PEM. 15 min. of time window has been selected and shown the predicted data compared to measured data Figure 22 (a) to (g). It does produce sound scheme to track the zone temperature.

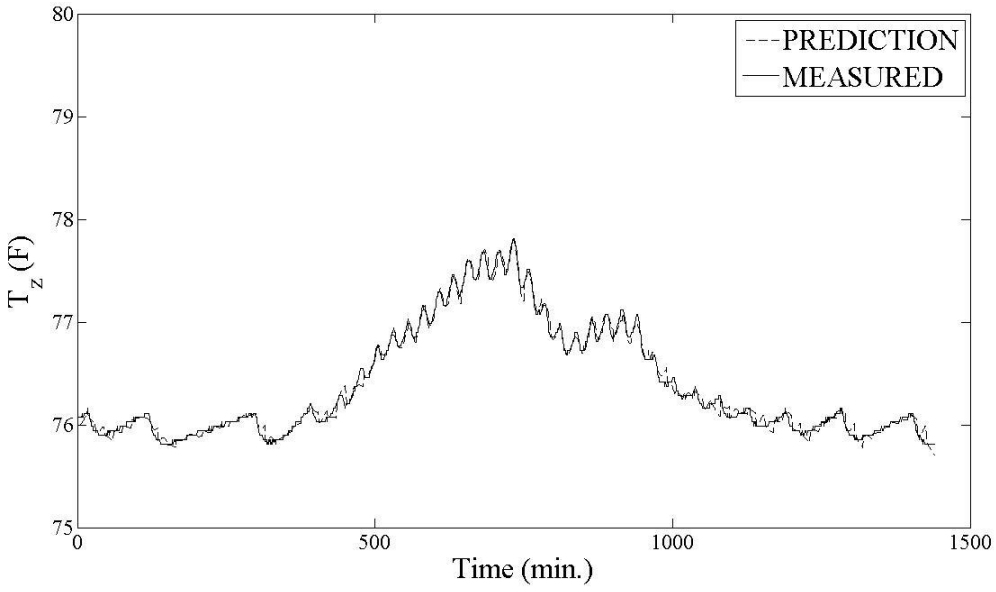

(a)

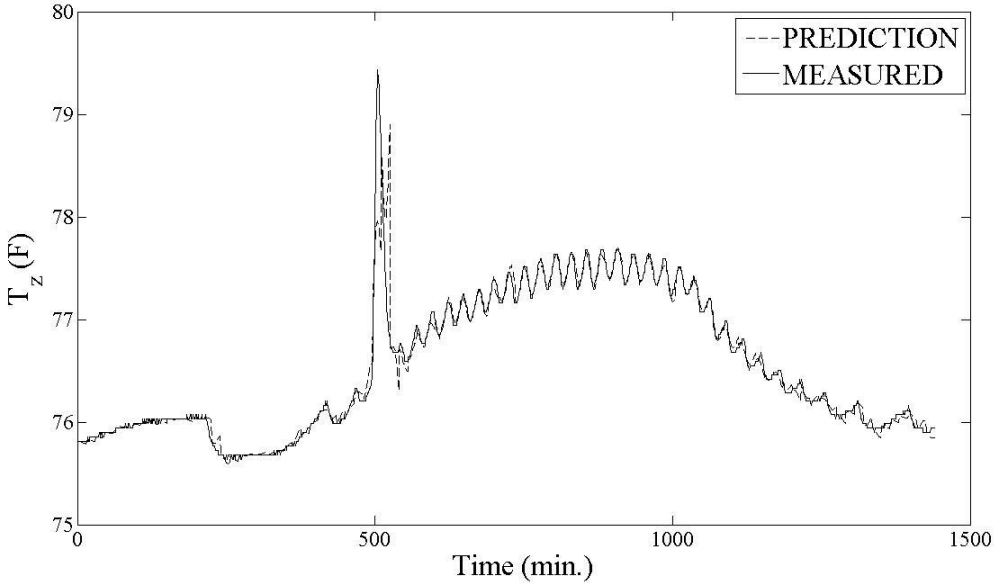
---PREDICTION
—MEASURED
80
79
78
77
76
75
T_z (F)
0
500
1000
1500
Time (min.)

(b)

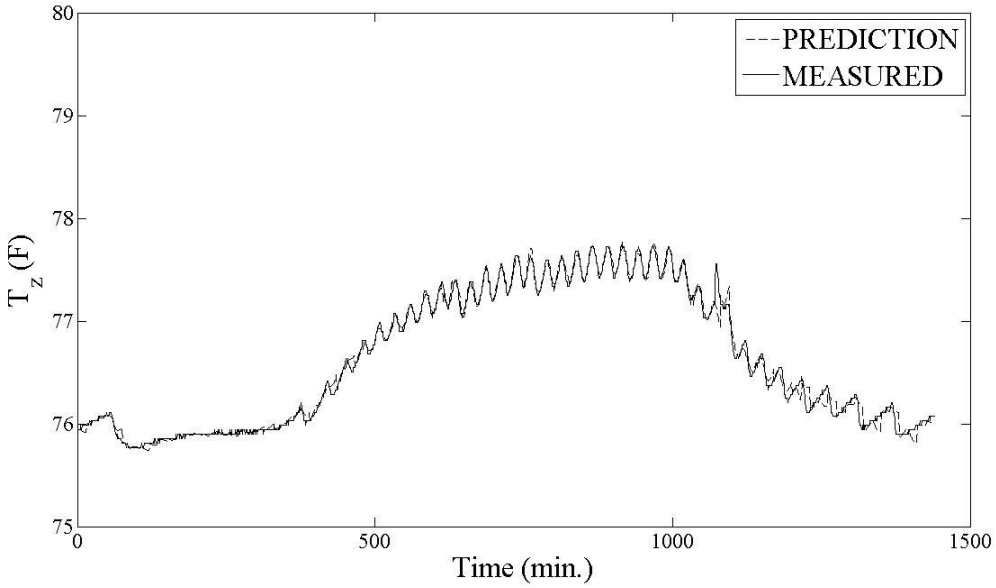
---PREDICTION
—MEASURED
80
79
78
77
76
75
T_z (F)
0
500
1000
1500
Time (min.)

(c)

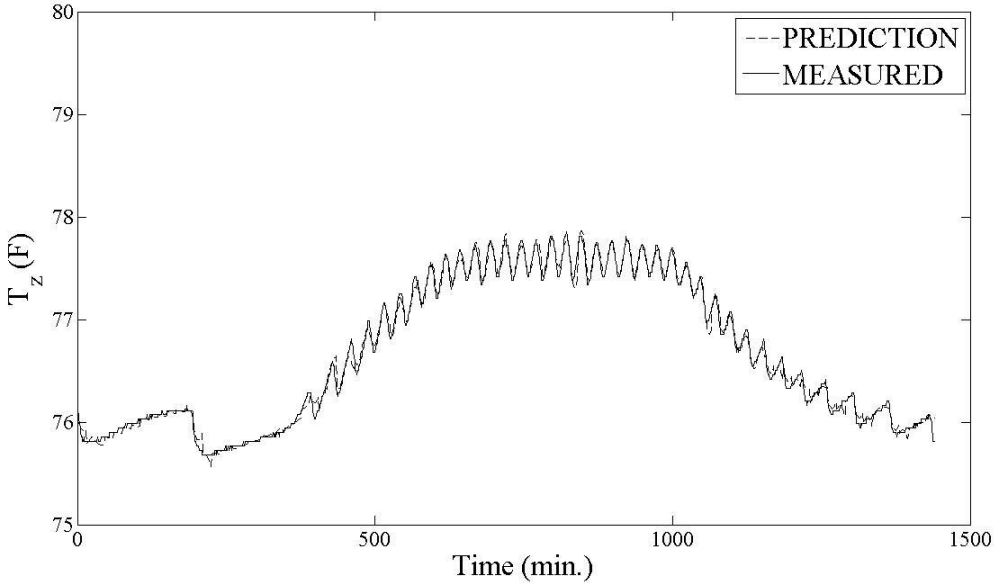
---PREDICTION
—MEASURED
80
79
78
77
76
75
T_z (F)
0
500
1000
1500
Time (min.)

(d)

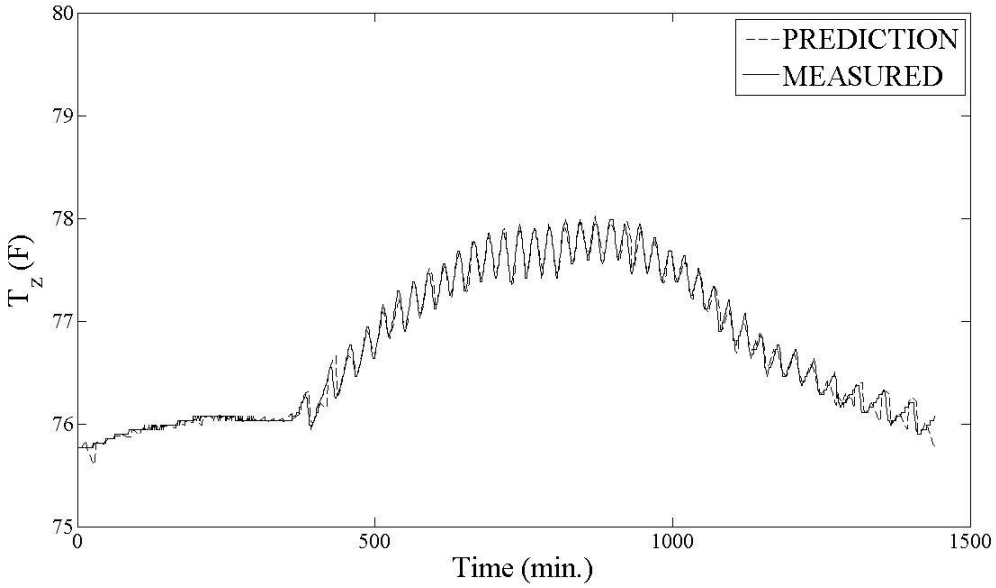
---PREDICTION
—MEASURED
80
79
78
77
76
75
T_z (F)
0
500
1000
1500
Time (min.)

(e)

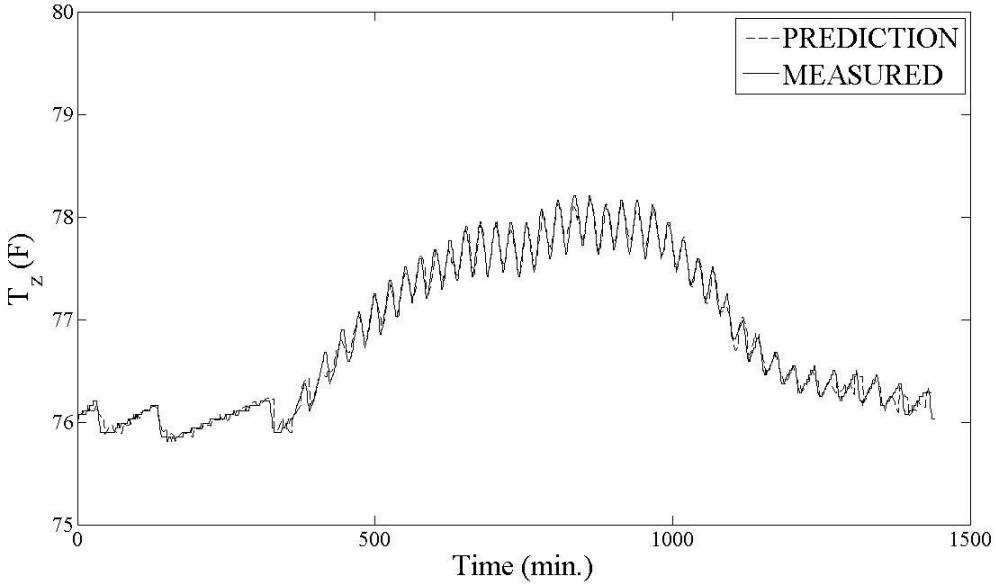

(f)

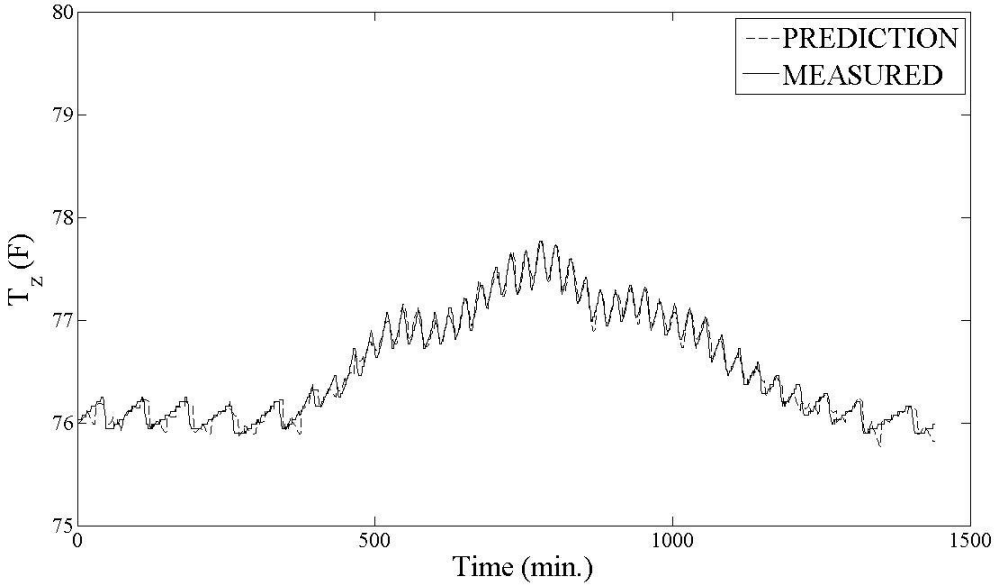

(g)

Figure 22: (a) to (g) Using recursive state estimation using PEM approach for Control Model Validation.

2. Kalman filter implementation for temperature prediction.

Kalman filter [75] has been discussed in the previous section in details. This has been implemented to track zone temperature accurately and it also produces interesting results. There is although a legitimate question about the use of this model in the proposed controls system. It does one step ahead prediction. The present research focusses on development of control system also. The model should have long time predictions. In that case it might seem little difficult to implement. However, this can be used independently, with any other control system or for just a solution to tracking problem.

Here are the results Figure 23 (a) – (g) using Kalman state estimation.

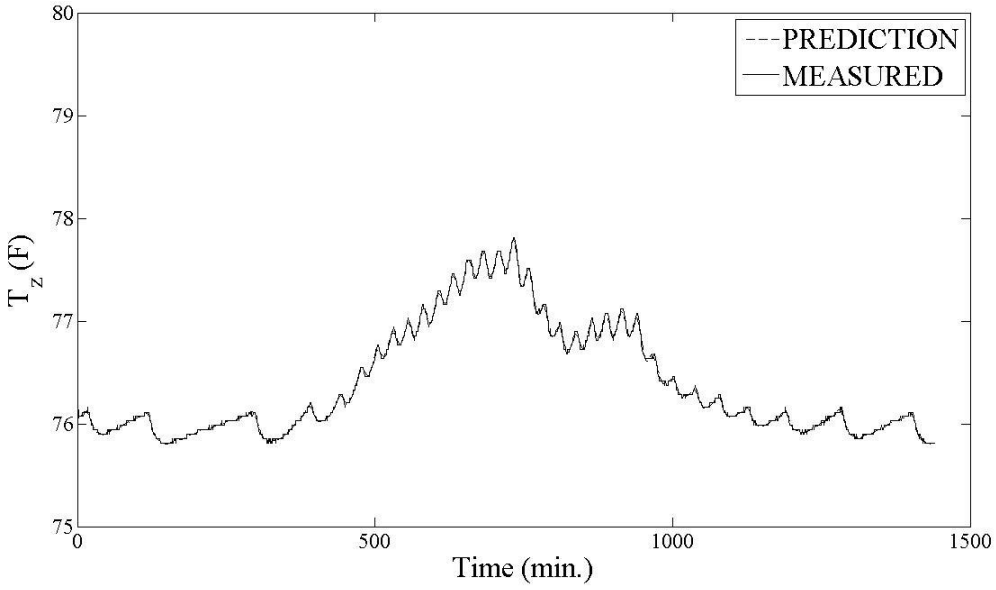

(a)

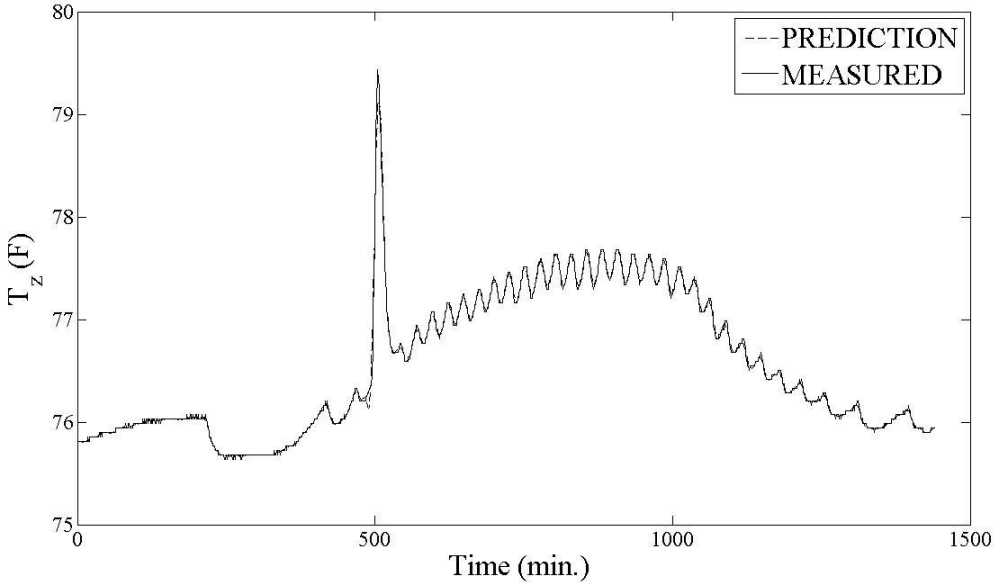
---PREDICTION
—MEASURED
80
79
78
77
76
75
T_z (F)
0
500
1000
1500
Time (min.)

(b)

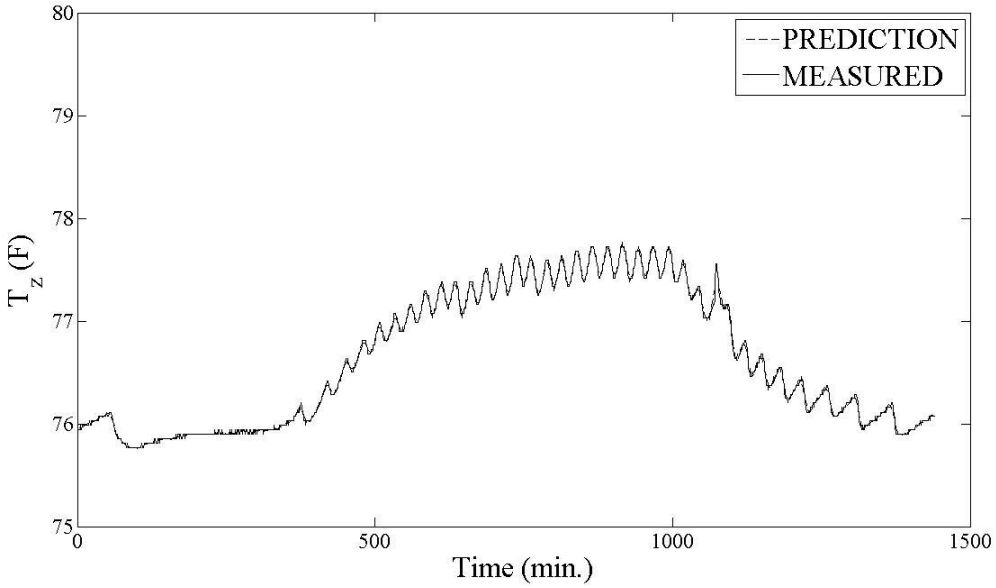
---PREDICTION
—MEASURED
80
79
78
77
76
75
T_z (F)
0
500
1000
1500
Time (min.)

(c)

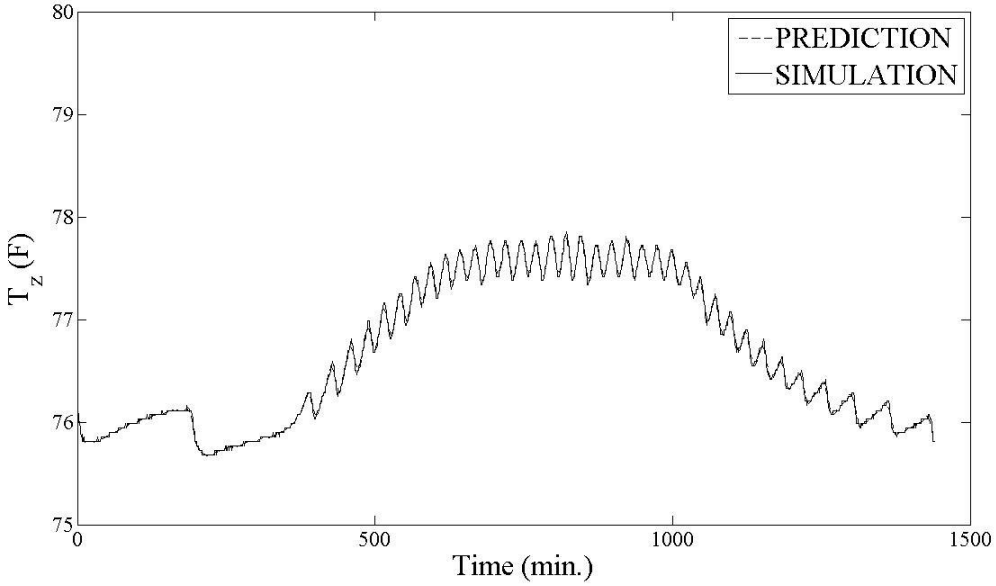
---PREDICTION
—SIMULATION
80
79
78
77
76
75
T_z (F)
0
500
1000
1500
Time (min.)

(d)

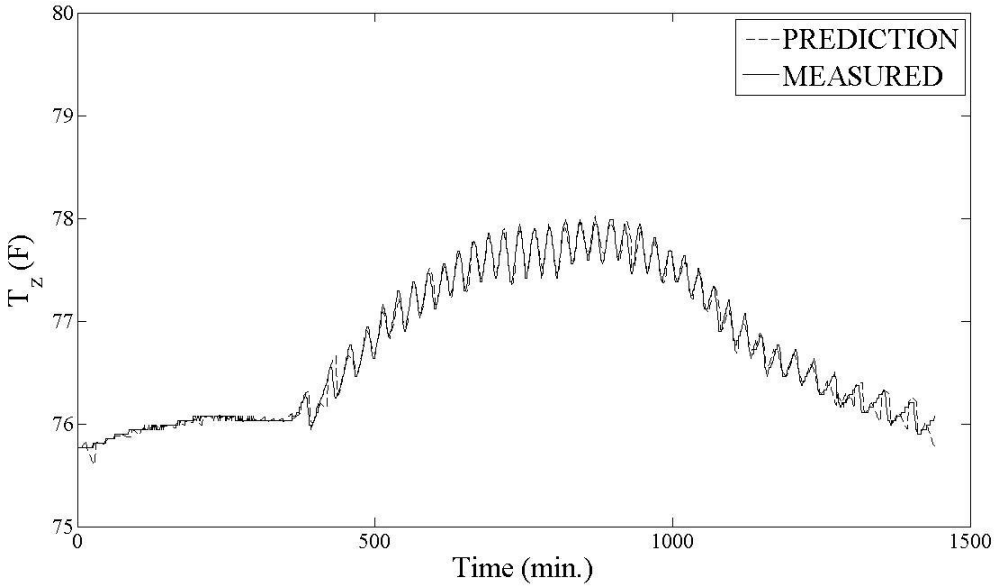
---PREDICTION
—MEASURED
80
79
78
77
76
75
T_z (F)
0
500
1000
1500
Time (min.)

(e)

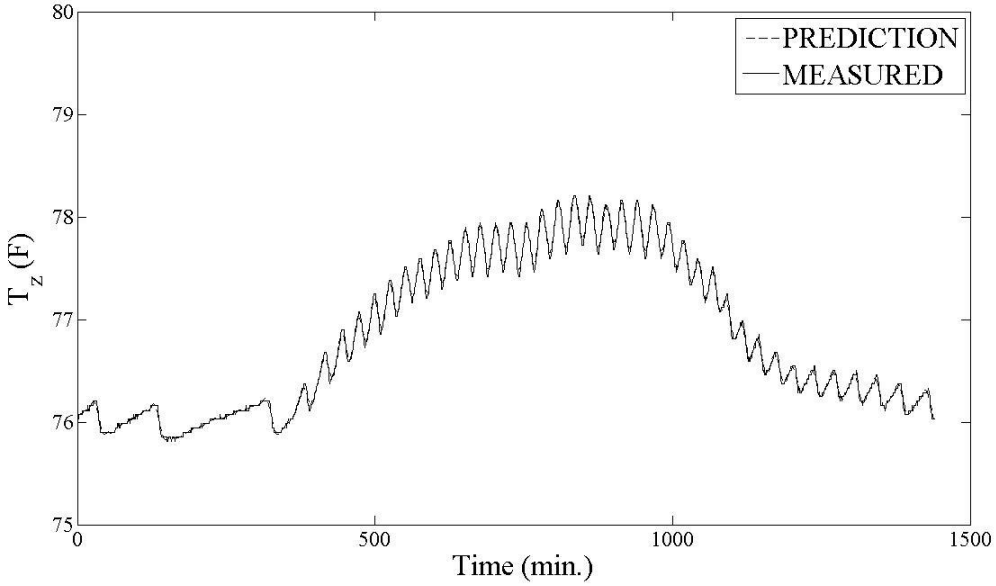

(f)

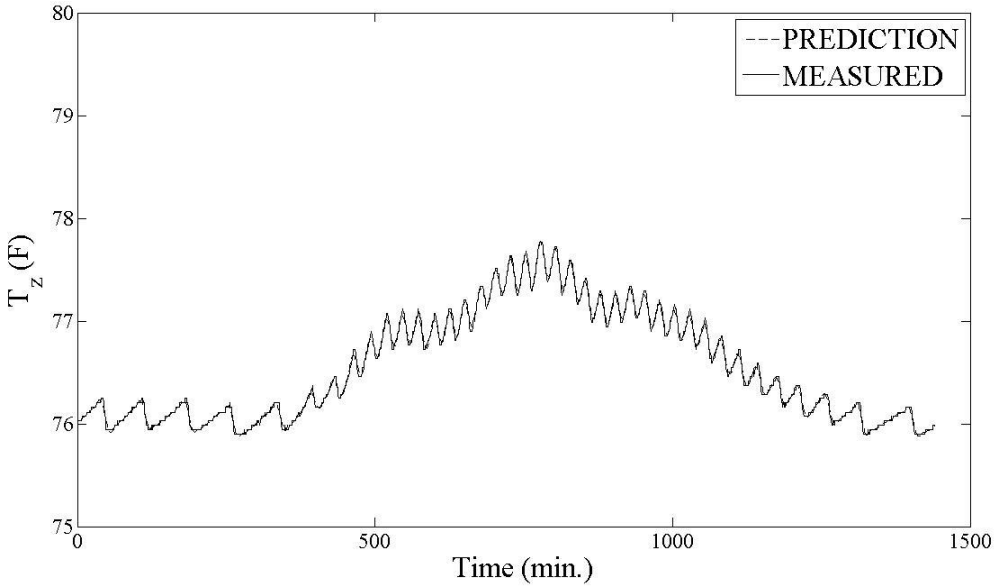

(g)

Figure 23: (a) to (g) Using Prediction based on Kalman Filter for Control Oriented Model Validation.

It can be concluded that model capability is enhanced by using previously available measurement data. In case of implementation in real system, all the sensors would be data loggers. The data will be taken to estimate states to track the system behavior.

CHAPTER 4: DEVELOPMENT OF CONTROL SYSTEMS

Ideal objective of a control system should be to meet the thermal comfort requirements at the expense of optimum amount of energy. So far efforts have been there to develop a thermal model of residential house. Having obtained one, it is worth to proceed towards building up controller. There are many well developed control strategies present for HVAC of building systems such as On-Off, PID and rule based. Building Energy Management Systems (BEMS) [76], [77] is used to control and better energy utilization in big buildings. [78] Demonstrates the uses of Matlab/Simulink to design building energy systems through S-function. There are various ways to implement the controllers, Variable Air valve system (VAV) and Variable capacity control (VCC). VAV is takes into account the efficient utilization inter zonal air distribution in which fan plays an important role [79]. Most of the existing systems have fixed speed compressor which is highly inefficient at part load conditions. Variable capacity control matches with part load, reduces on-off cycling losses to mechanical components in HVAC. It has already been proven that variable capacity control is an efficient way to maintain the comfort level [80]. Variable capacity control is realized through selecting the variable speed compressor. Mathematical relationship between number of variables such as, cooling capacity, input power, mass flow rate etc. to the rpm of compressor have been shown [81]. This can be taken as basis to convert thermal energy requirement to speed of compressor as an input.

Interestingly, focus towards residential houses has been the least. On-Off controller is the most popular and widely used in houses. It does address the need of thermal comfort but does not do anything as far as optimum amount of energy usage is concerned. Coming back straight to address the objective of a controller in residential houses, first of all it should fulfill the need of thermal comfort. This is the foremost important duty of any control system. Moving further, no existing controller decides the action based on weather forecast information which is available for any location in the country. New Time of Use (TOU) policy which is "time of use" will be reality in the near future. User should be able to deal with all the possible options in a dynamic fashion to keep the electric bill low. On top of that advent of smart grid technology, Utility and household will be communicating to each other. Our present system is not prepared to handle all the dynamics. Definitely, there is strong need for a new kind of control strategy to deal with all kind of situations.

Taking into account these challenges, present work proposes Model Predictive Control strategy in residential energy systems. This is a very popular and effective controller in process industry. The section 3.1 will be introducing the concepts behind existing systems and later proposed controller strategy will be discussed in detail with validation results.

4.1 Residential Temperature Control

As of today, the most popular controller in residential houses is on-off (bang-bang or hysteretic) control. It is quite simple in it its operation. A typical HVAC system has already been discussed. On-off control makes the compressor run in two states, no rotation or running at a fixed speed. The controller will switch whenever the measured

temperature crosses the set temperature. Figure 24 shows the operation of on-off controller. HVAC tries to follow the set value (SV). PV (process value) is improved once PI or PID controller is used.

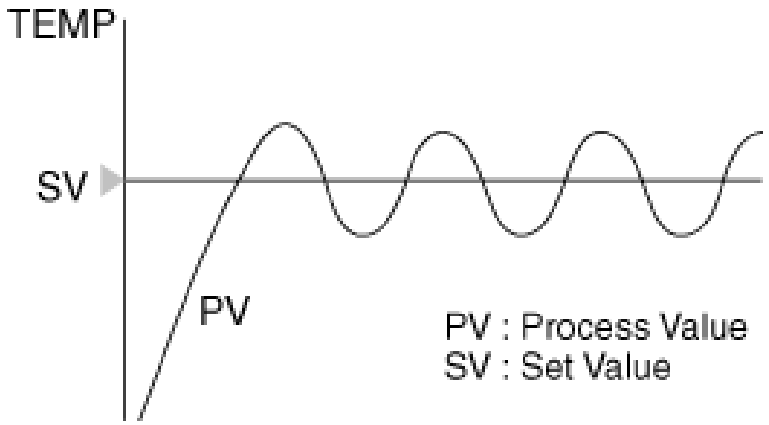

Figure 24: Showing temperature dynamics under on-off control.

For heating and cooling, equations (47) and (48) represent basic philosophy behind on-off control.

For heating

$$PV < SV - \frac{Deadbanb}{2} - HTS \tag{47}$$

Similarly, for cooling,

$$PV > SV + \frac{Deadbanb}{2} + CTS \tag{48}$$

Figure 25 shows various components in detail. Generally dead band are given to avoid frequently on-off cycles which are detrimental to the life of mechanical

components. HTS and CTS are two temperature settings for heating and cooling respectively. Further, SV (set value) has been defined in equation (48)

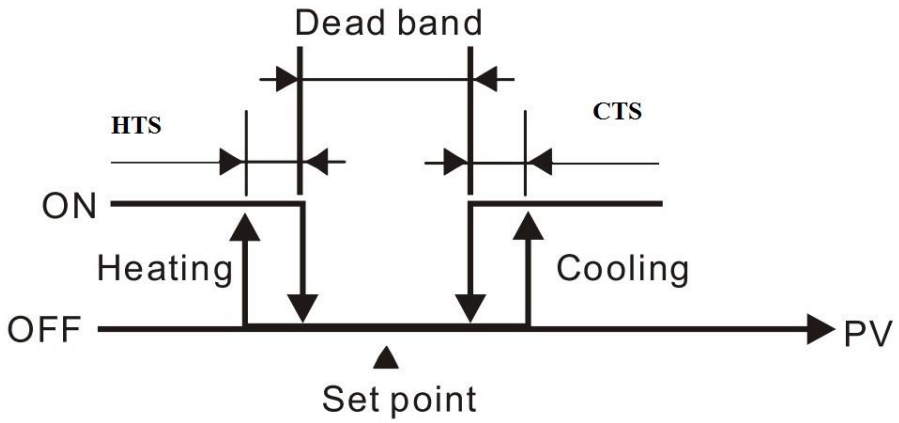

Figure 25: Pictorial representation of an on-off control strategy.

The Dead Band is the range around the PV in which the heating / cooling outputs remain off. Here dead band can be defined as

$$SV = \pm \frac{Deadband}{2} \tag{3}$$

Present work is going to focus on the development of a controller which can, handle model variations, deal with constraints on both inputs and outputs, take into account weather forecast information, handle multiple objectives, optimize energy consumption and suitable for on-line usage.

Model Predictive Controller has been selected for the residential HVAC control. It deals with problems especially in process industry. Effort has been made through the proposed work to bring this technology down from process industry to residential energy systems. Model Predictive Control (MPC) is a set of algorithms based on the models. It is known in the industry for its capability to handle systems and processes with not so

perfect models. Prediction model is the starting point for MPC. Generally, a prediction model can be defined as a model which can produce future outputs based on collected information of the past and anticipated future inputs. For example, a set of differential equations, state space equation and transfer function can be prediction models. MPC does not have a strict requirement on the model structure, which is different from the traditional control techniques and therefore MPC can handle any format of model. It is a general practice that the most convenient modeling methods are selected based on the information available to develop MPC.

Model Predictive control approach: - This technique can handle several constraints over inputs and outputs both. It is formulated as QP (quadratic Programming) problems. As far as minimization of performance function J alone is concerned, it's similar to LQG/LQR problem. A typical formulation for MPC has been given below.

General formulation,

$$min.J = \sum_{k=0}^{N}(r_k - y_k)^T Q(r_k - y_k) + u_k^T R u_k + \Delta u_k^T S \Delta u_k \quad (50)$$

$$y_{min} \leq y_k \leq y_{max} \quad (51)$$

$$u_{min} \leq u_k \leq u_{max} \quad (52)$$

$$\Delta u_{min} \leq \Delta u_k \leq \Delta u_{max} \quad (53)$$

Where, r= *reference input,*

u=input, y=output, Δu*= change in u.*

Q, R, S are weights

However, there are other parallel developments too. In [82], authors have explored to make a control law for a discrete time invariant system which minimizes performance function for finite horizon (Model Predictive Control) and infinite horizon

(Linear Quadratic Regulator). Although, it needs continuous effort in the future too. In the same vein, [83] summarizes various multi-objective optimization and search methods.

4.2 Model Predictive Control

4.2.1 Introduction

Model predictive control (MPC) is a process control technology that is being increasingly popular and being put in practice across several industries [84], [85], [86]. During late seventies, the concept was initiated at Shell Oil. As of date it is the most applied advanced control technique, around 67% in the process industries i.e. 4600 installations worldwide. There are several expert players in this technology, Aspen Technology, Honeywell, Invensys, ABB, Adersa etc.

Over the last decades Model Predictive Control (MPC) has evolved an extremely important tool in industry to solve complex dynamic problems [87]. MPC popularity can be attributed to its easy way of integrating constraints, handling multiple process variables, and dealing with uncertainties. As of now MPC has been present in process industry but recently, it is gaining momentum and has also started to be used in traffic control [88]. MPC has been demonstrated to control different traffic measures at the same time: ramp metering and variable speed limits, route guidance and ramp metering, and ramp metering and main-stream metering. MPC can also be used in implementation of controlling mixed urban and freeway traffic, where the objective is to make traffic in urban areas and on freeways smoothly interact with each other in such a way that total time spent in the network is minimized.

As discussed before, MPC uses a model of the system to be controlled, a performance function to characterize the desired behavior, constrains to limit the

variables of the system. MPC calculates required actions over a finite horizon that which will take the system to the desired state. MPC uses receding horizon optimization which is different from other widely used controller. The concept behind receding horizon optimization will be discussed in the following section. It takes into account the model-plant mismatch, time-varying behavior and disturbances. Therefore, it is always based on real scenarios, and the control moves are optimal. For a real complicated industrial process, the uncertainties incurred by model-plant mismatch, time-varying behavior and disturbances are unavoidable and, hence, the receding finite-horizon optimization can be more powerful than the global one-time optimization.

4.2.2 Formulation

Before going further deep in understanding MPC technology and implementation of it, few terminologies need be addressed first. Some of the important terms are explained below. These terms are shown in Figure 27.

Rolling or Receding horizon: - The problem of robustness is due to the fact that models are inherently inaccurate. A model is always an approximation of the system under consideration. Predictions about the behavior of the system become more and more inaccurate when considered further in the future. MPC techniques use a rolling horizon to increase robustness. The rolling horizon principle consists of synchronizing the state of the model with the state of the true system at every decision step. At every decision step the MPC agent observes the state of the true system updates its model of the system and tries to find the best sequence of actions given the updated model. Typically the agent only executes the first action of this sequence. It then observes the system's state again

and finds a new sequence of actions. Thus, the rolling horizon principle implements as a sequence of optimization problems for each decision step.

Finite Horizon: - Concept of Finite horizon opposed to global or infinite horizon is used for optimization of performance function. Longer the horizon better is the result. This is much faster in response and cheap in computational cost compared to infinite horizon. Although judicious decision on selection of size of horizon is necessary because performance function optimization is tied up with this timeframe.

Prediction horizon: - This refers to the timeframe which is used up for prediction model to produce future outputs. These outputs are taken as basis by MPC to plan for actions ahead of time.

Control horizon: - Having known the desired outputs control actions are calculated inside a certain time interval by optimizing the performance function. Control horizon has to be smaller than prediction horizon,

Soft constraints: - The constraints which are applied on outputs are called soft constraints. These constraints are relatively easy to handle compared to the constraints on inputs. Equation (50) is the example for soft constraints.

Hard constraints: - These constraints are applied on inputs and relatively difficult to deal with. Equation (51) is the example for hard constraints.

Apart from above mentioned parameters, there are other important factors too such as weights for input variables, output variables and rates. These weights are decided depending upon preferences of each variables and sensitivities associated with that to design MPC.

Laying out foundation for MPC, working principle and implementation process will be discussed briefly. MPC interacts with a dynamic system at every discrete time instant. Action is decided to force on the system after estimating state of the system on each time interval. The agent decides which action is selected based on a policy. The policy indicates what action the agent will make in each state. The goal of the control agent is to find a policy that maps states to actions in such a way that the system behaves in the best way possible. In order for the agent to evaluate how well the system is behaving, there typically is some kind of performance function. This function indicates how well it is to make a certain state-action-state transition. The agent has to find a policy that chooses actions in states in such a way that the overall performance is maximized.

MPC [89], [90], [91], [92] uses a model of the system and information of the desired behavior to determine required actions to take. The system model is used as a predictions model to understand the behavior of the system under various actions. The algorithm tries to find a sequence of actions that bring the system to a desired state. It finds out sequence of actions that which don not violate any constraints. Looking further ahead helps in understanding if there are possible constraint violations. In summary, the task is to determine a sequence of actions based on predictions using the system model that optimizes the performance of the system in terms of the desired behavior model, while preventing violation of system and action constraints.

MPC takes finite horizon by using a control horizon, a prediction horizon, and a performance function. The control horizon helps in finding appropriate actions. Prediction horizon predicts the autonomous behavior of the system. The performance function is related to the performance that MPC will obtain from the state at the end of

the prediction horizon. Typically both horizons are much shorter than infinity, while the prediction horizon is larger than the control horizon. This is the case since in particular when considering systems that have autonomous behavior, actions are used to steer the system in a certain direction after which it can autonomously evolve further. By considering a prediction horizon that is larger than the control horizon, the agent can analyze where the system ends up after the agent has executed its actions over the control horizon [93], [94], [95].

Figure 26 is the block diagram representation of MPC. In the figure, MPC and Plant have been shown with their respective inputs and outputs.

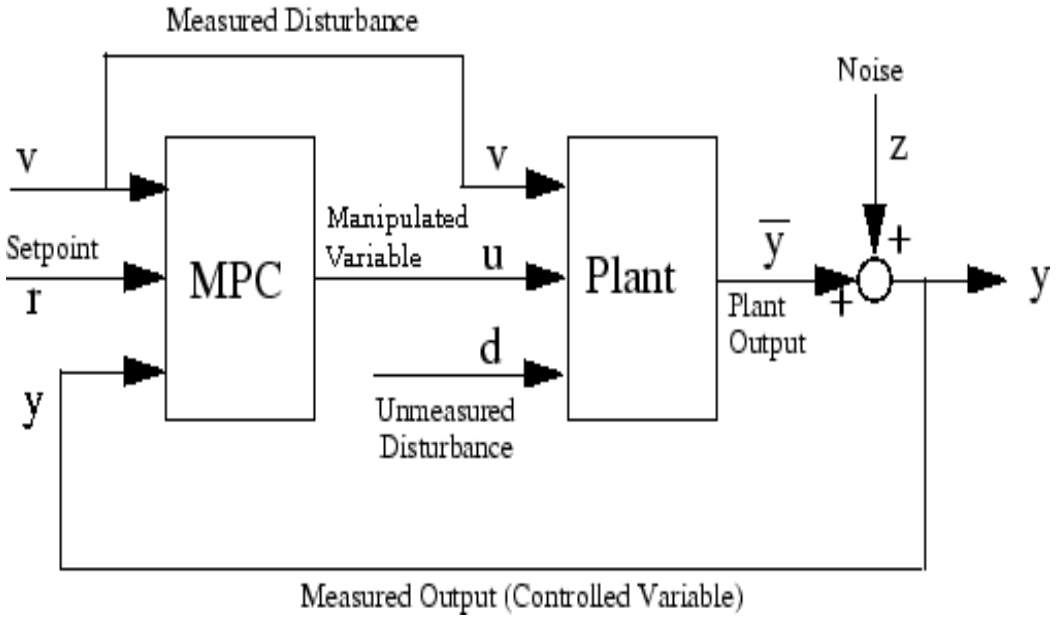

Figure 26: Block diagram representation of a typical MPC system.

There are three different kinds of inputs in general, i.e. Measured disturbance, Manipulated variable and Unmeasured disturbances. Each one of them has been described in brief.

Measured disturbance: - It is a measured quantity which affects the plant in consideration. It cannot be changed just measured. For example in thermal modeling of house, ambient temperatures, solar radiations are measured disturbances.

Manipulated variable: - It is a measured quantity which can be manipulated as per the plan or necessity. It is the control input and designing controller directly addresses deciding the manipulated variable.

Unmeasured disturbances: - It is non-measurable random quantity. Because of the randomness, it introduces plant and model mismatch and to counter this model should be robust enough.

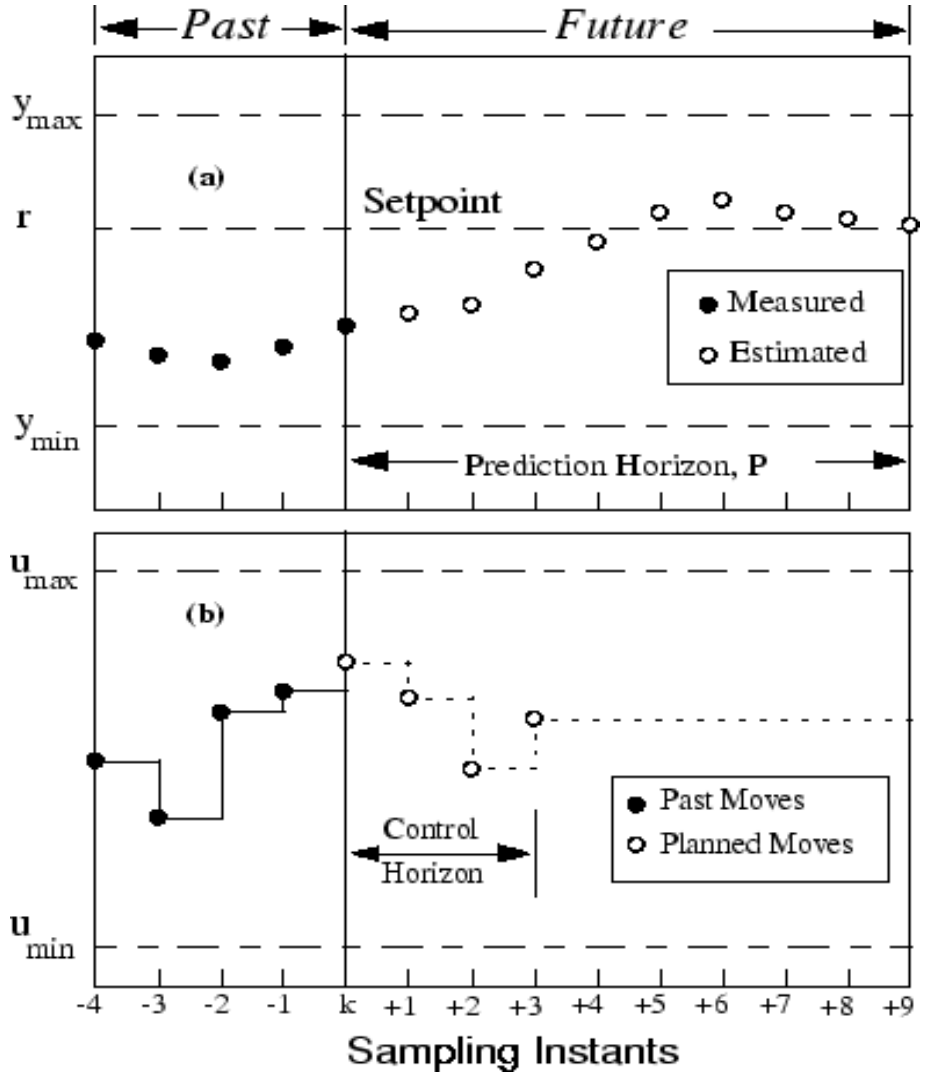

Figure 27: Description of MPC strategy.

In Figure 26, measured disturbance, manipulated variable and unmeasured disturbance is represented by v, u and d respectively. r is reference or set-point, y is output and z is the noise. MPC and the plant have been shown in closed-loop where y is fed back to the MPC block. MPC produces a manipulated variable to control the plant.

Figure 27 is the detailed representation of MPC strategy. It is extremely important to understand the figure. u_{max} , u_{min}, y_{max} and y_{min} are the limits or constraints on inputs and outputs. At any instant k, prediction and control horizons are

defined. As mentioned before too, Prediction horizon is always greater than Control horizon. Based on the prediction model and model variable measurements future moves are estimated. Interestingly, just one of the future inputs is applied and rest is discarded and MPC moves to the next instant, i.e. k+1.

Continuing with the MPC, there are enough credible works available which suggest its immense capability. The detailed methodologies have been discussed in [96], [97]. In [98] foundation of functional, parametric optimization has been addressed in detail. This could be one starting point to understand the concept behind MPC. Industrial processes of multivariable with constraints are controlled through digital process control [99]. Further, stability and robustness of MPC methods and constraints handling have been discussed in [100], [102], [103]. It has been observed so far that MPC outperforms traditional controllers because of its inherent features. Further, MPC has been compared with PID controller. [104] has shown MPC performance is better than PID. Also, a robustness characteristic, i.e. noise affecting output of MPC is better than PID [105].

4.2.3 Implementation of MPC in Residential HVAC systems.

In the previous section, model predictive control has been presented in detail and its capability discussed with few examples. One of the objectives of the proposed work has been to bring this technology from process control to residential energy systems. This is preferred from other competing controllers for obvious reasons that it is fully capable to optimize multi-objectives and constraints. It does not fully rely on the model provided for the system to be controlled rather on continuous measurements to do course of action at each sampling time. It can be implemented on an approximate model, should not be

100% perfect. Therefore time spent in building up models is less. There are few successful applications of MPC in energy system also. [106] presents an interesting work where MPC is used to control a solar refrigeration plant. The goals are different at various operating point which makes the problem as multi-objective optimization problem. A preliminary study of cooling of a building by water chiller plants using thermal energy storage has been done in University of Cal. Merced campus [107]. It was a joint research and other members are Univ. of Cal. Berkley, and UTRC. A MPC for the chillers operation is designed in order to optimally store the thermal energy in the tank by using predictive knowledge of building loads and weather conditions. There is another contribution in MPC domain called economic MPC. In it economic MPC is minimized opposed to general MPC where weighted least square objective is minimized. Economic MPC operates on power generators and consumers such that cost of power production is minimized [108]. Going through numerous examples and discussions, the confidence in MPC is vindicated.

Therefore, Model predictive controller has been proposed for the energy control of residential houses. This is going to utilize the online weather forecast [109] info to plan actions ahead of time to minimize energy consumption, and better control the comfort level in the house.

Proposed thermal model of a residential house described by discretized state space equation (53) and (54). This is the fourth order linear time invariant system. This is a control oriented model. The model has been identified and presented already in chapter-3.

$$\underline{x}_{k+1} = \underline{\underline{A}}(\theta)\underline{x}_k + \underline{\underline{B}}(\theta)\left[\dot{Q}_k \; T_{o,k} \; S_k\right] + \underline{\underline{K}}(\theta)\underline{e}_k \tag{54}$$

$$T_{z,k} = \underline{\underline{C}}(\theta)\underline{x}_k + \underline{e}_k \tag{55}$$

Here, $T_{z,k}$, $T_{o,k}$ and S_k are zone temperature, ambient temperature and solar irradiation at any instant k. $\dot{Q}_k$ is the cooling capacity.

To develop model predictive control, Matlab toolbox "mpctool" was used [110]. The identified control oriented plant model was imported through mpctool GUI. MPC has been defined with three inputs i.e. ambient temperature, T_o and solar irradiance, S as measured disturbances and $\dot{Q}$ as manipulated variable. Zone temperature T_z is output. Here are the values of several factors needed for MPC formulation,

Prediction horizon = 4 hrs. ,

Control Interval = 1 min,

Control Horizon = 15 min,

Simulation run time = 24 hrs.

Max cooling capacity, $\dot{Q} = 3500$ kW,

Reference temperature, $T_{Ref} = 77°$ F

Zone Temperature, $T_z = \begin{Bmatrix} \leq & 78 \\ \geq & 76 \end{Bmatrix}$

Figure 28 represents simulation of residential house with MPC. The experiment has been developed in Simulink with feedback Controller and plant imported from Matlab.

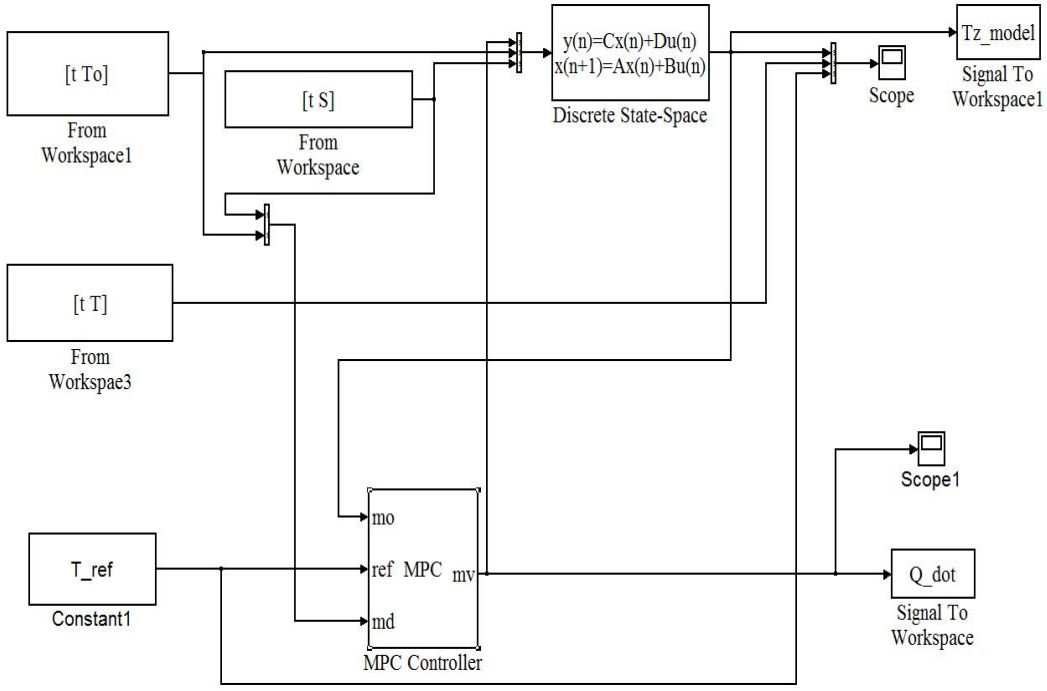

Figure 28: Simulink model for model predictive controller in a residential house.

The plant model which represents the house has discrete state space representation. In symbolic terms “mo”, “ref”, “md” and “mv” stand for measured output, reference, measured disturbance and manipulated variable respectively. In the simulation, manipulated variable generated by MPC is fed to the plant to generate the desired zone temperature. In the simulation, “T” is the zone temperature recorded while when on-off system was operational. The simulation is run for 24 hrs. The primary purpose of this simulation is show that same zone temperature can be created with the less amount of thermal energy. Energy saving is the key of this work. There are other equally important motives are to explore smaller thermal unit size, smooth operation of mechanical components for longer life span and better zonal comfort as there is no on-off cycle. The scheme has been implemented to show the capability of MPC. Energy usage has been compared for the same days when On-Off has been operational.

Figure 29(a)-(b) and Figure 30 (a)-(b) show the MPC against On-Off controller.

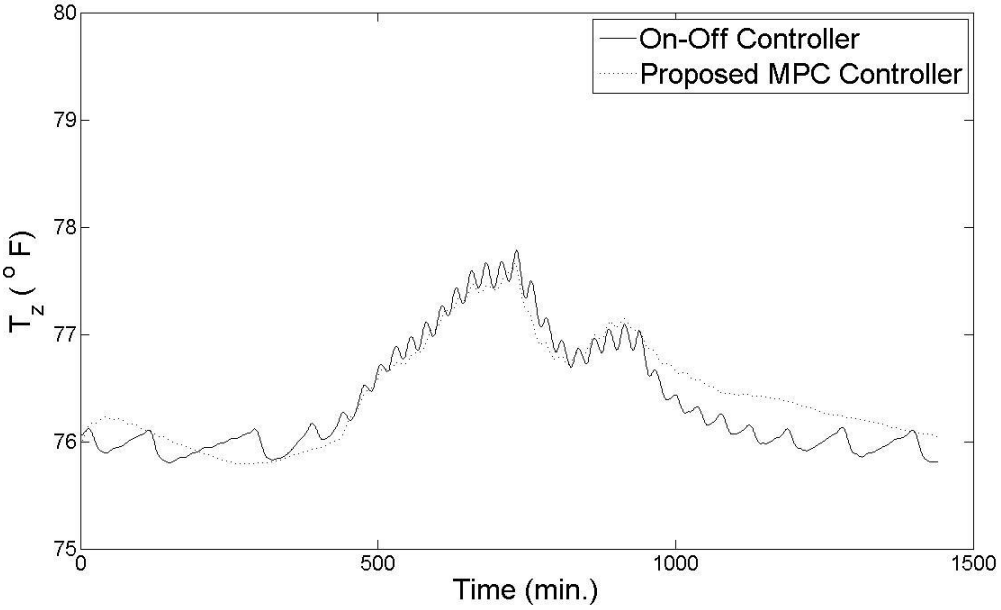

(a)

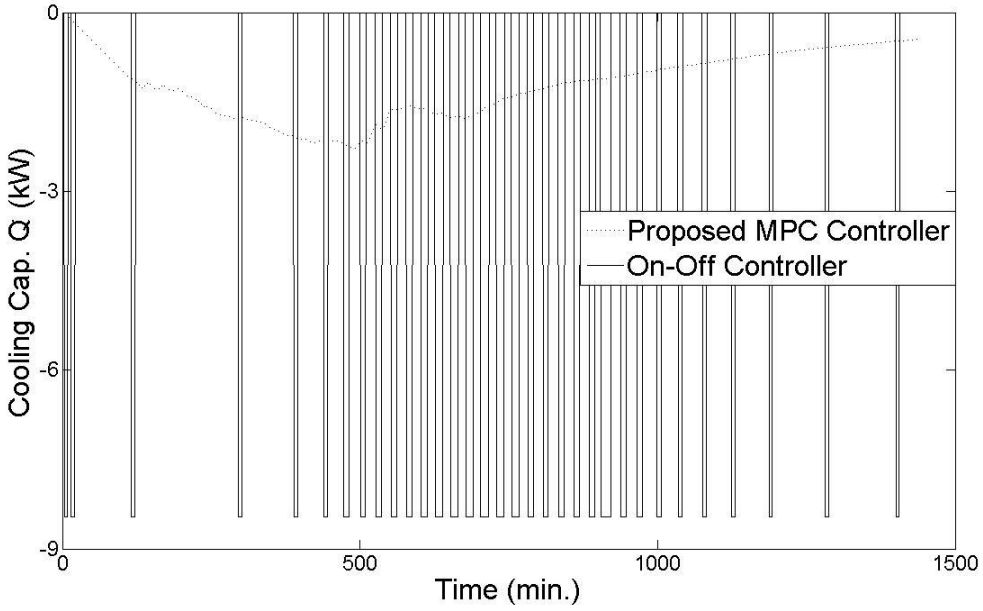

(b)

Figure 29: Day-1-Comparison of On-Off Controller vs. MPC with Prediction Horizon 4 hrs.

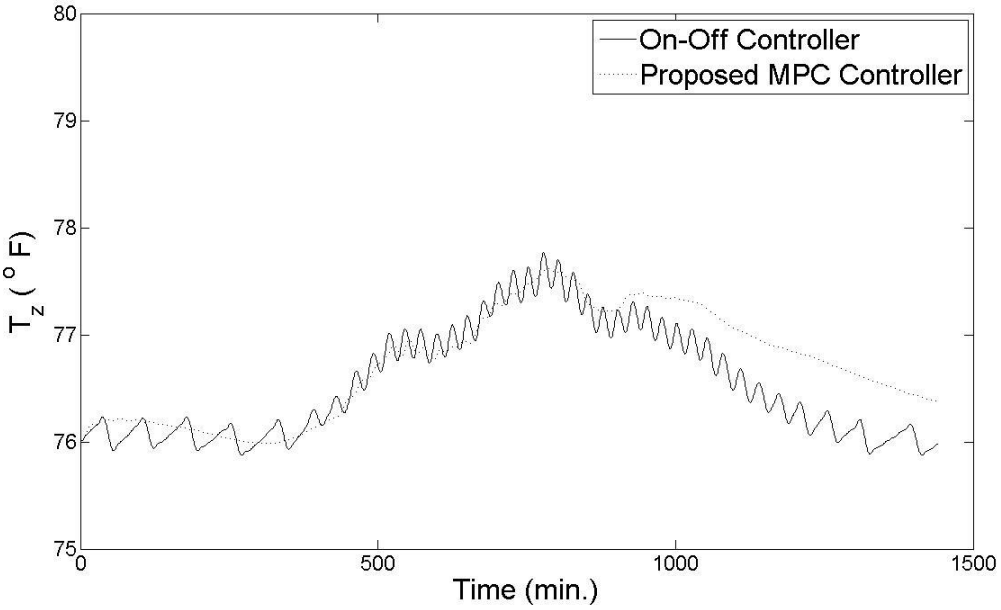

(a)

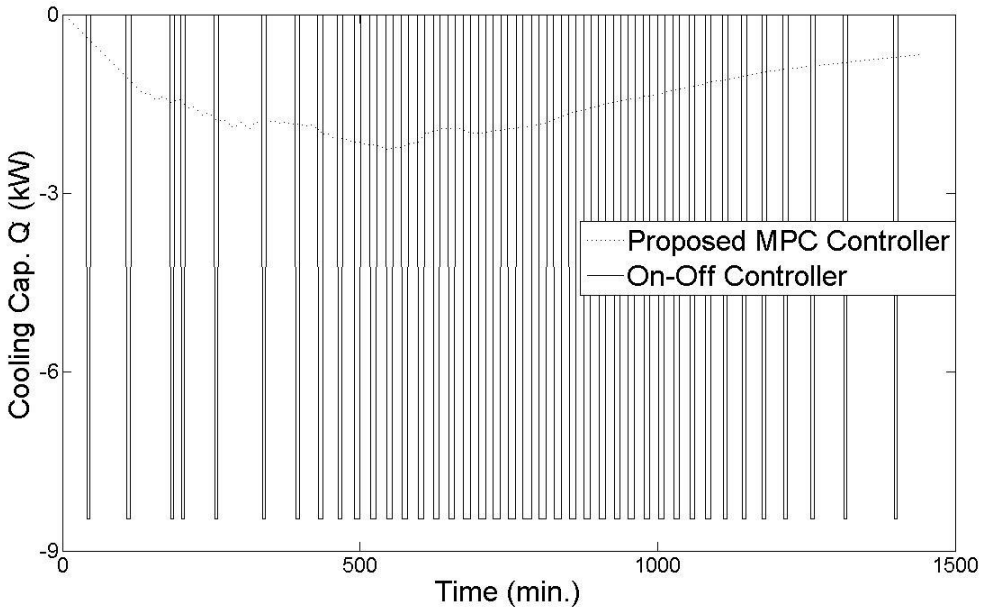

(b)

Figure 30: Day-2 Comparison of On-Off Controller vs. MPC with Prediction Horizon 4 hrs.

Using MPC controller, the system will consume less thermal energy. The following plot shows the zone behavior if the MPC is placed in the same residential house. This is a typical reference tracking problem where measured zone temperature has been taken as a reference trajectory.

Table 2: Performance comparison of On-Off Controller and MPC.

Days	On-Off Controller	MPC Controller	% Improvement
1	-44.27	-29.26	33.91
2	-52.88	-36.72	30.56
3	-54.85	-41.93	23.55
4	-58.37	-40.85	30.01
5	-59.36	-45.44	23.45
6	-66.69	-47.69	28.49
7	-52.88	-34.49	34.77

To dig further in MPC scheme, it can explore that forecast info plays an important role in the formulation and energy savings. Above plots have been generated on the basis of 4 hours of forecast information. Exactly same study is being done to understand the significance of forecast information on the MPC controller performance. Following plots have been generated based on 2 hours of forecast information.

This time also MPC over performs On-Off controller by 29.91 % but little less compared to previous controller. The reason is attributed to the fact that longer the forecast horizon better is action plan for energy usage, i.e. optimum performance. Also, it can be easily noticed that proposed controller has its peak almost close to peak temperature whereas in the previous plot peak occurs way before the temperature hits its highest measurement.

It is quite noticeable from the shown plots that smaller the forecast horizon, steeper rise will be in the control action to meet the demand.

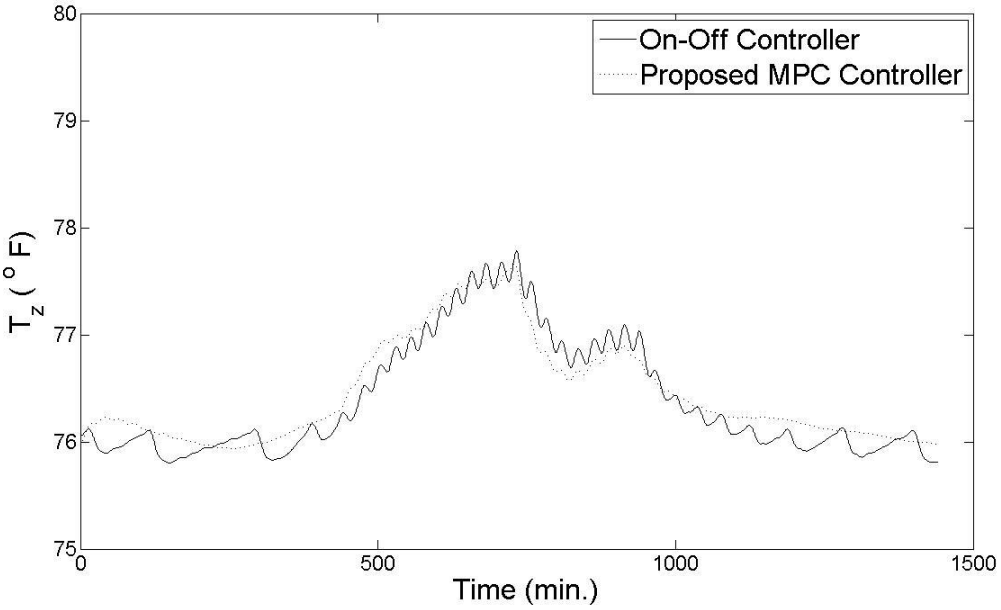

(a)

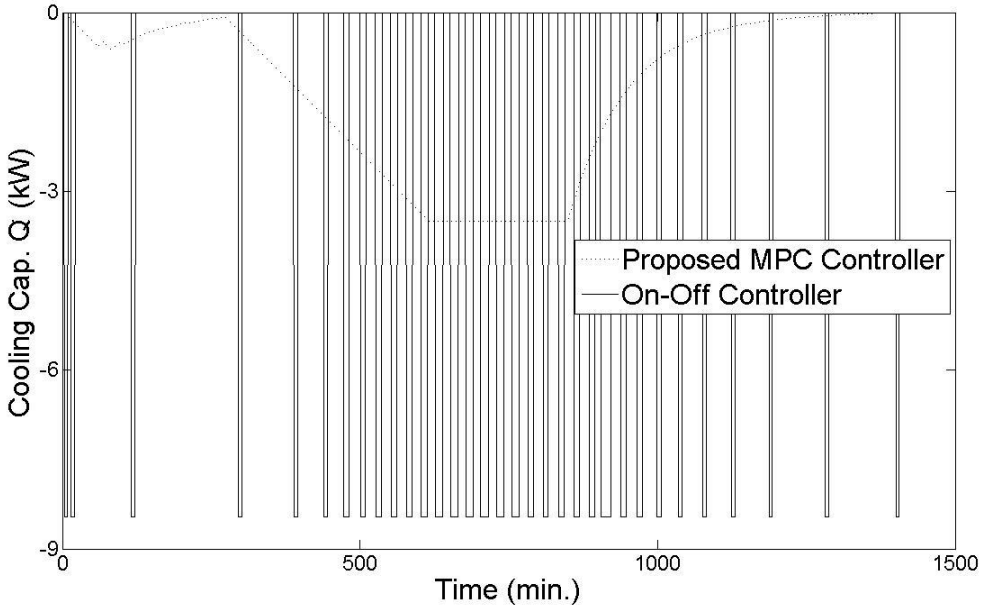

(b)

Figure 31: Comparison of On-Off Controller with MPC taking Prediction horizon as 2 hrs.

CHAPTER 5: DEVELOPMENT OF ENERGY PERFORMANCE MODEL

Energy demand forecasting is an integral part of demand side management. The prior knowledge of future demand helps to understand whether there is shortage of supply, overabundance or need for new unit as a whole. The energy usage model has tremendous applications for utilities and consumers both. On hand it gives a scientific tool to utility to plan strategy for energy distribution and establish a robust relationship between demand and supply.

5.1 Energy Performance- Oriented System Identification

As noted previously, two different models have been formulated, one for control in homes with next-generation HVAC systems and one for Energy Usage forecasting which can be extended to a model for diagnostics in homes with traditional HVAC systems. This section considers the specifics of both formulations, and presents experimental results from a single-zone test home with a three-ton air-vapor-compression air-conditioning unit. The home is located approximately 40 miles west of Charlotte, North Carolina.

The Energy usage forecasting model formulation is represented as shown in Figure 32. The model is provided with measurements of the outdoor temperature (T_o), the internal zone temperature (T_z), the solar irradiance (S). The output is the thermal energy input to the home since the beginning of the day. This quantity is defined as

$$E_{COOL} = \int_0^t \dot{Q}\, d\tau \tag{56}$$

where $\dot{Q}$ is the heating/cooling capacity of the HVAC system. Note that this quantity should be negative during the cooling season. In homes with heat pumps, this value would be positive during the heating season. The above formulation comes down to cumulative sum of heating/cooling capacity when applied to a discrete system. This has been tested for a discrete system with constant step measured variables.

The discrete system representation of a house for Energy usage will be represented as follows:

$$\underline{x}_{k+1} = \underline{\underline{A}}(\theta)\underline{x}_k + \underline{\underline{B}}(\theta)\left[T_{z,k}\; T_{o,k}\; S_k\right] + \underline{\underline{K}}(\theta)\underline{e}_k \tag{57}$$

$$\underline{E}_{cool,k} = \underline{\underline{C}}(\theta)\underline{x}_k + \underline{e}_k \tag{58}$$

This innovation form representation has already been discussed in detail in chapter 3.

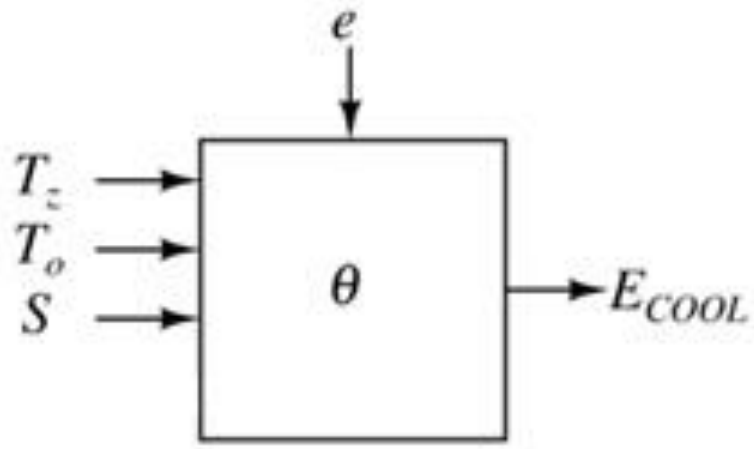

Figure 32: Energy usage-model formulation including random errors e.

This is 4th order state space based model. The block diagram for the above formulation can be represented as in Figure 32.

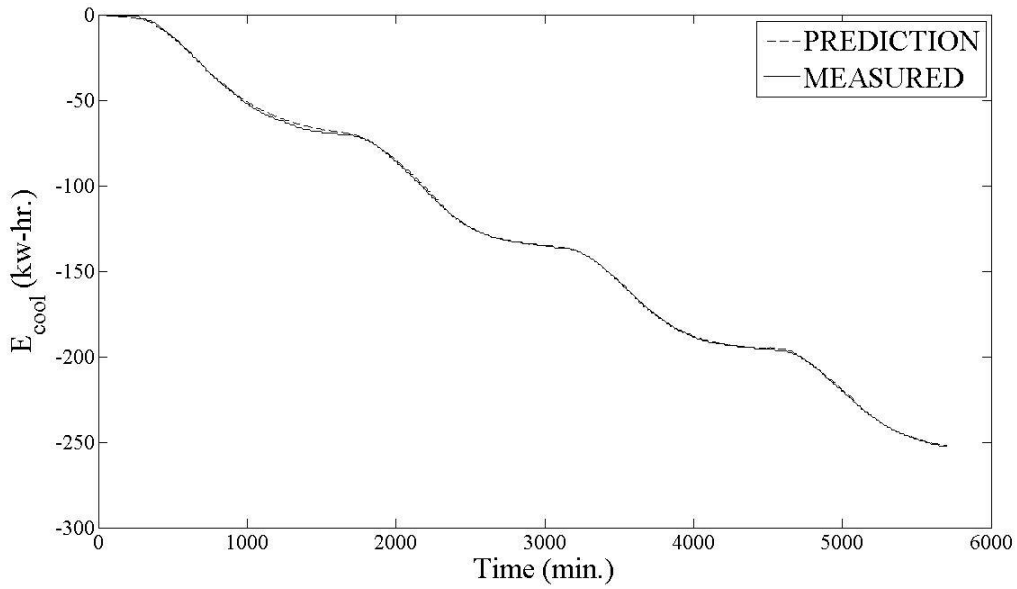

Figure 33: Measured (and Smoothen) and simulated data recorded during the training period.

The measured data have been used for training of the model and represented as shown in Figure 33. This experiment was done during summer and so cooling capacity has been used in model.

Identified model has been put for the validation through consecutive days. To minimize the effect of error propagation and disturbance, simulation is run for each full day independently.

The model clearly tracks all the variations in the thermal energy consumption. It does have tendency to deviate from actual as time progresses. Later in this work, two methods have been proposed to track the energy usage more precisely, i.e. Kalman filter and Prediction Error method based recursive state estimation.

5.2 Energy Performance Model validation

To validate the identified house model ambient temperature, zone temperature, solar irradiance and compressor on-off time are measured. The first three terms are used to find out total thermal energy consumed during entire day and compared to the measured thermal energy using on-off time of compressor. Sampling rate is 1 data/min and therefore 1440 measured values are there in single day.

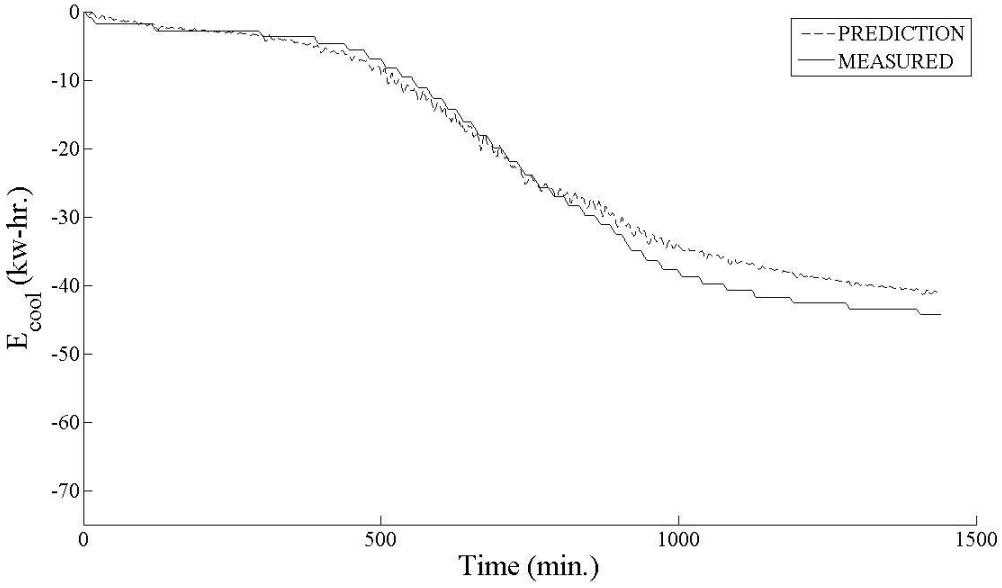

(a)

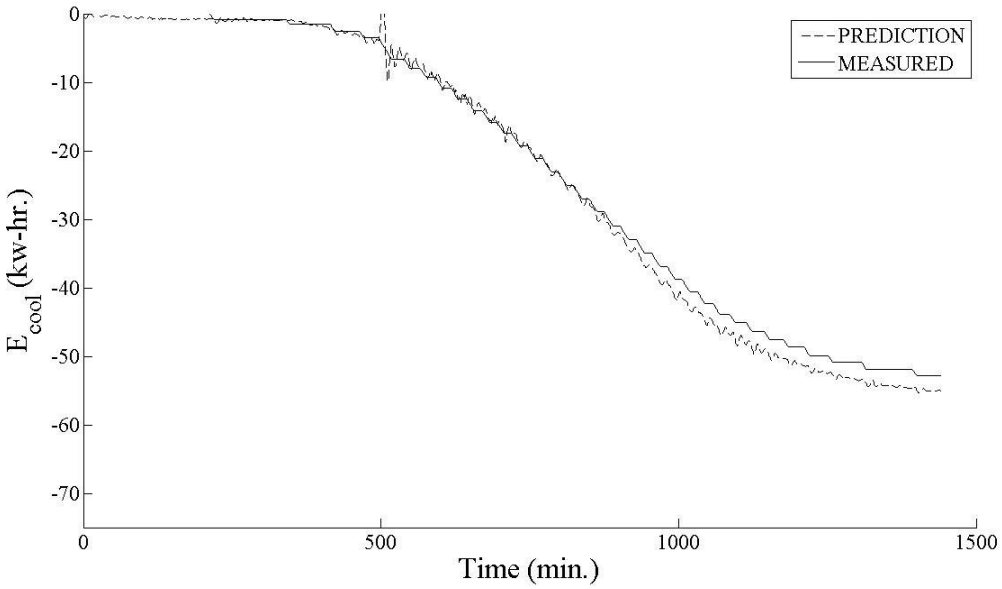
PREDICTION
MEASURED
E_{cool} (kw-hr.)
0
-10
-20
-30
-40
-50
-60
-70
0
500
1000
1500
Time (min.)

(b)

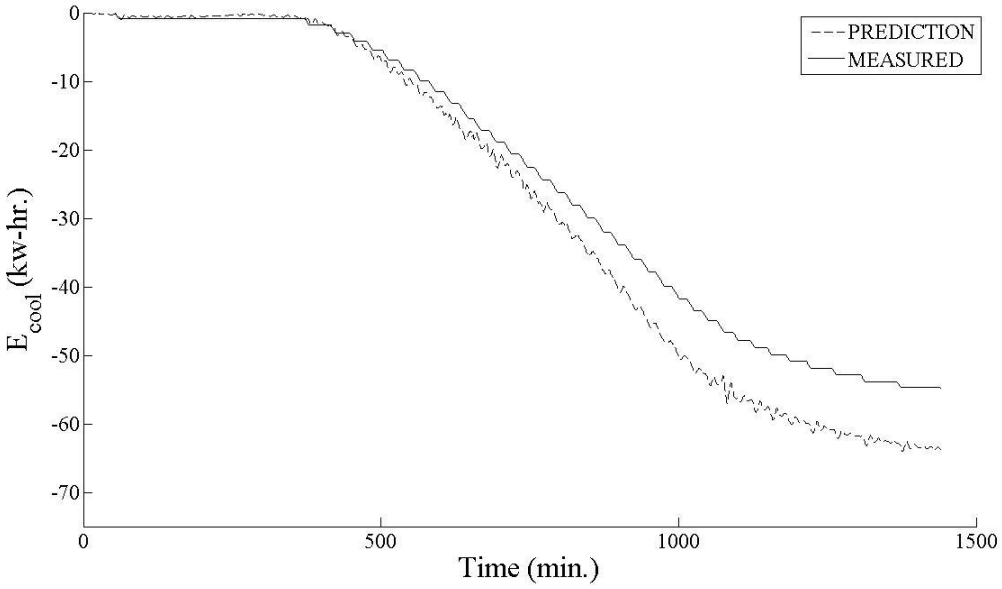
PREDICTION
MEASURED
E_{cool} (kw-hr.)
0
-10
-20
-30
-40
-50
-60
-70
0
500
1000
1500
Time (min.)

(c)

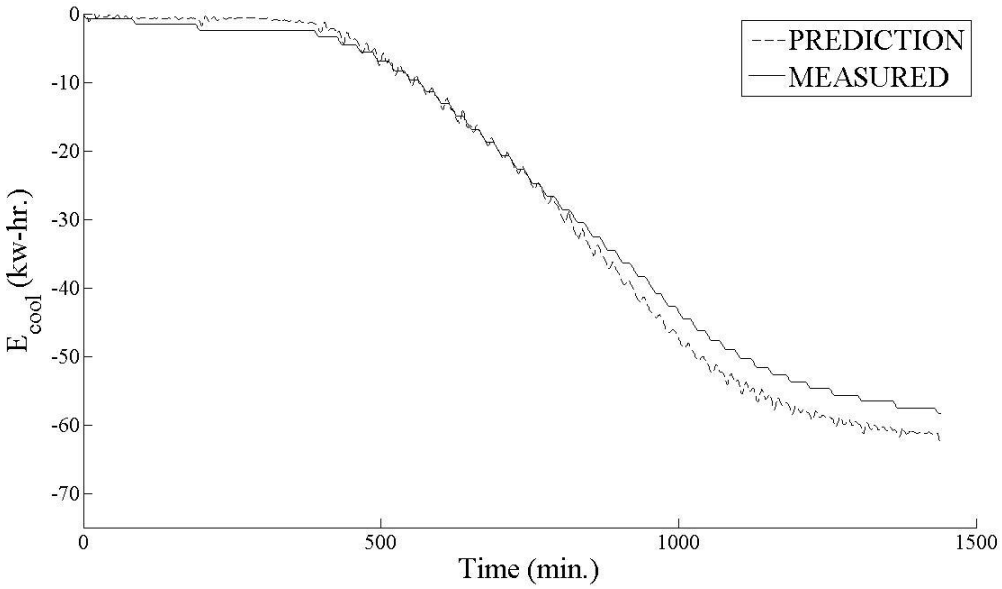
PREDICTION
MEASURED
E_{cool} (kw-hr.)
0
-10
-20
-30
-40
-50
-60
-70
0
500
1000
1500
Time (min.)

(d)

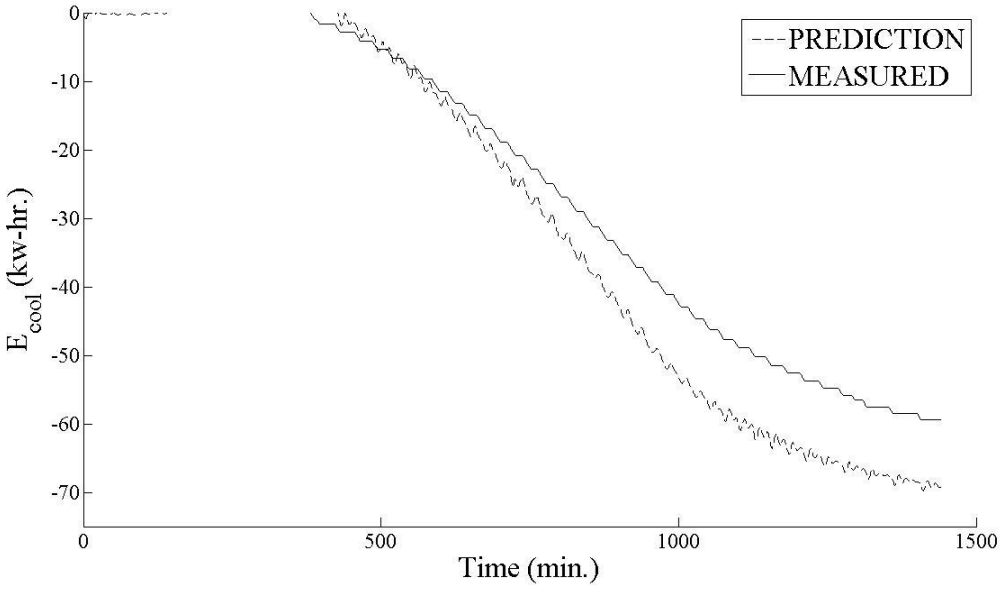
PREDICTION
MEASURED
E_{cool} (kw-hr.)
0
-10
-20
-30
-40
-50
-60
-70
0
500
1000
1500
Time (min.)

(e)

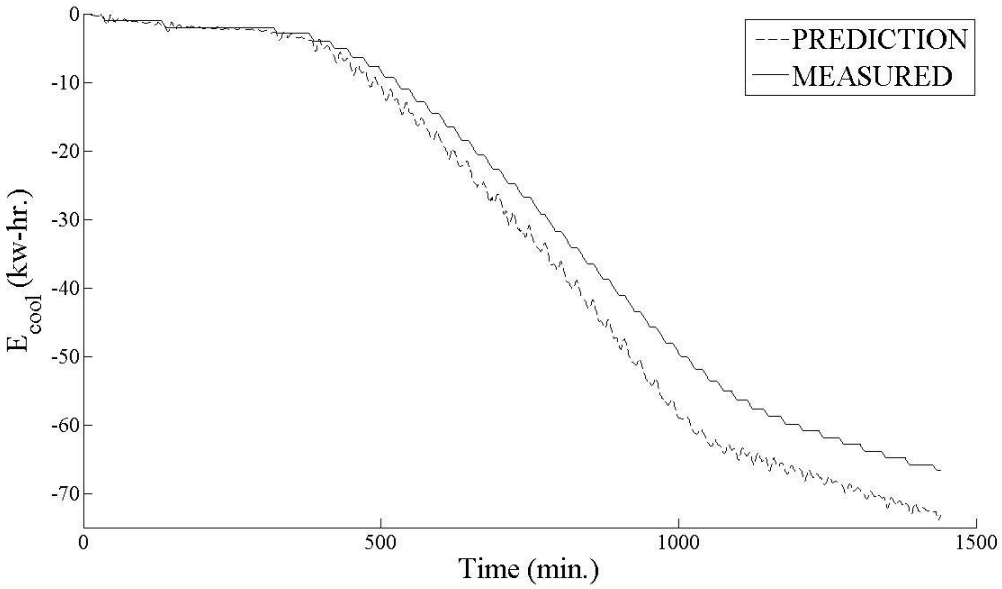

(f)

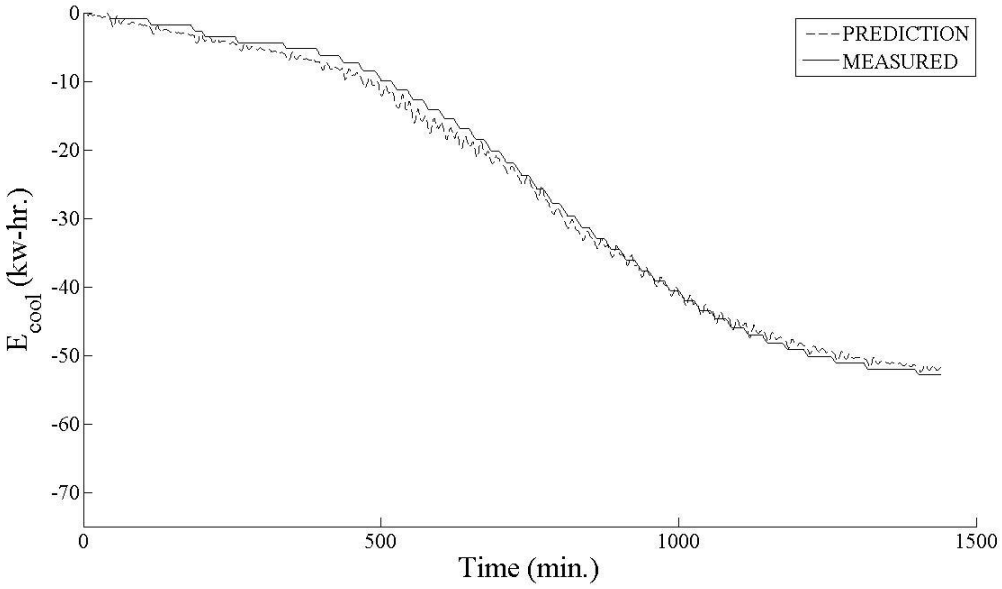

(g)

Figure 34: (a)-(g) show Energy Usage Model Validation.

As discussed above the method recursively estimates states using PEM. 1 hr. of time window has been selected and shown the predicted data compared to measured data. Hourly prediction from recursive PEM

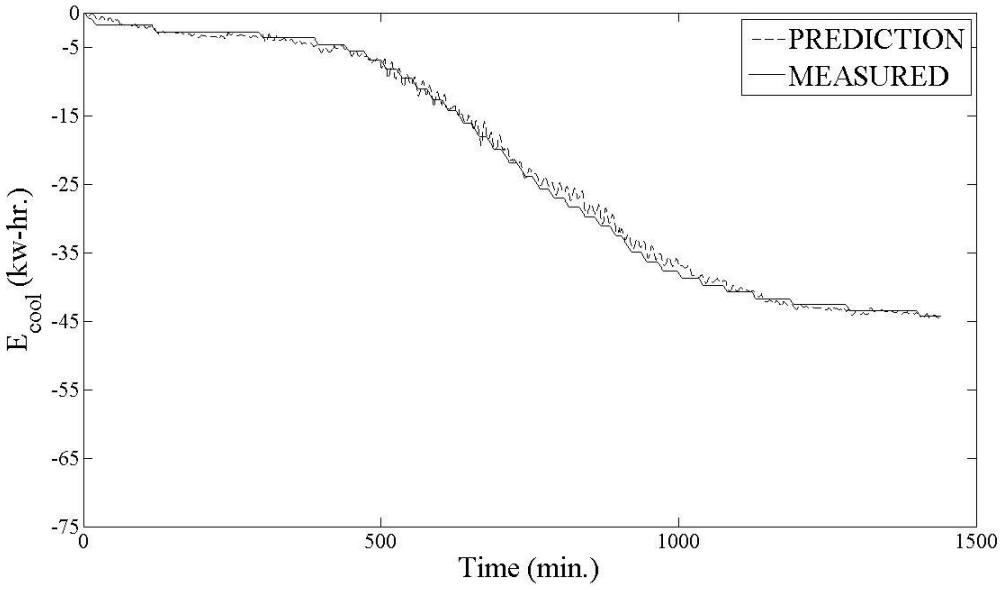

(a)

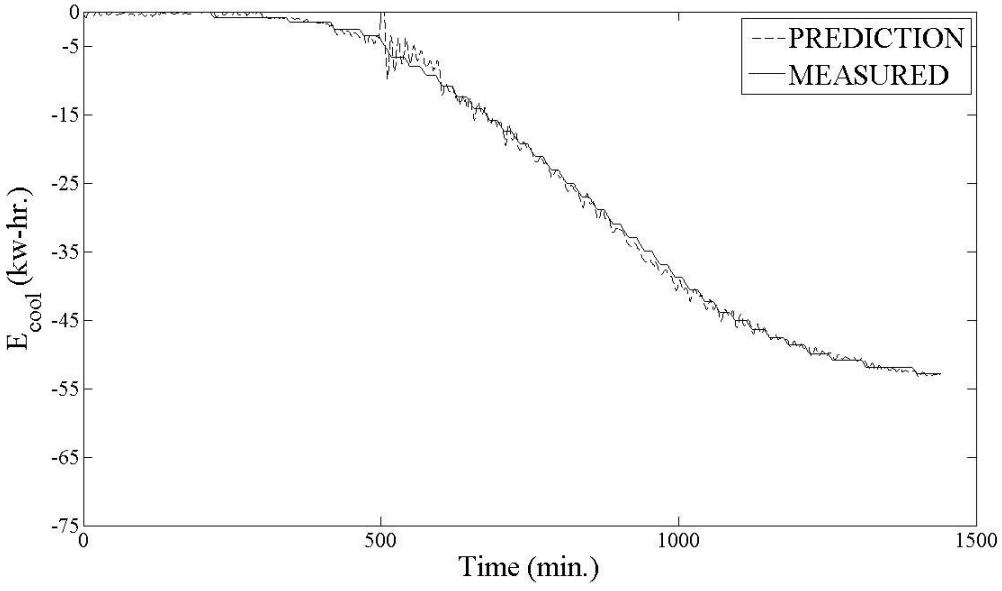

(b)

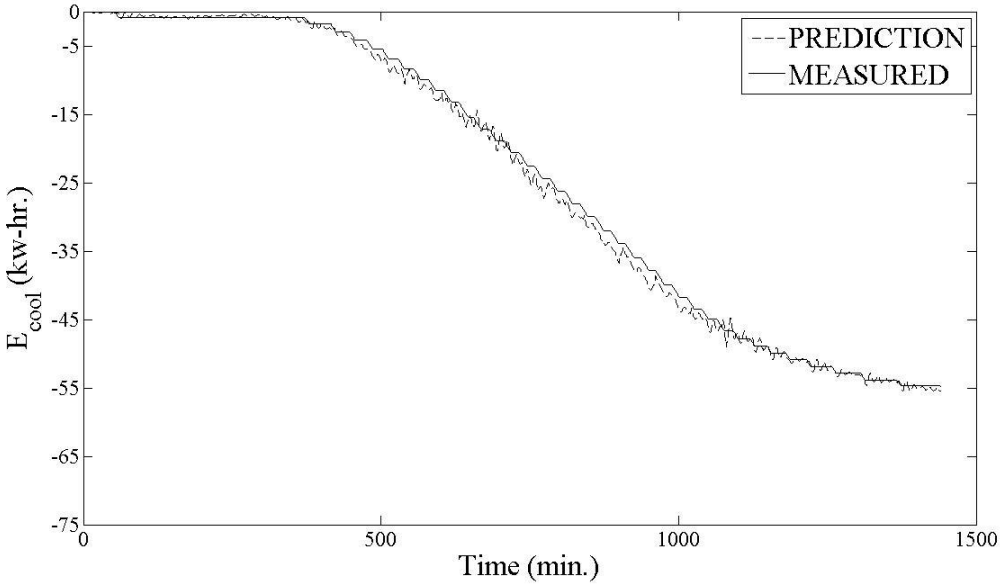
PREDICTION
MEASURED
E_{cool} (kw-hr.)
Time (min.)
0
-5
-15
-25
-35
-45
-55
-65
-75
0
500
1000
1500

(c)

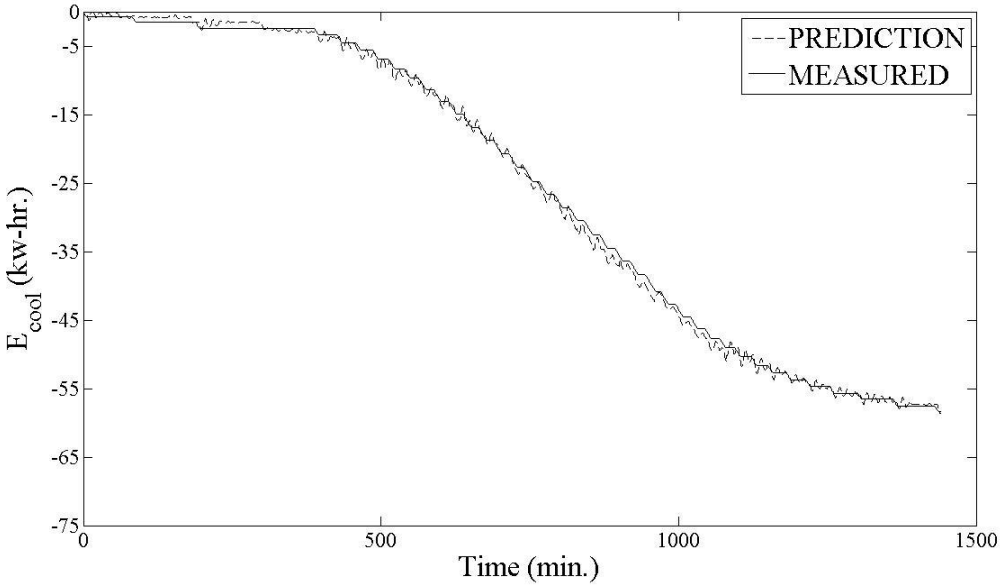
PREDICTION
MEASURED
E_{cool} (kw-hr.)
Time (min.)
0
-5
-15
-25
-35
-45
-55
-65
-75
0
500
1000
1500

(d)

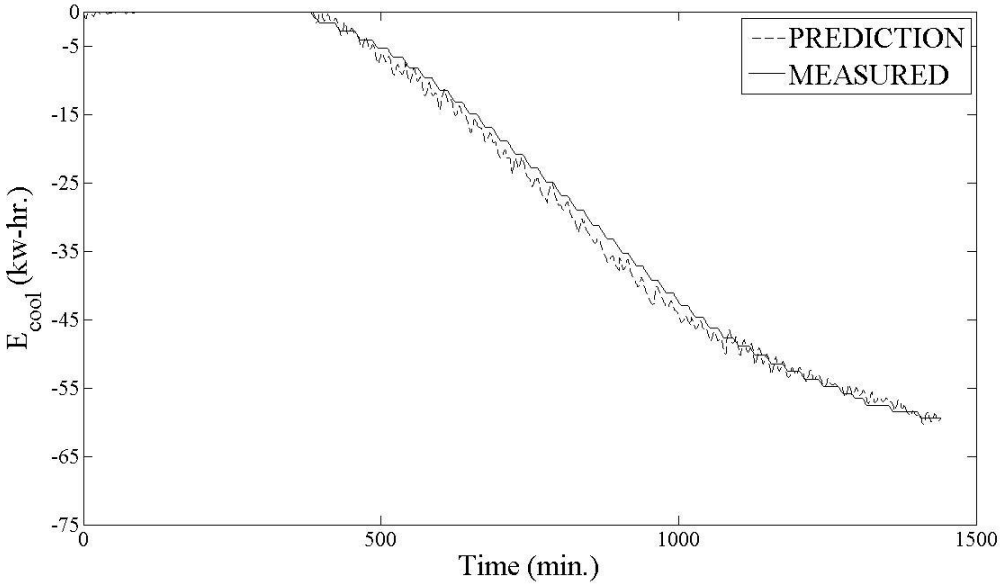
PREDICTION
MEASURED
E_{cool} (kw-hr.)
Time (min.)
0
-5
-15
-25
-35
-45
-55
-65
-75
0
500
1000
1500

(e)

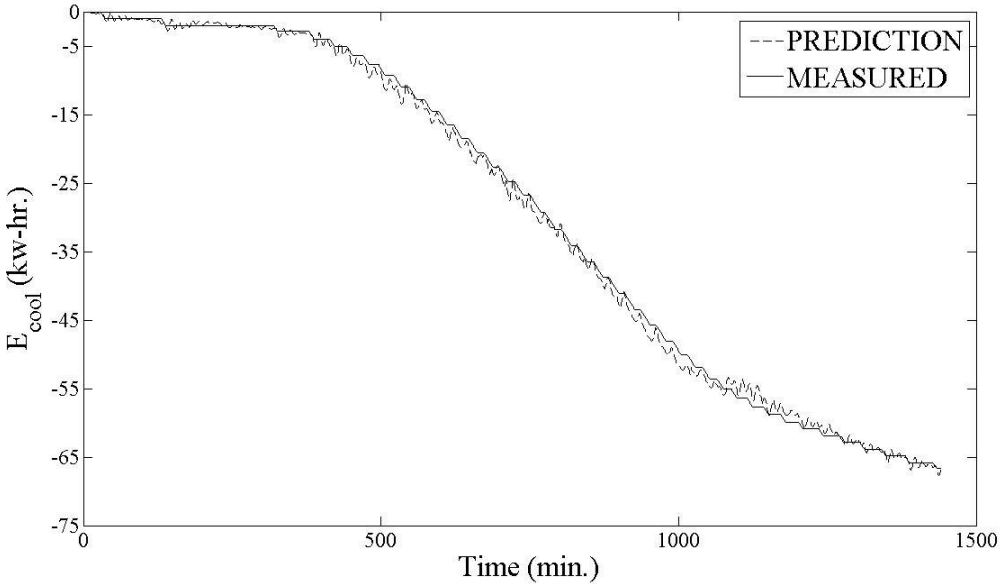
PREDICTION
MEASURED
E_{cool} (kw-hr.)
Time (min.)
0
-5
-15
-25
-35
-45
-55
-65
-75
0
500
1000
1500

(f)

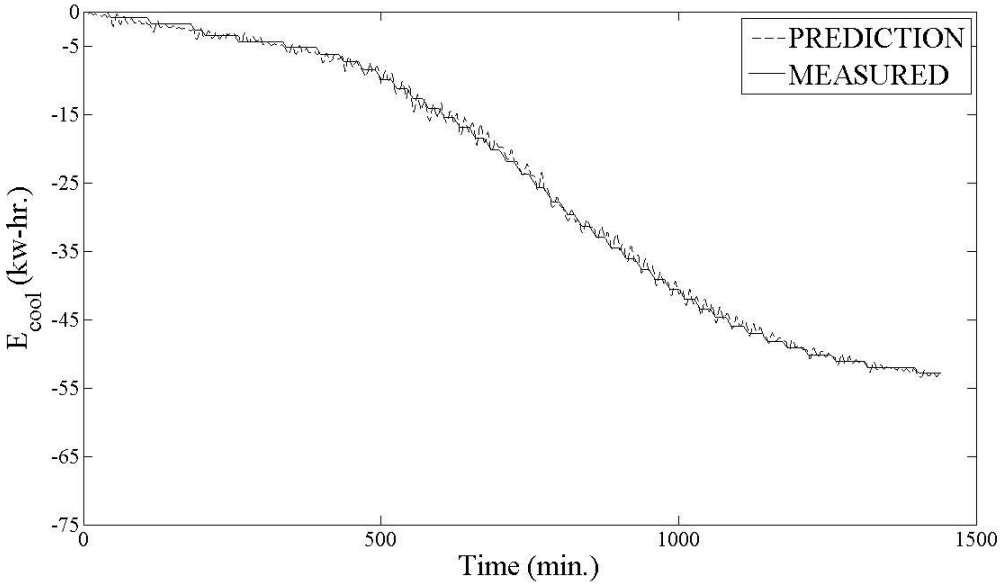

(g)

Figure 35: (a) to (g) Using Prediction based on recursive PEM approach for Energy Usage Model Validation.

Kalman Filter implementation for energy usage prediction.

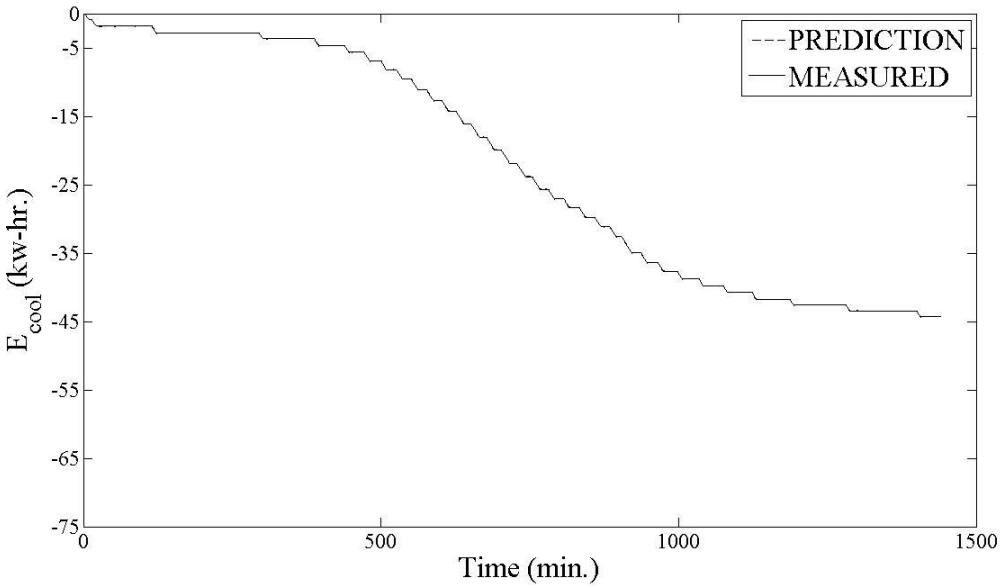

(a)

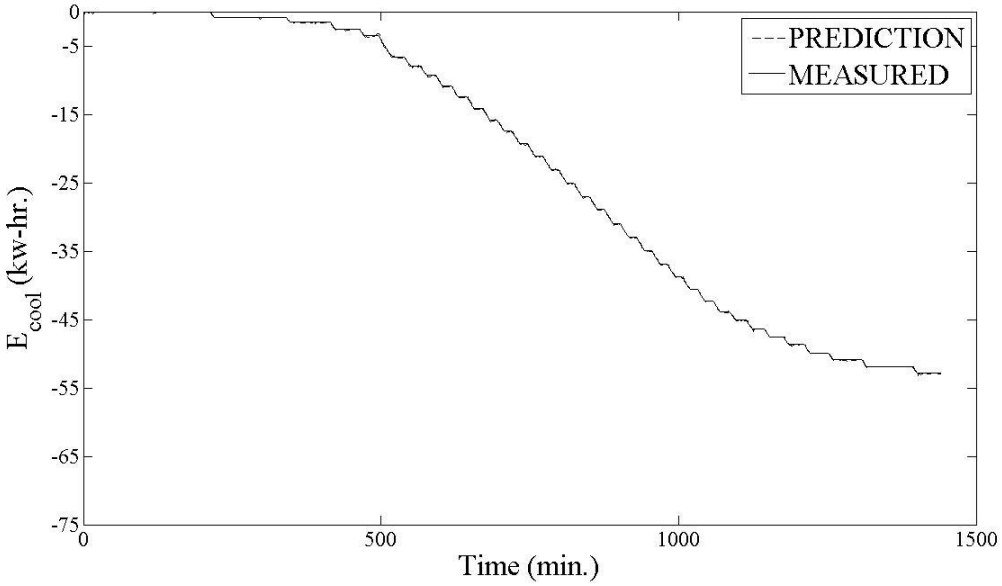
PREDICTION
MEASURED
E_{cool} (kw-hr.)
0
-5
-15
-25
-35
-45
-55
-65
-75
0
500
1000
1500
Time (min.)

(b)

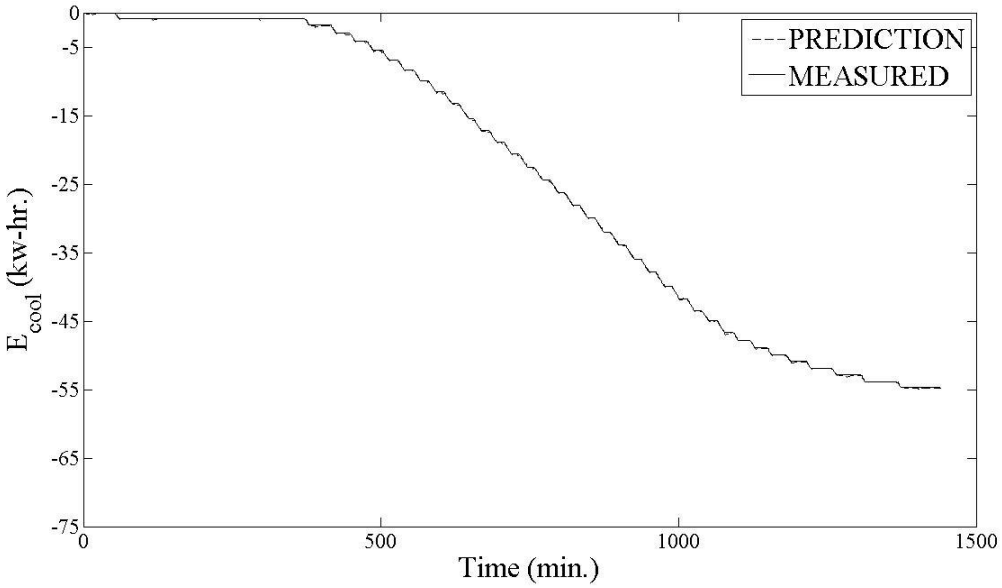
PREDICTION
MEASURED
E_{cool} (kw-hr.)
0
-5
-15
-25
-35
-45
-55
-65
-75
0
500
1000
1500
Time (min.)

(c)

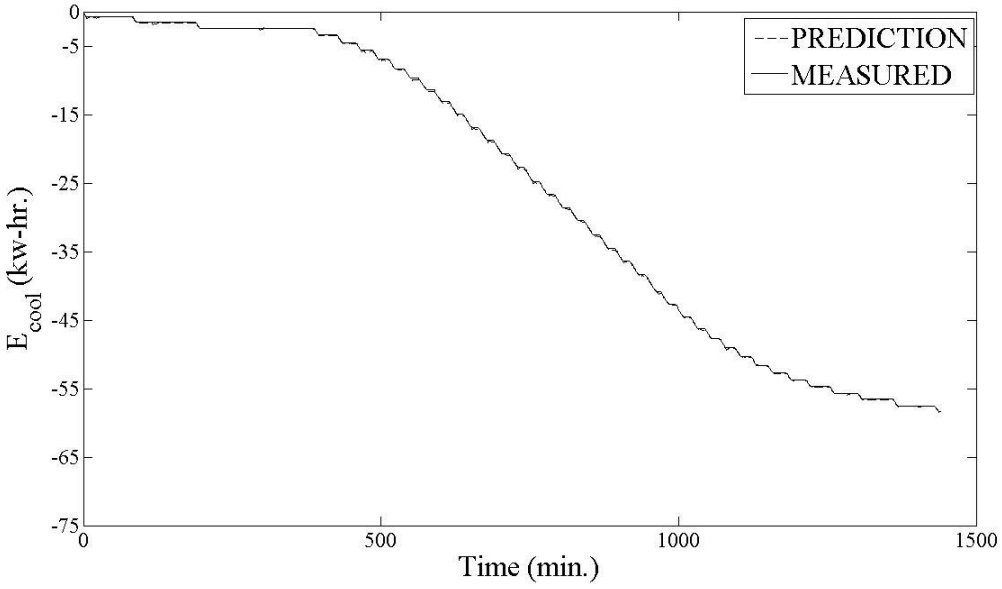
---PREDICTION
—MEASURED
0
-5
-15
-25
-35
-45
-55
-65
-75
E_{cool} (kw-hr.)
0
500
1000
1500
Time (min.)

(d)

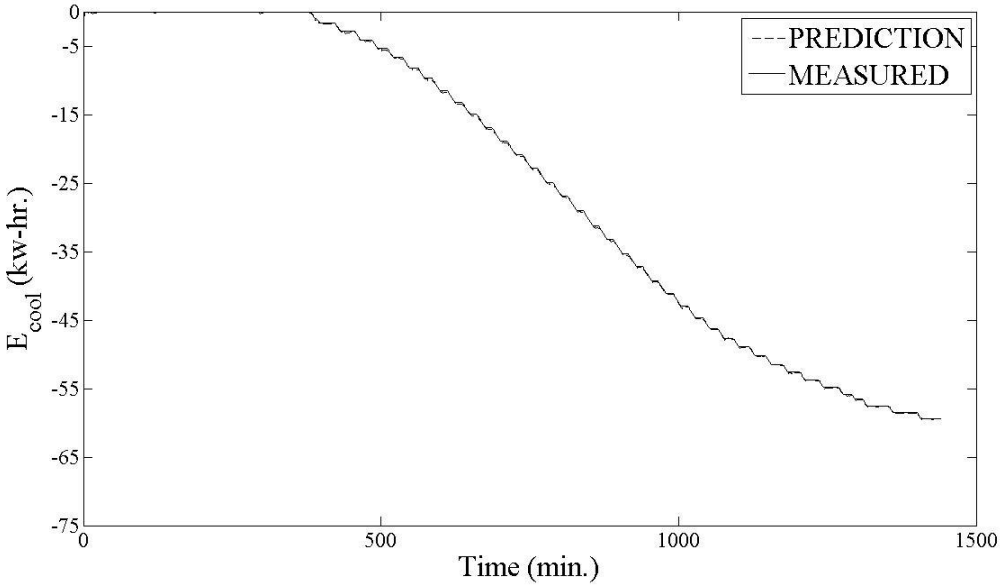
---PREDICTION
—MEASURED
0
-5
-15
-25
-35
-45
-55
-65
-75
E_{cool} (kw-hr.)
0
500
1000
1500
Time (min.)

(e)

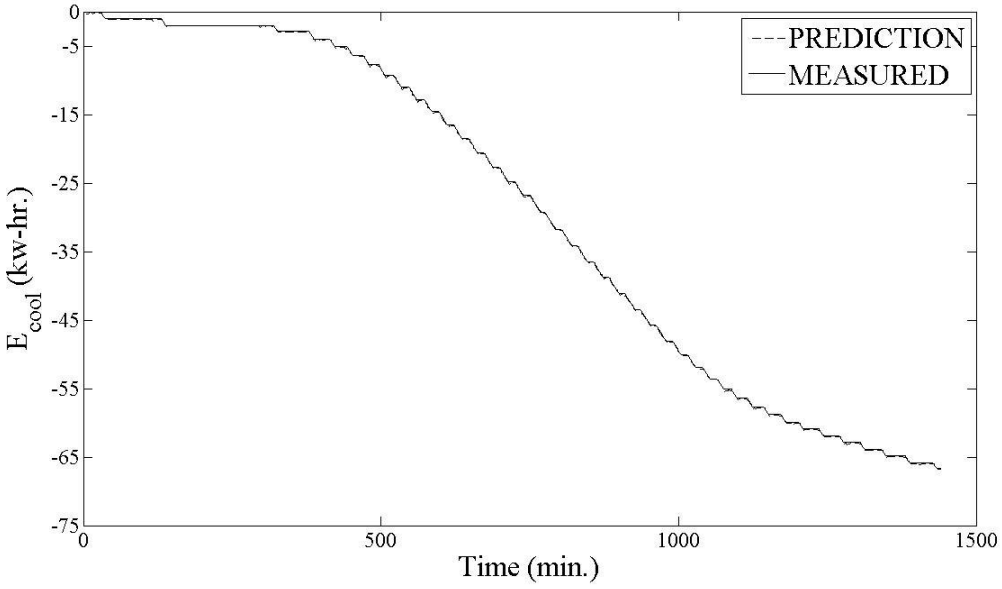

(f)

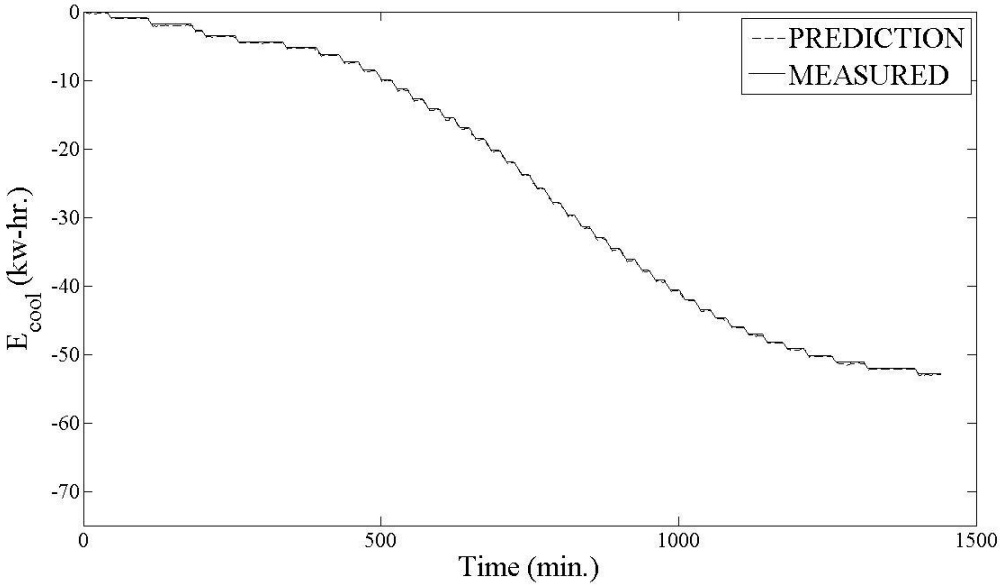

(g)

Figure 36: (a) to (g) Using Prediction based on Kalman filter approach for Energy Usage Model Validation.

Recursive state estimation using PEM does produce sound scheme to track the Energy usage. The long one-hour window tool can be proven to be quite helpful to utilities.

5.3 Energy Performance Model as Diagnostic Tool

Fault detection and diagnosis have been extremely important and challenging problems in engineering. It becomes even more critical when high level of automation is employed and system is being monitored and controlled. Revenue loss is very significant due to the fault in the system. To understand the faults imply understanding the performances. PNNL has done detailed research on the performance of HVAC [111].

Fault is generally defined as deviation from acceptable band or normal behavior. Typically faults from different sources [112] in any controlled process can be represented as in Figure 37.

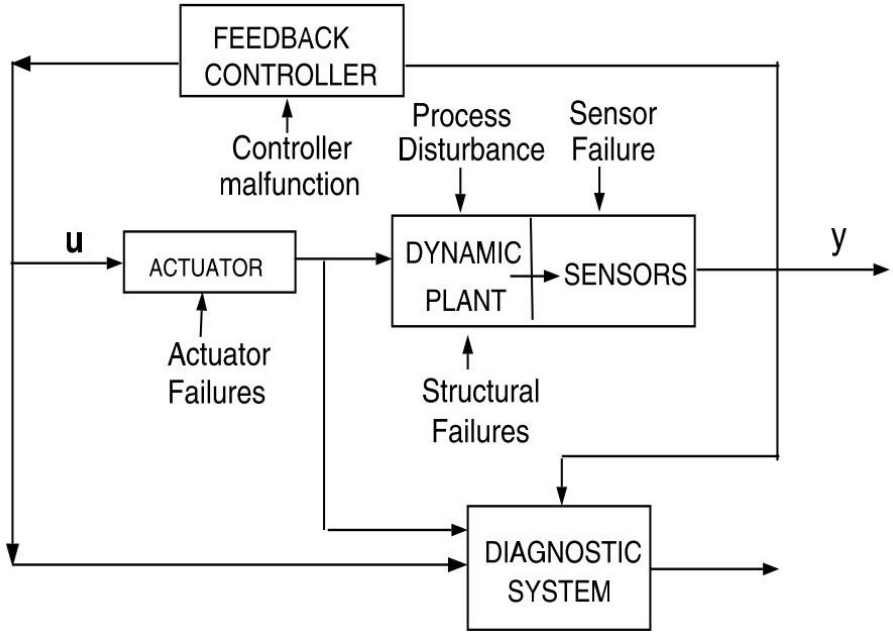

Figure 37: General Framework of a Diagnostic System.

The block diagram has been shown to display failures related to each individual component.

In general there are three different classes of faults [112], i.e. Gross parameter change in model, Structural changes and Malfunctioning sensors-actuators. Parameter failures arise when there is a disturbance entering the process from the environment through one or more exogenous variables. Structural change refers to the change in the process itself. Structural malfunctions are the result of failure of information flow between variables. Malfunctioning of sensors and actuators could be due to a fixed failure, a constant bias (positive or negative) or an out-of range failure. A failure in one of the instrument could cause the plant state variables to deviate beyond acceptable limits. Broadly, there are three general methods for the development of a fault detection and diagnostic system. These are Quantitative model-based methods [112], Qualitative model-based methods [113] and process history based methods, shown below [114] in Figure 38.

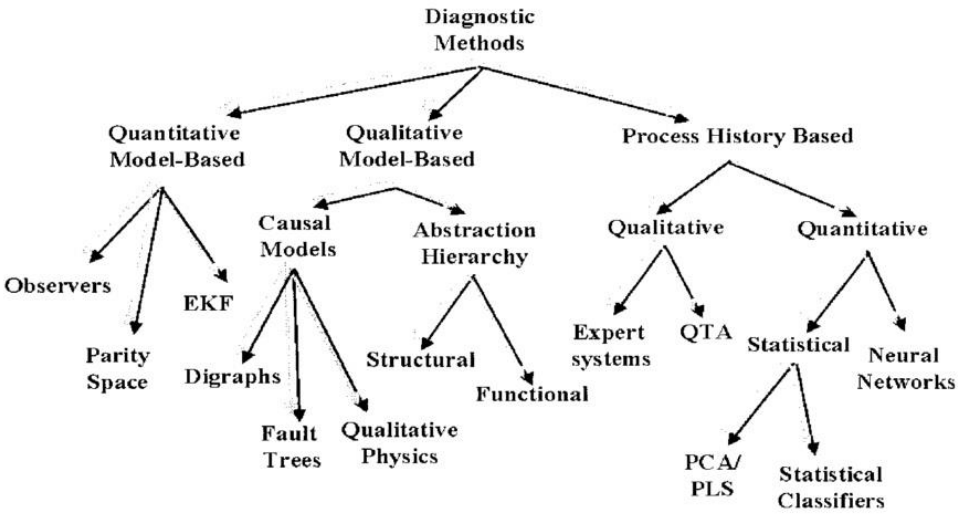

Figure 38: Diagnostic Algorithm classification.

All the popular methods have been shown under a tree structure of Diagnostics formulation method.

In Quantitative model based techniques, faults are identified as residuals between expected behavior of model and actual observation. There are wide ranges of quantitative based models such as state space based input-output, first principle and frequency response etc. The first principle method has been popular because of the mathematical complexity involved in the formulation step itself. Most of the Fault, Detection and Isolation (FDI) methods use black-box approach.

Qualitative model based technique has some understanding of behavior of the process or system. This is not in terms of explicit mathematical representation but in causal representation. The diagnostic system has some symptomatic feature or look table.

Lastly, Process history based method has just historical data and no priory information of the system. This data is used for feature extraction which gives information about the fault in the system. Feature extraction methods are either statistical or non-statistical. Neural networks falls under are non-statistical whereas Principle Component Analysis (PCA) and Partial Least Square (PLS) are statistical based feature extraction methods.

The proposed method falls under Quantitative model based diagnostic technique. It is measurement based discrete state space model. Here residual has been defined as the difference between observed and estimated through model. The entire approach has been explained below.

In practice, the NILM calculates E_{COOL} at each time step over an individual day. To do so, the NILM assumes a fixed cooling capacity value. This quantity is determined

from a one-time measurement performed during initial commissioning of the system. Each time the compressor is energized, it is assumed that the system delivers its measured capacity. The assumed heat input from the HVAC system is thus of the form shown in Figure 41 b, and the corresponding measured and simulated values of E_{COOL} are shown in Figure 41 a. Note that because of the assumed form of the cooling capacity, the measured value of E_{COOL} changes linearly when the system is on and remains constant when it is off.

As refrigerant charge leaks out of the HVAC equipment, the actual value of the cooling capacity drops, forcing the predicted value of E_{COOL} to deviate from the measurement. The homeowner can be alerted when differences arise and provided with information about how much excess money has been spent as a result of the fault. Model parameters have been estimated using data recorded over a three-day period. Once parameters are known, the thermal energy consumption is predicted and compared to measurements.

To elaborate these methodologies further, following examples would cast light on it. Thermal capacity can be represented by a collection of unit step functions where t_1, t_2, t_3…….t_n are time instants to represent compressor on-off schedule.

$$\dot{\mathrm{Q}} = \mathrm{q} * [\mathrm{U(t)} - \mathrm{U(t - t_1)} + \mathrm{U(t - t_2)} - \mathrm{U(t - t_3)} \ + \cdots + \mathrm{U(t - t_{n-1})} - \mathrm{U(t - t_n)}] \quad (59)$$

q is estimated based on the above equations using measured data. Later, the estimated q is used to as reference to investigate the system performance.

Further, $\dot{Q}$ is integrated over time to get total energy imparted during the time. Ramp signal E,

$$E = \int_0^t \dot{Q} = q * [t * U(t) - (t - t_1) * U(t - t_1)] + q * [(t - t_2) * U(t - t_2) - (t - t_3) * U(t - t_3)] + \cdots + q * [(t - t_{n-1}) * U(t - t_{n-1}) - (t - t_n) * U(t - t_n)] \quad (60)$$

Both the plots, Thermal capacity and total thermal energy input to the house have been shown here.

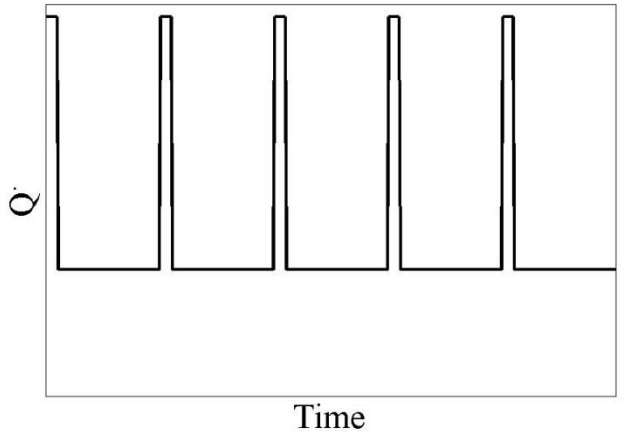

(a)

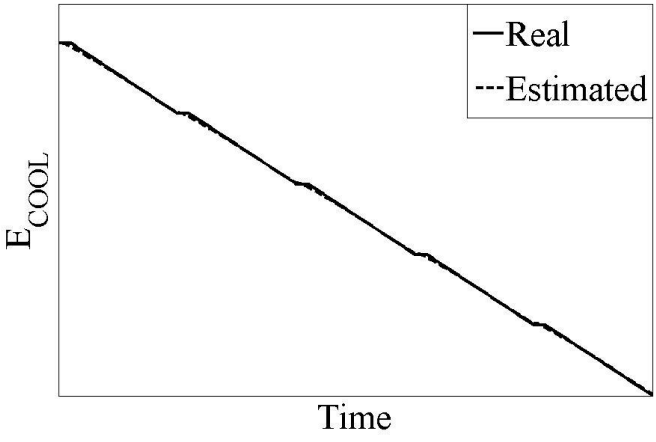

(b)

Figure 39: (a) Cooling capacity, (b) Measured vs. Estimated cumulative cooling energy to show system performance with no fault.

Here E_1, E_2…, E_n are defined as total thermal energy input to the system up tot_1, t_2, t_3…….t_n from the beginning.

$$E_1 = \int_0^T \dot{Q}\ , E_2 = \int_0^{2T} \dot{Q}\ , E_3 = \int_0^{3T} \dot{Q}\ , \ldots.\ E_{n-1} = \int_0^{(n-1)T} \dot{Q}\ ,\ E_n = \int_0^{nT} \dot{Q}$$

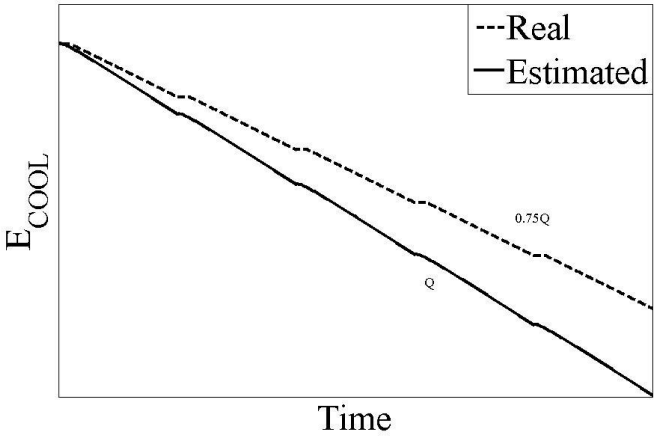

Figure 40: Measured vs. Estimated cumulative cooling energy to show system performance with fault.

As discussed before, this methodology of fault diagnosis comes under Quantitative model based approach. Validation of this approach has been dealt in the following section. To give emphasis further, the results have been revalidated through Process history based approach. This particular approach for faults diagnosis was used by Chris Laughman.

5.4 Diagnostic Tool demonstration

To explore the diagnostic capabilities of this approach, a small amount of refrigerant (~25%) was removed from the system. This value was selected for two reasons. First, research suggests that many systems are undercharged by about this amount [3]. Additionally, this value is low enough that energy consumption increases, but not by an amount that most consumers can detect from billing data.

To demonstrate the comparison between healthy performance and with fault, simulation was done with no fault. Figure 41 (a) displays cooling energy E_{COOL} simulation against time and Figure 41 (b) is the cooling capacity input to the house. Clearly, measured and simulated values are close to each other. This can be called normal or expected performance of the system.

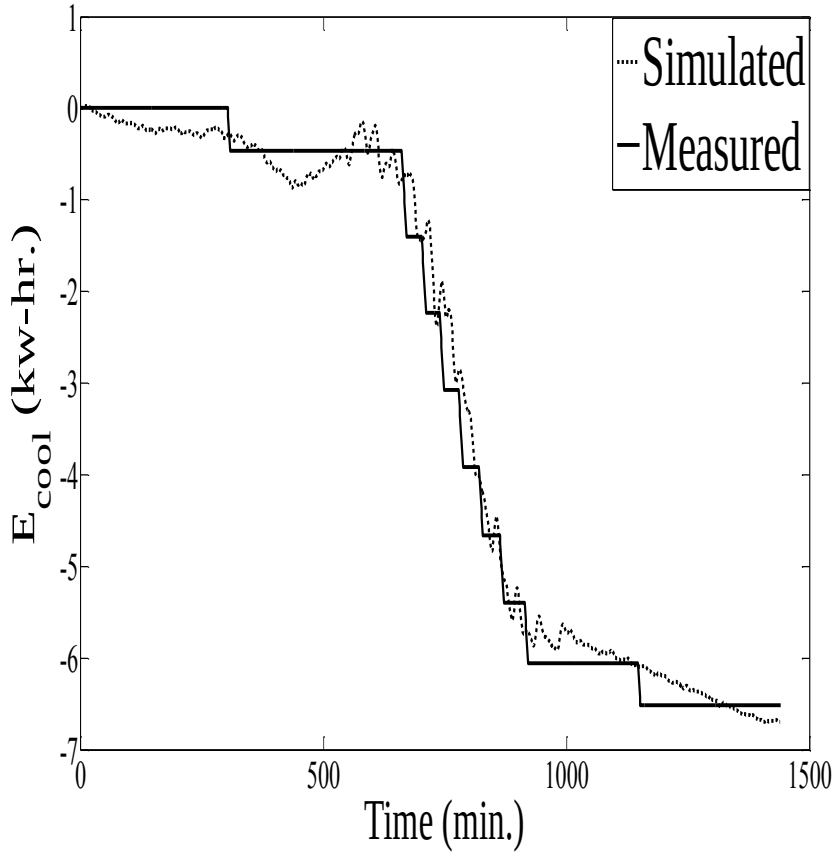

(a)

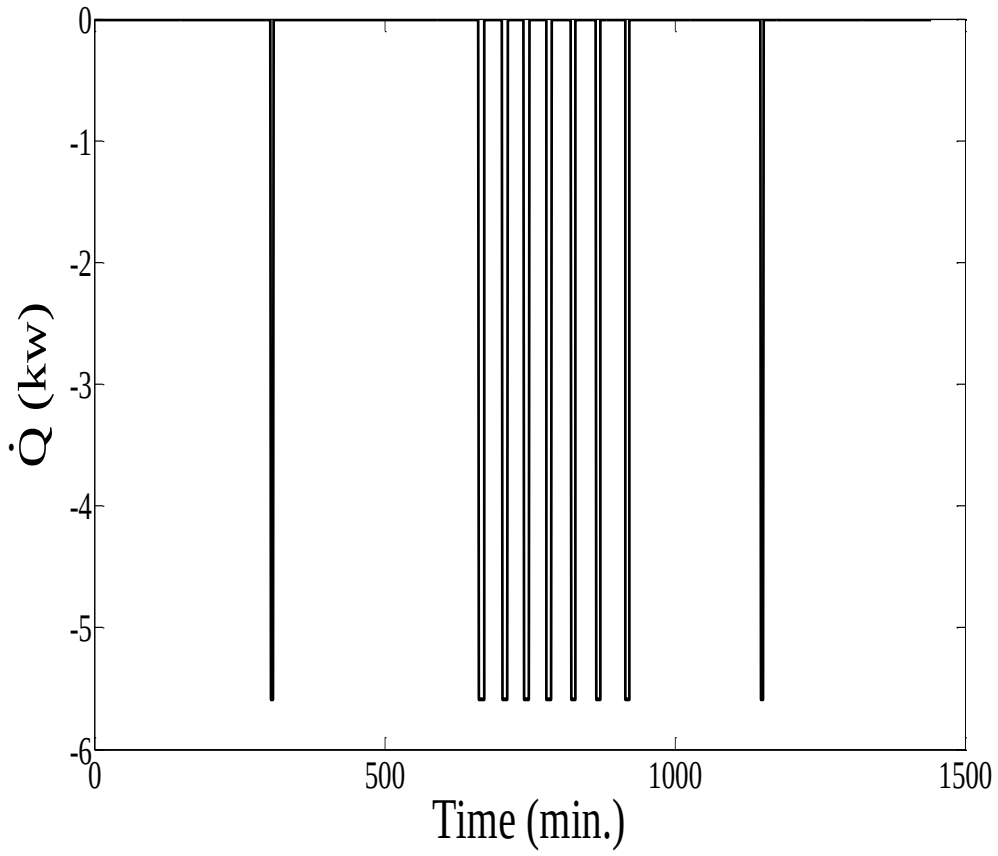

(b)

Figure 41: (a) Simulated and measured values of E_{COOL} over a single day when the experimental system has normal refrigerant charge. (b) The corresponding cooling capacity as a function of time.

As discussed before, if refrigerant leaks and the performance of the system deteriorate, it will be reflected in the monthly electricity bill. In reality, it is difficult to notice such an issue simply from the bill. To demonstrate a more robust approach, some refrigerant was removed from the test system. Figure 42 shows how the estimated and measured values of E_{COOL} deviated during this test. Note that several different measured curves are shown. The lowest of these is the one that was initially recorded assuming that the cooling capacity was still at its initial value $\dot{Q}_{init}$. With that assumption, the magnitude of the corresponding final measured value of $E_{COOL}$is approximately 5kW-hrs

greater than the final simulated value. To account for the refrigerant loss, the assumed cooling capacity is thus reduced. Measured curves are shown for $\dot{Q}_{init}$, $.9\dot{Q}_{init}$, $.8\dot{Q}_{init}$, and $.72\dot{Q}_{init}$, respectively. Note that the curve corresponding to 72% of the initial cooling capacity provides the best fit.

Understanding the significance of Figure 42 can be difficult. Part of the challenge lies in the fact that the figure suggests that a 27% drop in cooling capacity causes a corresponding drop in thermal energy. This may at first seem counterintuitive since the lower $\dot{Q}$ is expected to increase energy consumption. The overall energy draw did, however, increase relative to normal conditions. Figure 42 is thus misleading on this point. Consider, for example, Figure 41, which shows results under normal conditions (i.e.$\dot{Q} = \dot{Q}_{init}$) on a day with similar weather conditions.

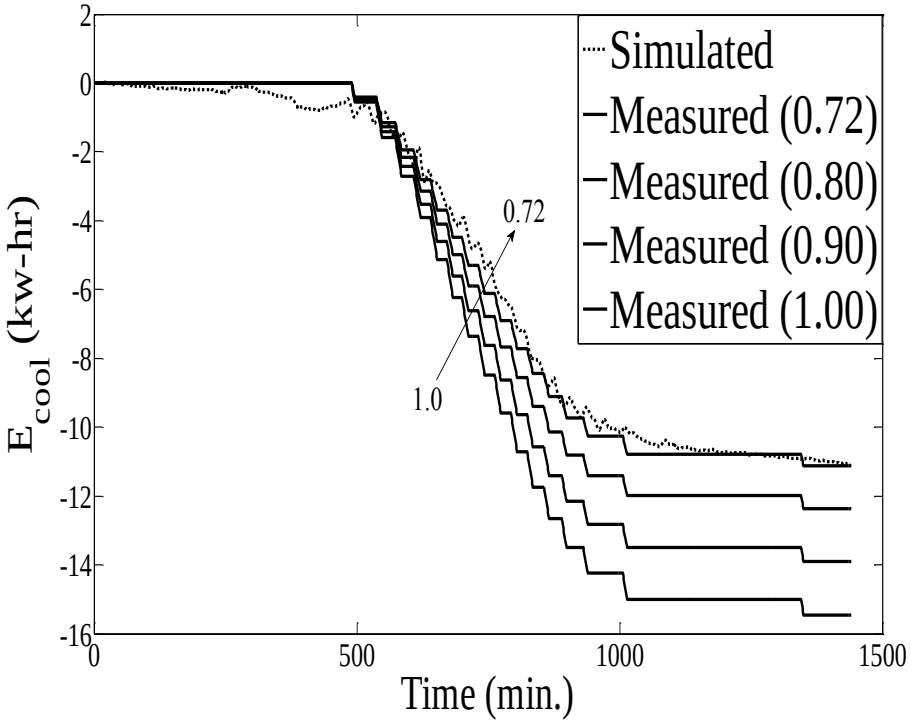

Figure 42: Measured and simulated values of ECOOL when the system is undercharged by about 25%.

Note that the overall amount of thermal energy increased from approximately 6.5kW-hrs on the normal day to approximately 11kW-hrs after the refrigerant was removed and the cooling capacity was reduced. This difference results from an increase in system run time after refrigerant removal. The various measured curves correspond to different assumptions for the cooling capacity, from 100% of its initial value (bottom) to 72% of its initial value (top).

To analyze performance through coefficient of performance (COP), it has been calculated and presented in Figure 43. As per definition,

$$COP = \frac{|E_{cool}|}{W} \tag{61}$$

Where $W = \int P$, P represents electrical power input.

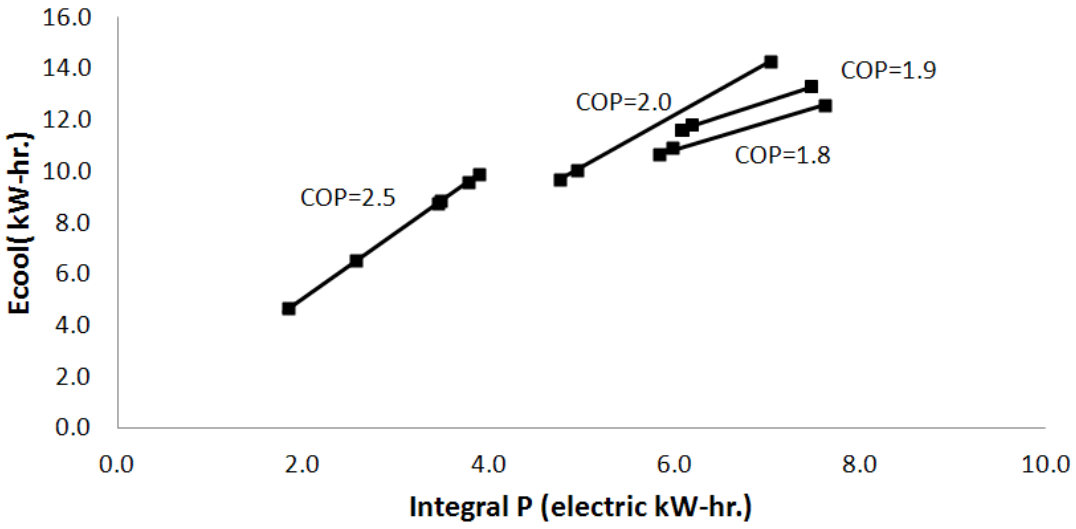

Figure 43: Coefficient of Performance (COP) based analysis of the system.

In this figure, each data point represents a single day observation of COP as it has been calculated for each day.

The figure shows two groups of days. COP for optimum performing days is high compared to low performing days. Therefore, as the performance starts derogating, slopes become more flat, i.e. low COP.

Figure 44 shows residuals calculated over days to study the performance. Residual is defined as the difference between simulated and measured data. This has been taken as one of the possible identifier to judge the system performance. A threshold value of 15% has been taken to make difference between normal operation and faulty one. Although this is just an assumption to show the system behavior. It could be a value different than 15%..

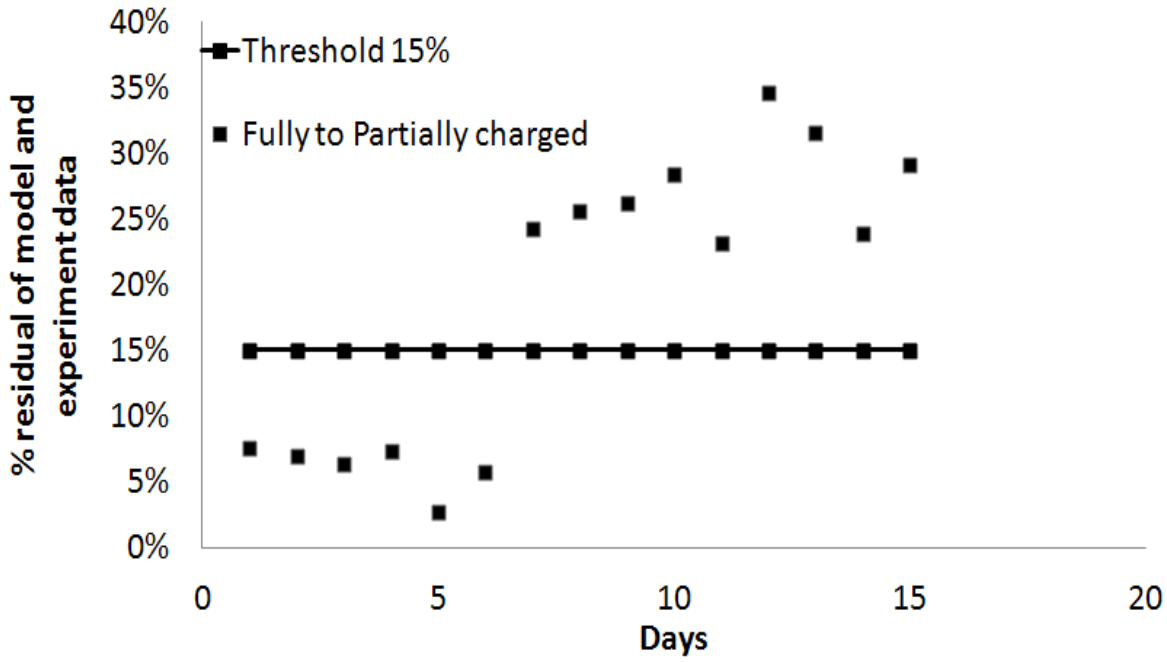

Figure 44: Residuals calculated each day to judge the system performance.

It is evident from Figure 44 that on days when the system was fully charged with refrigerant comes under threshold limit else they go well beyond limit when they are partially charged.

Now, simulated total thermal energy data for each day calculated and compared with the measured one. % absolute error has been determined too. Table 3 summarizes the observations. "-" in front of each no. to show that the system is cooling. It will be replaced with "+" for heating.

Table 3: Comparison of measured and simulated total thermal energy, % difference for (a) fully charged with refrigerant, (b) partially charged with refrigerant.

Table3: (a) fully charged with refrigerant

Regular charged			
Sl. No.	Measured (kW-hr.)	Simulated (kW-hr.)	% error (abs)
1	-8.8	-9.4	7.60%
2	-8.8	-9.5	6.90%
3	-9.9	-9.3	6.40%
4	-4.7	-5	7.40%
5	-6.5	-6.7	2.70%
6	-9.6	-10.2	5.70%

Table 3: (b) partially charged with refrigerant.

Partially charged			
Sl. No.	Measured (kW-hr.)	Simulated (kW-hr.)	% error (abs)
1	-17.9	-13.6	24.20%
2	-12.6	-9.4	25.60%
3	-12.1	-8.9	26.20%
4	-15.5	-11.1	28.30%
5	-15.7	-12.1	23.20%
6	-19	-12.4	34.60%
7	-19.4	-13.3	31.60%
8	-14.8	-11.3	23.80%
9	-15.2	-10.8	29.10%

Having visited Quantitative model based diagnosis; it is worth to check the fault by process history based approach now. It has been tried out to see the same data through different angle. To start with, (T_o-T_z) has been calculated and plotted against Δt. The term Δt is time interval of compressor on time. Here, objective is to look for Δt, the time interval for the same temperature difference (T_o-T_z). Two data sets have been chosen for display, i.e. first 7 days and last 7 days of system performance. After close analysis of this plot, it can be inferred that to maintain the same temperature compressor runs for long time in last 7 days which confirms underperformance of the system.

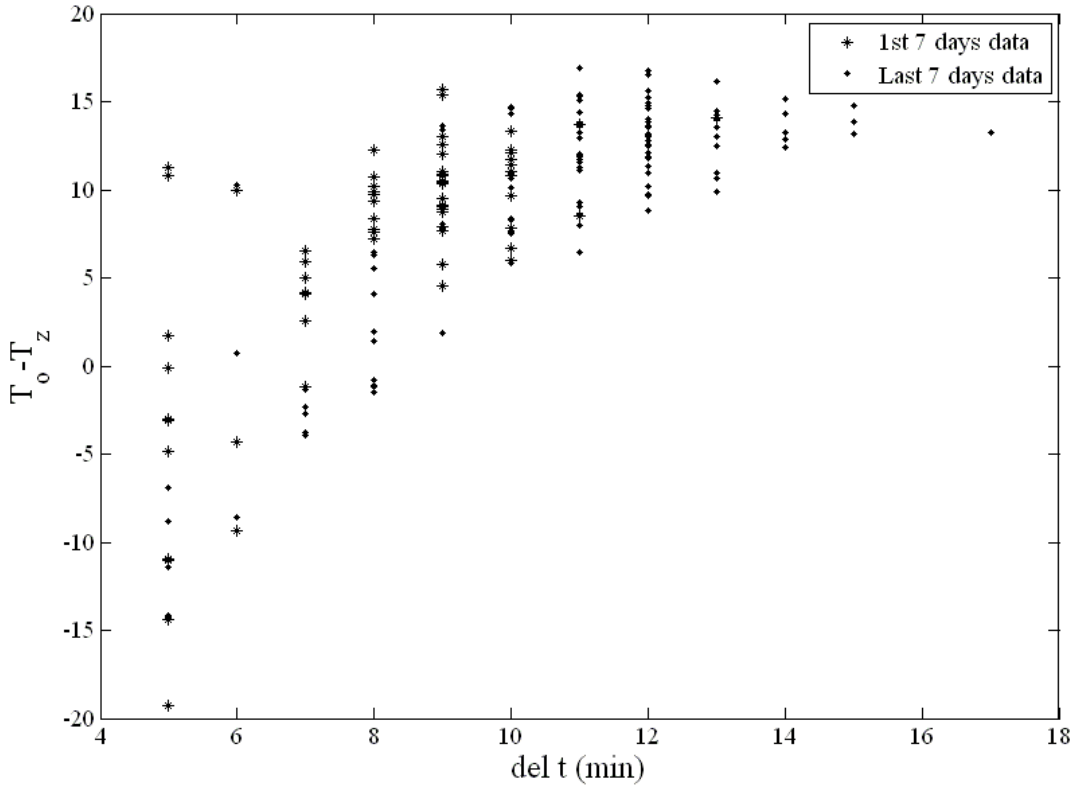

Figure 45: System performance study through compressor running time.

The chapter has dealt with the diagnostic scheme developed for residential or low rise buildings. It takes the same measurement data which will be used in control oriented model formulation. It has the potential to be quite useful for health determination of HVAC system in house.

CHAPTER 6: CONCLUSION AND FUTURE WORK

This research has demonstrated the effectiveness of the proposed thermal modeling procedure and considered two applications, i.e. a Model Predictive Control strategy and a system for fault diagnosis [115], [116], [117]. The entire formulation has been developed with the intention of limited or no human interaction. The work will assist utilities to better understand energy demand; it will also empower consumers with tools for cost savings.

6.1 Conclusions

The focus of this research has been towards developing an accurate thermal model that can be used to monitor and potentially control energy conversion in homes and small buildings while maintaining the same level of comfort. Two different applications have been considered, one for control and the other for energy usage. The demonstrated models have been developed purely based on measured data, which makes it attractive in applications where the first-time cost can be problematic.

Two different models have been built, i.e. a control-oriented model and energy-performance model. The control-oriented model takes as inputs cooling capacity, ambient temperature, and solar irradiance; zone temperature is the output. In the case of the energy-performance, zone temperature, ambient temperature and solar irradiance are the inputs; and cooling energy is the output. Both models are cast in state-space form and system identification is performed using the Prediction Error Method (PEM). Field

testing has demonstrated that four days of data is sufficient and that a fourth-order model is sufficient.

To improve the performance of the models for prediction, recursive PEM and a Kalman filter have been used. It has been demonstrated that both are very powerful and greatly improve the capability of the models. The research also demonstrates some of the finer details about smoothing of recorded data for model identification. Field validation has been performed through measurements in a small single-zone home. The entire scheme uses as small a set of sensors as possible, which thus reduces overall installation cost. Since this is a sensor-based and potentially online scheme, no human training is required.

The control-oriented model has been used to develop a predictive control strategy. Simulation results show energy costs can be reduced by about 30% if the proposed model-predictive scheme is employed. It should be noted here this scheme would take into account the weather forecast information to decide control actions in advance.

The energy-performance model would be used potentially by utilities where the agencies can plan ahead for resource allocation. This is the key for demand side management.

Further, the energy usage model has been used to detect refrigerant leaks. In this case, a partially charged unit was detected in the field. The refrigerant level was reduced by approximately 25% from its normal value, which causes over-consumption but not by an amount that is detected by most homeowners. Thus, such a system could detect issues before they were to become extremely problematic.

6.2 Future Directions

At present, new research students are beginning to use the models developed herein for more detailed fault detection and diagnostics. The team has installed the monitoring systems at two Wells Fargo retain bank branches in the greater Charlotte, North Carolina, area. The systems have successfully detected faults in one building near the UNC Charlotte campus. The team is currently working to automate the modeling process described in this thesis so that the system could potentially be deployed across a large number of retail sites. Such facilities are similar in size to many homes, and the fact that an enterprise customer has so many buildings motivates the desire to better understand and monitor performance. The team is also combining through the individual sensor streams to determine the exact cause of a fault. The present model would not necessarily isolate such a fault.

Another major application of the modeling process is in the context of demand-side management. Utilities have a strong desire to shed HVAC equipment during periods of peak demand. This allows them to optimize the use of "peak" power sources. To date, most load-shedding schemes are very simplistic. The approach used here is being considered for more optimal control of such shedding activities.

REFERENCES

[1] *2011 Building Energy Data Book*, U.S. Department of Energy, Office of Energy Efficiency and Renewable Energy, *March 2012*.

[2] T. Lui, W. Stirling, and H. Marcy, "Get smart," IEEE Power and Energy Magazine, vol. 8, no. 3, pp. 66-78, May/Jun 2010.

[3] R.J. Mowris, A. Blankenship, and E. Jones, "Field measurements of air conditioners with and without txvs. in *2004 ACEEE Summer Study on Energy Efficiency in Buildings*, pp 212–227, 2004.

[4] W. Kim, J.E. Braun, and H. Li, "Evaluation of a virtual refrigerant charge sensor," in *Proc. International Refrigeration and Air-Conditioning Conference at Purdue*, 2008.

[5] S. R. Shaw, S. B. Leeb, L. K. Norford, and R. W. Cox, "Nonintrusive load monitoring and diagnostics in power systems," *IEEE Trans. Inst. and Meas.*, vol. 57, pp. 1445-1454, 2008.

[6] A. Oppenheim, A. Willsky, and I. Young, *Signals and Systems*, Englewood Cliffs, NJ: Addison-Wellesley, 1988.

[7] S. B. Leeb, S. R. Shaw, and J. L. Kirtley, "Transient event detection in spectral envelope estimates for nonintrusive load monitoring," *IEEE Trans. Power Del.*, vol. 10, no. 3, pp. 1200–1210, Jul. 1995.

[8] K. D. Lee, "Electric load information system based on non-intrusive power monitoring," Ph.D. dissertation, Massachusetts Institute of Technology, 2003.

[9] W. Wichakool, A.-T. Avestruz, R. W. Cox, and S. B. Leeb, "Modeling and estimating current harmonics of variable electronic loads," IEEE Trans. on Power Electronics, vol. 24, no. 12, pp. 2803-2811.

[10] Energy plus Engineering reference guide.

[11] S. Wang and X. Xu," Parameter estimation of internal thermal mass of building dynamic models using genetic algorithm", Energy Conversion and Management 47 (2006) 1927–1941.

[12] D. G. Stephenson and G. P. Mitalas, "Calculation of heat conduction transfer functions for multi-layer slabs," *ASHRAE Trans.* vol. 77, pp. 117–126, 1971.

[13] P. R. Armstrong, "Model identification with application to building control and fault detection", PhD dissertation, MIT, 2004.

[14] J. E. Seem, "Modeling of heat transfer in buildings", PhD dissertation, UW, Madison 1987.

[15] D.G. Stephenson, G.P. Mitalas, "Room thermal response factors", *ASHRAE Trans.* vol. 73, pp. III1.1–1.7, 1967.

[16] N. W. Wilson, W. G. Colborne and R. Ganesh, "Determination of thermal parameters for an occupied house", *ASHRAE Trans.* vol. 90, pp. 39–50, 1984.

[17] T. L. McKinley , A. G. Alleyne, "Identification of building model parameters and loads using on-site data logs", *Third National Conference of IBPSA-USA,* Berkeley, 2008.

[18] G. J. Rios, M. T. Perea, R. C. Miranda, V. M. Guzman, G. H. Ruiz, "Modeling temperature in intelligent buildings by means of autoregressive models," *Automation in Construction,* vol. 16, no. 5, pp. 713-722, Aug. 2007.

[19] K.A. Antonopoulos, E.P. Koronaki, "Thermal Parameter Components of Building Envelope", *Applied Thermal Engineering 20(2000) 1193-1211*.

[20] D.A. Coley, J.M. Penman, "Simplified Thermal Response Modeling in Building Energy Management. Paper III: Demonstration of a Working Controller", *Building and Environment, vol. 31, no. 2, pp. 93-97, 1996.*

[21] H. Madsen and J. Holst, "Estimation of continuous-time models for the heat dynamics of a building," Energy and Buildings, vol. 22, no. 1, pp. 67–79, 1995.

[22] S. C. Bhattacharyya and G. R. Timilsina, "Energy Demand Models for Policy Formulation A Comparative Study of Energy Demand Models", the World Bank Development Research Group Environment and Energy Team March 2009.

[23] J. S. Armstrong, " Principle of Forecasting: A handbook for researchers and practitioners,", Norwell, MA: Kluwer Acadmic 2001,

[24] G. Levermore, " Building Energy Management Systems: an application to heating and control", London: E& FN SPON; 1992.

[25] A.I. Dounis and C. Caraiscos,"Advanced control systems engineering for energy and comfort management in a building environment – a review", Renewable and Sustainable Energy Reviews 13 (2009) 1246-1261.

[26] D. Kolokotsa," Comparison of the performance of fuzzy controllers for the management of the indoor environment", Department of Natural Resources Engineering, Technological Educational Institute of Crete, 73133 Chania, Crete, Greece.

[27] ASHRAE. 2005. 2005 ASHRAE Handbook—Fundamentals, chapters 3 (Heat Transfer) and 30 (heat-balance method). Atlanta: American Society of Heating, Refrigerating and Air-Conditioning Engineers, Inc.

[28] A. Gelb, "*Applied Optimal Estimation*, Cambridge", MA: MIT Press, 1974.

[29] G. A. Einicke, "Smoothing, Filtering and Prediction: Estimating the Past, Present and Future", InTech 2012, Croatia.

[30] NIST/SEMATECH e-Handbook of Statistical Methods: Single Exponential Smoothing.

[31] S. B Achelis," *Technical Analysis from A to Z*", Second printing, McGraw-Hill, 1995.

[32] Cleveland, W.S. (1979), "Locally Weighted Regression and Smoothing Scatterplots," *Bell Laboratories Memorandum*.

[33] Cleveland, William S. (1977), "Robust Locally Weighted Regression and Smoothing Scatterplots," *Journal of the American Statistical Association*, Vol. 74, pp. 829-836.

[34] Cleveland, W.S. and Devlin, S.J. (1988), "Locally Weighted Regression: An Approach to Regression Analysis by Local Fitting," Journal of the American Statistical Association, Vol. 83, pp. 596-610.

[35] NIST Engineering Statistics Handbook, 4.1.4.4. LOESS (aka LOWESS).

[36] Fan, J. and Gijbels, I. (1996). Local Polynomial Modelling and its Applications. Chapman and Hall, London.

[37] Green, P.J. and Silverman, B. (1994). Nonparametric Regression and Generalized Linear Models: A roughness penalty approach. Chapman and Hall, London.

[38] H¨ardle, W. (1990). Applied Nonparametric Regression. Cambridge University Press, Cambridge.

[39] Hart, J.D. (1997). Nonparametric Smoothing and Lack-of-Fit Tests. Springer, New York.

[40] Efromovich, S. (1999). Nonparametric Curve Estimation. Springer, New York.

[41] Fan, J. and Yao, Q. (2003). Nonlinear Time Series: Nonparametric and Parametric Methods. Springer-Verlag, New York.

[42] A. Savitzky and M. J. E. Golay, vol. 36, no. 8, july 1964 “Smoothing and Differentiation of Data by Simplified Least Squares Procedures”.

[43] Box, George E. P.; Norman R. Draper (1987). Empirical Model-Building and Response Surfaces, p. 424, Wiley. ISBN 0471810339

[44] K. Åström, and P. Eykhoff, ” System identification – A survey” , Automatica7 : 123–162. , 1971.

[45] P. Sjovall and T. Abrahamsson, “Component System Identification and State Space Model Synthesis”, Mechanical Systems and Signal Processing 21(2007) 2697-2714.

[46] W. Fred Ramirez. Process control and identification. Academic Press, New York, NY, 1994.

[47] L. Ljung, *System Identification: Theory for the User*. (2nd ed.), Upper Saddle River, NJ: Prentice Hall, 1999.

[48] L. Ljung, “Prediction error estimation methods”, *Circuits, Systems, and Signal Processing,* vol. 21, no. 1, pp. 11-21, 2002.

[49] R. Qinchang,”Prediction Error Method for Identification of a Heat Exchanger”, ISBN 90-6144-237-0, Jan 1990.

[50] P.V. Kabaila,” On Output-Error Methods for System Identification”, IEEE Transaction on Automatic Control, Vol. AC-28, No. 1, Jan. 1983.

[51] H. Dai and N.K. Sinha, “ A Robust Off-Line Output Error Method for System Identification”, IEEE Transaction on Industrial Electronics, Vol. 39. 4 Aug. 1992.

[52] P. V. Overschee, B. D. Moor,”Subspace Identification for Linear Systems”, Katholieke Universiteit Leuven, Belgium.

[53] S. J. Qin, “ An Overview of Subspace Identification “, Computers & Chemical Engineering 30 (2006) 1502-1513.

[54] System Identification Toolbox, Matlab.

[55] G. Welch and G. Bishop, “An Introduction to Kalman Filter”, Dept. of Computer science, UNC Chapel Hill, July 2006.

[56] R. E. Kalman, “A New Approach to Linear Filtering and Prediction Problems” Transaction of the ASME-Journal of Basic Engineering, 82 (Series D): 35-45, 1960.

[57] H. Wang, H. Zhang and G. Duan, "Kalman Filtering Descriptor Systems with Current and Delayed Measurements" International Conference on Control, Automation, Robotics and Vision, Dec. 2004.

[58] Kalman Filter design, Matlab.

[59] http://www.onsetcomp.com/

[60] ASHRAE. 2005. 2005 ASHRAE Handbook—Fundamentals, chapters 1 Thermodynamics and Refrigeration Cycles.

[61] M.J.Moran, H. N. Shapiro, D.D. Boettner and M.B. Bailey ," Fundamental of Engineering Thermodynamics".

[62] D.M. Admiraal and C. W. Bullard (Aug. 1993), "Heat transfer in Refrigerator, Condenser and Evaporator", Air Conditioning and Refrigeration Center, TR-48.

[63] X. Fang (Aug. 1999), "Advances in fixed area Expansion Devices", Air Conditioning and Refrigeration Center, CR-20.

[64] D. A. Aaron and P. A. Domanski (July 1989),"An Experimental Investigation and Modeling of the Flow rate of Refrigerant 22 through the Short Tube Restrictor", NISTIR 89-4120.

[65] S.A. Klein, D.T. Reindl (May 1999), "Develop Data Base for Determining Optimum Compressor Rating Points for Residential Refrigerator and Freezer Compressors" ASHRAE RP-870.

[66] Air-Conditioning and Refrigeration Institute (1991): Standard 540-91 "A method for presentation of compressor performance data".

[67] http://www.bristolcompressors.com/BCWC02.aspx?ModelNo=H25B35QABC&CylRunning=2&Frequency=60&System=M

[68] http://www.emersonclimate.com/enus/Products/Compressors/Scroll_Compressors/copeland_scroll_residential/Pages/CopelandScrollZRK5Compressor.aspx

[69] R.C. Arora, "Refrigeration and Air Conditioning" ISBN 978-81-203-3915-6.

[70] ASHRAE standard for duct air flow measurement.

[71] B. Friedland, "Control System Design: An Introduction to state-space methods".

[72] K. Ogata, "State space analysis of a control system".

[73] J. Golten and A. Verwer, "Control System Design and Simulation".

[74] R. C. Dorf, “Modern control systems”.

[75] R.E. Kalman and R.S. Bucy. New results in linear filtering and prediction theory. Trans. ASME, J. Basic Engineering, pages 95–108, March 1961.

[76] V. Lemort, A. Rodriguez and J. Lebrun, “Simulation of HVAC components with the help of an Equation Solver”, *IEA SHC Task 34/ECBCS Annex 43, Subtask D: Mechanical Equipment and Control Strategy, Mar. 2008.*

[77] M. Trcka and J. L. M Hensen, “Overview of HVAC system simulation”, *Automation in Construction, 19 (2010) 93-99.*

[78] A. Schijndel and M. de Wit, “Advanced simulation of building systems and control with Simulink,” Building Simulation, pp. 1185–1192, 2003.

[79] G. R. Zheng, M. Z. Uddin, “Optimization of Thermal Processes in a Variable Air Volume HVAC System” *Energy vol. 21, no. 5, pp. 407-420, 1996.*

[80] T.Q. Qureshi and S.A. Tassou, “Variable-Speed Capacity Control in Refrigeration System”, *Applied Thermal Engineering, vol. 16, no. 2, pp.103-113, 1996.*

[81] S. Shao, W. Shi, X. Li and H. Chen, “Performance representation of variable-speed compressor for inverter air conditioners based on experimental data” International *Journal of Refrigeration 27(2004) 805-815.*

[82] Bemporad, A., M.Morari, V. Dua, E. Pistikopoulos (2002), “The explicit linear quadratic regulator for constrained systems”, Automatica, 38(1), pp. 3–20.

[83] Andersson, J., A survey of multiobjective optimization in engineering design. Technical report LiTH-IKP-R-1097, Department of Mechanical Engineering, Linköping University, Linköping, Sweden, 2000.

[84] Camacho, E., C. Bordons (1995) Model Predictive Control in the Process Industry, Springer-Verlag, Berlin, Germany.

[85] M. Morari and J.H. Lee. Model predictive control: Past, present and future. In Proceedings of PSE/Escape ’97, Trondheim, Norway, 1997.

[86] S.J. Qin and T.A. Badgwell. An overview of industrial model predictive control technology. In J.C. Kantor, C.E. Garcia, and B. Carnahan, editors, AIChE Symposium Series: Fifth Int. Conf. on Chemical Process Control, volume 316, pages 232–256, 1997.

[87] R.R. Negenborn, B. De Schutter, M.A. Wiering, and J. Hellend oorn,“Experience-based model predictive control using reinforcement learning,” Proceedings of the 8th

TRAIL Congress 2004 – A World of Transport, Infrastructure and Logistics – CD-ROM, Rotterdam, The Netherlands, 18 pp., Nov. 2004.

[88] Ir. M. Berg and Dr. Ir. A. Hegyi, "A model predictive control approach based on mixed integer linear programming", TRAIL Research school, Delft, Oct. 2008.

[89] Camacho, E. F. and C. Bordons Model predictive control. Springer: Advanced Textbooks in Control and Signal Processing Series, London, 2004.

[90] Garc´ıa, C., D. Prett, M. Morari (1989) Model predictive control: Theory and practice —A survey, Automatica, 25(3), pp. 335–348.

[91] Maciejowski, J. M. (2002) Predictive Control with Constraints, Prentice Hall, Harlow, England.

[92] Rossiter, J. A., Model-based predictive control: A practical approach. Crc Press: Control Series, Boca Raton, 2003.

[93] W.H. Kwon, "Advances in predictive control: Theory and application" In Proceedings of first Asian Control Conference, Tokyo, 1994.

[94] R. de Keyser, "A gentle introduction to model based predictive control", In EC-PADI2 Int. Conference on Control Engineering and Signal Processing,

[95] K.R. Muske and J.B. Rawlings, "Model predictive control with linear models", AIChE Journal, 39(2):262–287, 1993.

[96] J.B. Rawlings. Tutorial: Model predictive control technology. In Proc. American Control Conference, pages 662–676, San Diego, California, June 1999.

[97] M. Morari, 'Model Predictive Control: Multivariable Control Technique of Choice". 1990.

[98] A.E. Bryson and Y-C. Ho., "Applied optimal control: optimization, estimation and control" Hemisphere, Washington, 1975.

[99] J. Richalet, A. Rault, J.L. Testud, and J. Papon., "Model predictive heuristic control: Applications to industrial processes", Automatica, 14:413–428, 1978.

[100] N.M.C. Oliveira and L.T. Biegler, "Constraint handling and stability properties of model predictive control" AIChE J., 40:1138–1155, 1994.

[101] J.B. Rawlings and K.R. Muske. The stability of constrained receding horizon control. IEEE Transactions on Automatic Control, 38(10):1512–1516, 1993.

[102] E. Zafiriou. Robust model predictive control of processes with hard constraints. Comp. & Chem. Eng., 14(4/5):359–371, 1990.

[103] Eric C. Kerrigan and Jan M. Maciejowski, Soft constraints and exact penalty functions in model predictive control.

[104] Nilson Monteiro de Oliveira, Miguel Angel Rodriguez Borroto, "Comparative Performance Analysis between PID Controller and MPC Controller applied to an Inverted Pendulum".

[105] C. Bonivento, P. Castaldi and D. Mirotta, "Predictive Control vs PID Control of an Industrial Heat Exchanger".

[106] Zambrano, D., and E.F Camacho, "Application of MPC with multiple objectives for a solar refrigeration plant", Proceedings of the IEEE Conference on Control Applications, 1230-1235, Glasgow. September. 2002.

[107] Y. Ma, F. Borrelli, B. Hencey, A. Packard and S. Bortoff , " Model Predictive Control of Thermal Energy Storage in Building Cooling Systems".

[108] T. G. Hovgaard, K. Edlund, and J. B. Jørgensen, "The potential of economic MPC for power management," in 49th IEEE Conference on Decision and Control, 2010, pp. 7533–7538.

[109] V. M. Zavala, E. M. Constantinescu, and T. K. amd Mihai Anitescu, "Online economic optimization of energy systems using weather forecast information," Journal of Process Control, no. 19, pp. 1725–1736, 2009.

[110] Model Predictive Control toolbox, Matlab.

[111] N. Lu, Y.L Xie and Z. Huang, "Air Conditioner Compressor Performance Model", *PNNL-17796, Aug. 2008.*

[112] V. Venkatasubramanian, R. Rengaswamy, K.Yin and S. N. Kavuri, "A review of process fault detection and diagnosis Part I: Quantitative model-based methods" Computers and Chemical Engineering 27 (2003) 293-311.

[113] V. Venkatasubramanian, R. Rengaswamy, and S. N. Kavuri, "A review of process fault detection and diagnosis Part II: Qualitative models and search strategies" Computers and Chemical Engineering 27 (2003) 313-326.

[114] V. Venkatasubramanian, R. Rengaswamy, S. N. Kavuri and K.Yin, "A review of process fault detection and diagnosis Part III: Process history based methods" Computers and Chemical Engineering 27 (2003) 327-346.

[115] M. N. Sinha and R. W. Cox," Improving HVAC System Performance Using Smart Meters". Energytech, 2011 IEEE, Pages 1-6.

[116] M. Sinha, B. Desai and R. W. Cox, "Using smart meters for diagnostics and model-based control in the thermal comfort systems", IECON Proceedings (Industrial Electronics Conference). 2012:3600-3605.

[117] D. Bruckner, J. Hasse, P.P. Sky and G. Zucker, "Latest trends in integrating building automation and smart grids", IECON 2012 -38th Annual Conference on IEEE Industrial Electronics Society, 6285-6290.

[118] "Reduce Energy Consumption by 20% with Little or No Cost: A Guide to Energy Efficiency Technologies," White Paper, The Carbon War Room, online: http://www.carbonwarroom.com

APPENDIX A: EXPERIMENTAL SITE DESCRIPTION

Description of Experimental site: -

No. of Windows = 8, No. of Doors = 2

Total dimensions: Length X Width X Height X Thickness = 70 ft X 14 ft X 8 ft X 4 inch

Table 4: Dimensions of (a) doors, (b) windows.

(a)

No.	Windows Dimension (inch) (Width X Height)
1	32 X76
2	32 X 76

(b)

No.	Windows Dimension (inch) (Width X Height)
1	28 X26
2	92 X 38
3	28 X 26
4	46 X 38
5	46 X 38
6	12 X 25
7	46 X 38
8	46 X 38

APPENDIX B: EXPERIMENTAL SET UP AND RESULTS

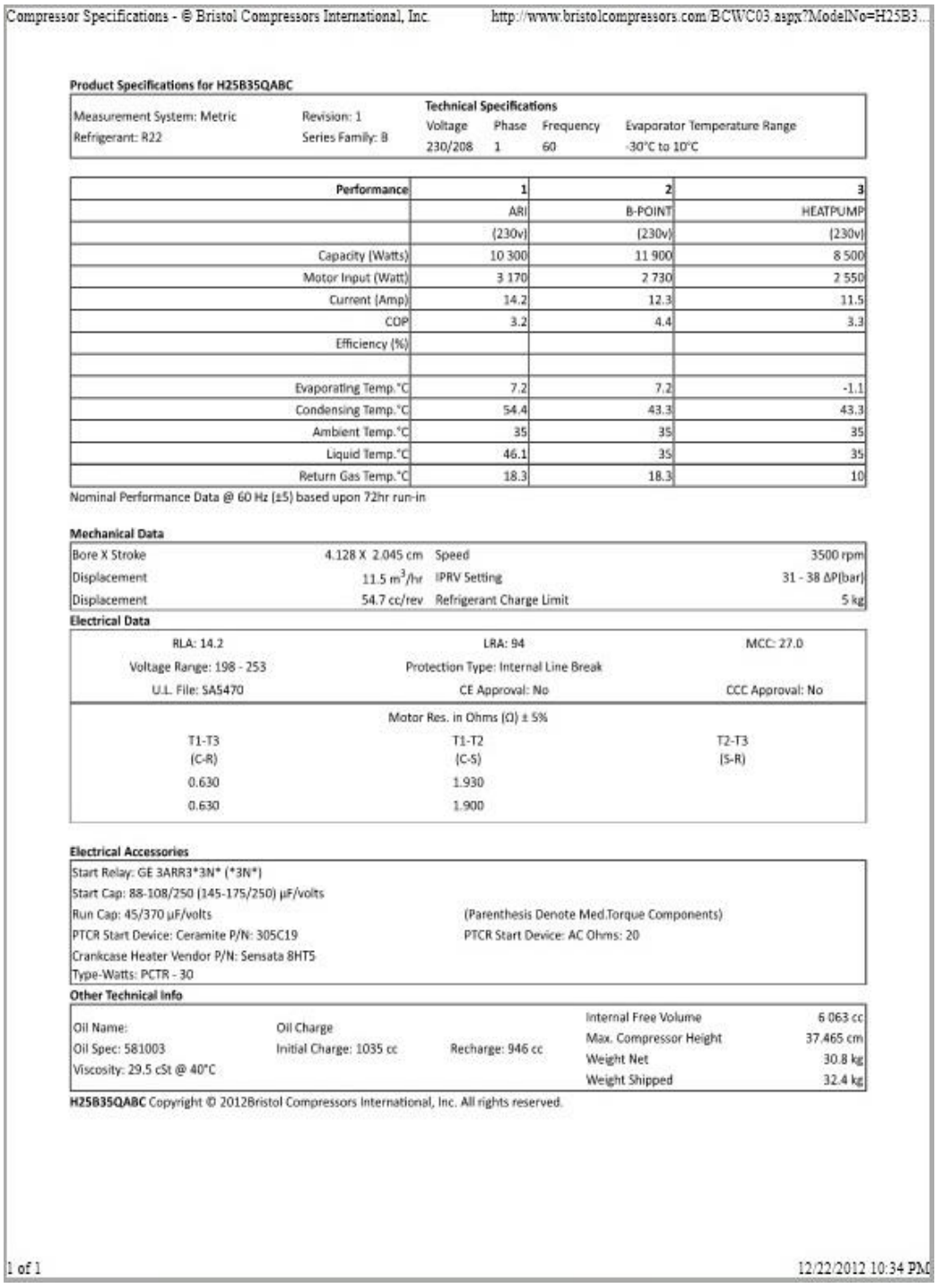

Compressor Specifications - © Bristol Compressors International, Inc. http://www.bristolcompressors.com/BCWC03.aspx?ModelNo=H25B3...

Product Specifications for H25B35QABC

		Technical Specifications			
Measurement System: Metric	Revision: 1	Voltage	Phase	Frequency	Evaporator Temperature Range
Refrigerant: R22	Series Family: B	230/208	1	60	-30°C to 10°C

Performance	1	2	3
	ARI	B-POINT	HEATPUMP
	(230v)	(230v)	(230v)
Capacity (Watts)	10 300	11 900	8 500
Motor Input (Watt)	3 170	2 730	2 550
Current (Amp)	14.2	12.3	11.5
COP	3.2	4.4	3.3
Efficiency (%)			
Evaporating Temp.°C	7.2	7.2	-1.1
Condensing Temp.°C	54.4	43.3	43.3
Ambient Temp.°C	35	35	35
Liquid Temp.°C	46.1	35	35
Return Gas Temp.°C	18.3	18.3	10

Nominal Performance Data @ 60 Hz (±5) based upon 72hr run-in

Mechanical Data

Bore X Stroke	4.128 X 2.045 cm	Speed	3500 rpm
Displacement	11.5 m^3/hr	IPRV Setting	31 - 38 ΔP(bar)
Displacement	54.7 cc/rev	Refrigerant Charge Limit	5 kg

Electrical Data

RLA: 14.2	LRA: 94	MCC: 27.0
Voltage Range: 198 - 253	Protection Type: Internal Line Break	
U.L. File: SA5470	CE Approval: No	CCC Approval: No

Motor Res. in Ohms (Ω) ± 5%

T1-T3 (C-R)	T1-T2 (C-S)	T2-T3 (S-R)
0.630	1.930	
0.630	1.900	

Electrical Accessories

Start Relay: GE 3ARR3*3N* (*3N*)
Start Cap: 88-108/250 (145-175/250) µF/volts
Run Cap: 45/370 µF/volts (Parenthesis Denote Med.Torque Components)
PTCR Start Device: Ceramite P/N: 305C19 PTCR Start Device: AC Ohms: 20
Crankcase Heater Vendor P/N: Sensata 8HT5
Type-Watts: PCTR - 30

Other Technical Info

Oil Name:	Oil Charge		Internal Free Volume	6 063 cc
Oil Spec: 581003	Initial Charge: 1035 cc	Recharge: 946 cc	Max. Compressor Height	37.465 cm
Viscosity: 29.5 cSt @ 40°C			Weight Net	30.8 kg
			Weight Shipped	32.4 kg

1 of 1 12/22/2012 10:34 PM

(a)

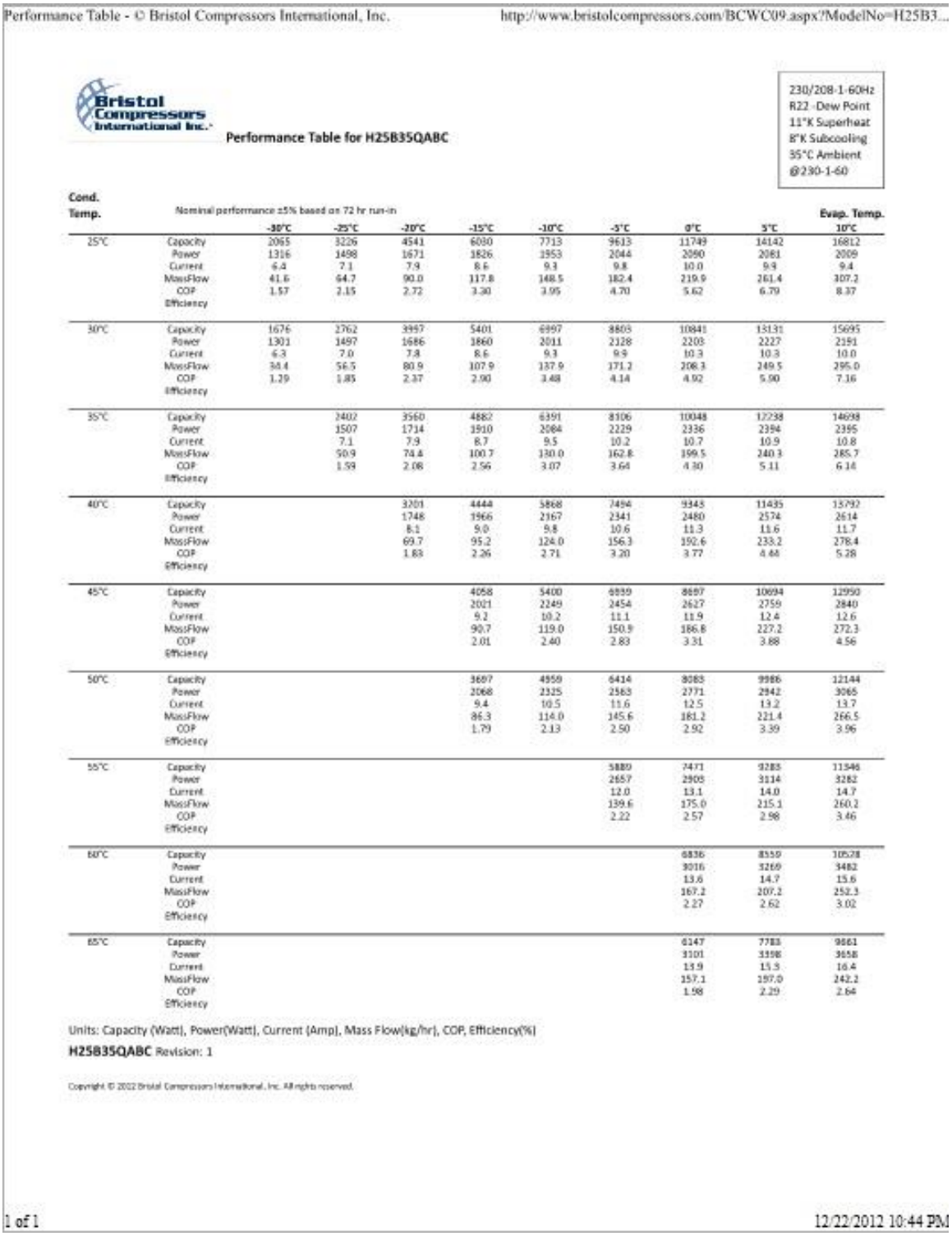

Performance Table - © Bristol Compressors International, Inc. http://www.bristolcompressors.com/BCWC09.aspx?ModelNo=H25B3...

Bristol Compressors International Inc.

Performance Table for H25B35QABC

230/208-1-60Hz
R22 -Dew Point
11°K Superheat
8°K Subcooling
35°C Ambient
@230-1-60

Cond. Temp.		Nominal performance ±5% based on 72 hr run-in								Evap. Temp.
		-30°C	-25°C	-20°C	-15°C	-10°C	-5°C	0°C	5°C	10°C
25°C	Capacity	2065	3226	4541	6080	7713	9613	11749	14142	16812
	Power	1316	1498	1671	1826	1953	2044	2090	2081	2009
	Current	6.4	7.1	7.9	8.6	9.3	9.8	10.0	9.9	9.4
	MassFlow	41.6	64.7	90.0	117.8	148.5	182.4	219.9	261.4	307.2
	COP	1.57	2.15	2.72	3.30	3.95	4.70	5.62	6.79	8.37
	Efficiency									
30°C	Capacity	1676	2762	3997	5401	6997	8805	10841	13131	15695
	Power	1301	1497	1686	1860	2011	2128	2203	2227	2191
	Current	6.3	7.0	7.8	8.6	9.3	9.9	10.3	10.3	10.0
	MassFlow	34.4	56.5	80.9	107.9	137.9	171.2	208.3	249.5	295.0
	COP	1.29	1.85	2.37	2.90	3.48	4.14	4.92	5.90	7.16
	Efficiency									
35°C	Capacity		2402	3560	4882	6391	8106	10048	12238	14698
	Power		1507	1714	1910	2084	2229	2336	2394	2395
	Current		7.1	7.9	8.7	9.5	10.2	10.7	10.9	10.8
	MassFlow		50.9	74.8	100.7	130.0	162.8	199.5	240.3	285.7
	COP		1.59	2.08	2.56	3.07	3.64	4.30	5.11	6.14
	Efficiency									
40°C	Capacity			3201	4444	5868	7494	9343	11435	13792
	Power			1748	1966	2167	2341	2480	2574	2614
	Current			8.1	9.0	9.8	10.6	11.3	11.6	11.7
	MassFlow			69.7	95.2	124.0	156.3	192.6	233.2	278.4
	COP			1.83	2.26	2.71	3.20	3.77	4.44	5.28
	Efficiency									
45°C	Capacity				4058	5400	6959	8697	10694	12950
	Power				2021	2249	2454	2627	2759	2840
	Current				9.2	10.2	11.1	11.9	12.4	12.6
	MassFlow				90.7	119.0	150.9	186.8	227.2	272.3
	COP				2.01	2.40	2.83	3.31	3.88	4.56
	Efficiency									
50°C	Capacity				3697	4959	6414	8083	9986	12144
	Power				2068	2325	2563	2771	2942	3065
	Current				9.4	10.5	11.6	12.5	13.2	13.7
	MassFlow				86.3	114.0	145.6	181.2	221.4	266.5
	COP				1.79	2.13	2.50	2.92	3.39	3.96
	Efficiency									
55°C	Capacity						5889	7471	9285	11346
	Power						2657	2903	3114	3282
	Current						12.0	13.1	14.0	14.7
	MassFlow						139.6	175.0	215.1	260.2
	COP						2.22	2.57	2.98	3.46
	Efficiency									
60°C	Capacity							6836	8559	10628
	Power							3016	3269	3482
	Current							13.6	14.7	15.6
	MassFlow							167.2	207.2	252.3
	COP							2.27	2.62	3.02
	Efficiency									
65°C	Capacity							6147	7783	9861
	Power							3101	3398	3658
	Current							13.9	15.3	16.4
	MassFlow							157.1	197.0	242.2
	COP							1.98	2.29	2.64
	Efficiency									

Units: Capacity (Watt), Power(Watt), Current (Amp), Mass Flow(kg/hr), COP, Efficiency(%)

H25B35QABC Revision: 1

1 of 1 12/22/2012 10:44 PM

(b)

Figure 46: Compressor details provided by manufacturer (a) Compressor specification datasheet, (b) Compressor map.

ZR32K5-PFV

HCFC, R-22, 60Hz, 1- Phase, 208/230 V
Air Conditioning

Production Status: Available for sale to all U.S. customers. Please check with your local Emerson Climate Technologies Representative for international availability.

Performance

Evap(°F)/Cond(°F)	45 / 130	50 / 100
RG(°F)/Liq(°F)	65 / 115	70 / 85
Capacity (Btu/hr)	32600	42600
Power (Watts):	2910	2020
Current (Amps):	13.30	9.20
EER (Btu/Wh):	11.20	21.10
Mass Flow (lbs/hr):	478	545
Sound Power (dBA):	68 Avg	73 Max
Vibration (mils)peak-	2.0 Avg	3.0 Max
Record Date:	2010-11-16	

Mechanical

Number of Cylinders:	0	Displ(in^3/Rev):	2.69
Bore Size(in):	0.00	Displ(ft^3/hr):	326.91
Stroke(in):	0.00		
Overall Length (in):	9.50	Mounting Length (in):	7.50
Overall Width (in):	9.50	Mounting Width (in):	7.50
Overall Height (in):	15.86	Mounting Height (in):	16.08 *

Suction Size (in):	3/4 Stub
Discharge Size (in):	1/2 Stub
Oil Recharge (oz):	19
Initial Oil Charge (oz):	25
Net Weight (lbs):	49.9
Internal Free Volume (in^3):	115.0
Horse Power:	

*Overall compressor height on Copeland Brand Product's specified mounting grommets.

Electrical

LRA-High*:	87.0	MCC (Amps):	24.0	UL File No:	SA-2337
LRA-Half Winding:		RPM:		UL File Date:	19-Nov-2009
LRA Low*:		Max Operating Current:	22.5		
RLA(=MCC/1.4;use for contactor selection):		17.1			
RLA(=MCC/1.56;use for breaker & wire size		15.4			

*Low and High refer to the low and high nominal voltage ranges for which the motor is approved.

Alternate Applications

Refrigerant	Freq (Hz)	Phase	Voltage	Application

Maruti Sinha
12/08/2011

(a)

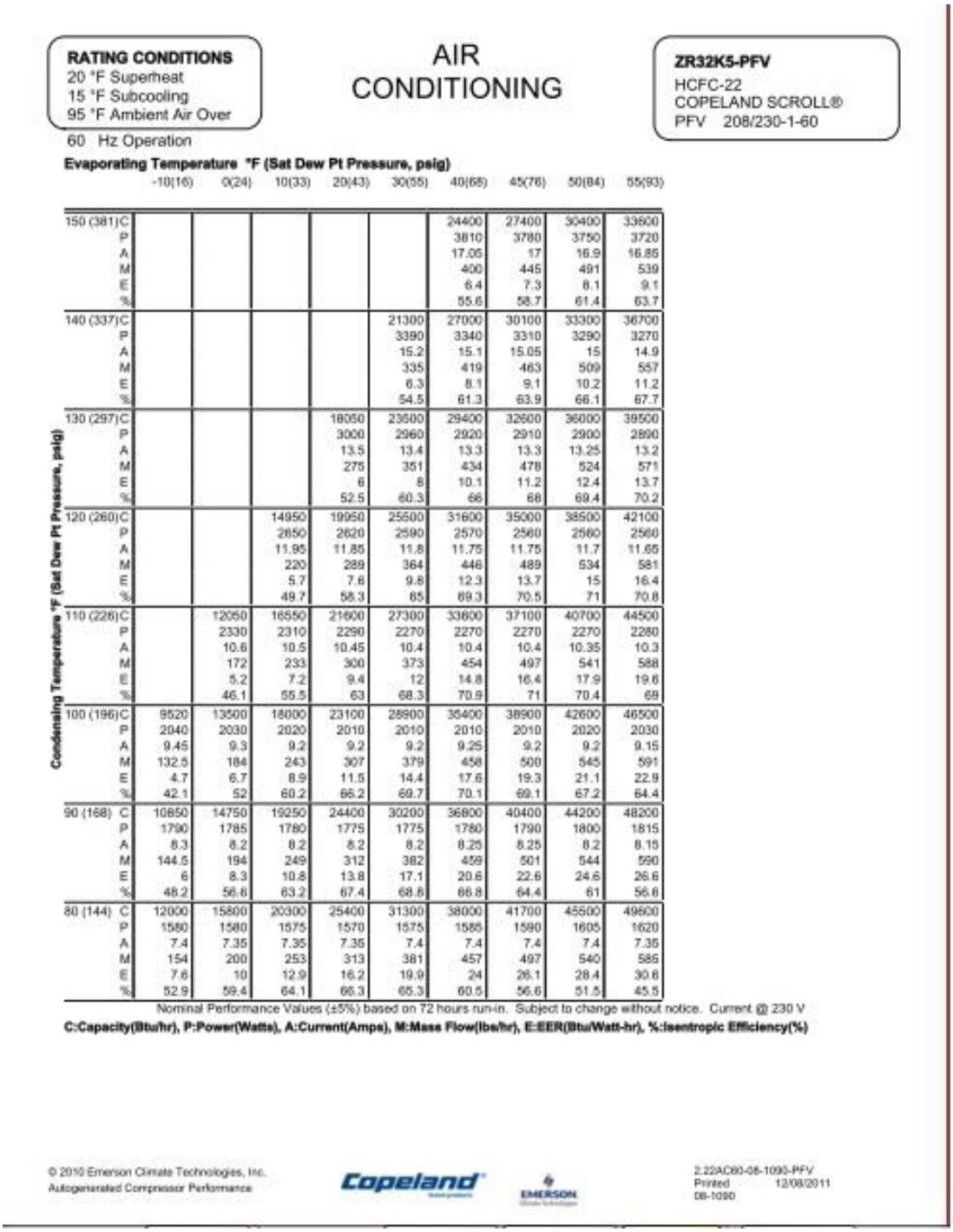

RATING CONDITIONS
20 °F Superheat
15 °F Subcooling
95 °F Ambient Air Over
60 Hz Operation

AIR CONDITIONING

ZR32K5-PFV
HCFC-22
COPELAND SCROLL®
PFV 208/230-1-60

Evaporating Temperature °F (Sat Dew Pt Pressure, psig)

Condensing Temperature °F (Sat Dew Pt Pressure, psig)		-10(16)	0(24)	10(33)	20(43)	30(55)	40(68)	45(76)	50(84)	55(93)
150 (381)	C						24400	27400	30400	33600
	P						3810	3780	3750	3720
	A						17.05	17	16.9	16.85
	M						400	445	491	539
	E						6.4	7.3	8.1	9.1
	%						55.6	58.7	61.4	63.7
140 (337)	C					21300	27000	30100	33300	36700
	P					3390	3340	3310	3290	3270
	A					15.2	15.1	15.05	15	14.9
	M					335	419	463	509	557
	E					6.3	8.1	9.1	10.2	11.2
	%					54.5	61.3	63.9	66.1	67.7
130 (297)	C				18050	23500	29400	32600	36000	39500
	P				3000	2960	2920	2910	2900	2890
	A				13.5	13.4	13.3	13.3	13.25	13.2
	M				275	351	434	478	524	571
	E				6	8	10.1	11.2	12.4	13.7
	%				52.5	60.3	66	68	69.4	70.2
120 (260)	C			14950	19950	25600	31600	35000	38500	42100
	P			2650	2620	2590	2570	2560	2560	2560
	A			11.95	11.85	11.8	11.75	11.75	11.7	11.65
	M			220	289	364	446	489	534	581
	E			5.7	7.6	9.8	12.3	13.7	15	16.4
	%			49.7	58.3	65	69.3	70.5	71	70.8
110 (226)	C		12050	16550	21600	27300	33600	37100	40700	44500
	P		2330	2310	2290	2270	2270	2270	2270	2280
	A		10.6	10.5	10.45	10.4	10.4	10.4	10.35	10.3
	M		172	233	300	373	454	497	541	588
	E		5.2	7.2	9.4	12	14.8	16.4	17.9	19.6
	%		46.1	55.5	63	68.3	70.9	71	70.4	69
100 (196)	C	9520	13500	18000	23100	28900	35400	38900	42600	46500
	P	2040	2030	2020	2010	2010	2010	2010	2020	2030
	A	9.45	9.3	9.2	9.2	9.2	9.25	9.2	9.2	9.15
	M	132.5	184	243	307	379	458	500	545	591
	E	4.7	6.7	8.9	11.5	14.4	17.6	19.3	21.1	22.9
	%	42.1	52	60.2	66.2	69.7	70.1	69.1	67.2	64.4
90 (168)	C	10850	14750	19250	24400	30200	36800	40400	44200	48200
	P	1790	1785	1780	1775	1775	1780	1790	1800	1815
	A	8.3	8.2	8.2	8.2	8.2	8.25	8.25	8.2	8.15
	M	144.5	194	249	312	382	459	501	544	590
	E	6	8.3	10.8	13.8	17.1	20.6	22.6	24.6	26.6
	%	48.2	56.6	63.2	67.4	68.8	66.8	64.4	61	56.6
80 (144)	C	12000	15800	20300	25400	31300	38000	41700	45500	49600
	P	1580	1580	1575	1570	1575	1585	1590	1605	1620
	A	7.4	7.35	7.35	7.35	7.4	7.4	7.4	7.4	7.35
	M	154	200	253	313	381	457	497	540	585
	E	7.6	10	12.9	16.2	19.9	24	26.1	28.4	30.6
	%	52.9	59.4	64.1	66.3	65.3	60.5	56.6	51.5	45.5

Nominal Performance Values (±5%) based on 72 hours run-in. Subject to change without notice. Current @ 230 V

C:Capacity(Btu/hr), P:Power(Watts), A:Current(Amps), M:Mass Flow(lbs/hr), E:EER(Btu/Watt-hr), %:Isentropic Efficiency(%)

Autogenerated Compressor Performance

Copeland EMERSON

2.22AC60-08-1090-PFV
Printed 12/08/2011
08-1090

(b)

Figure 47: Compressor (used in experiment) details provided by Emerson (a) Compressor specification datasheet, (b) Compressor map.

Table 5: Coefficients for Compressor Model H25B35QABC.

Coefficient	Capacity	Power	Current	Mass Flow
C1	63 419.510000000	3 223.298000000	20.972470000	918.813200000
C2	867.817300000	6.043080000	0.105030100	8.892987000
C3	-1 073.361000000	- 50.539860000	- 0.390878800	- 17.894800000
C4	4.682023000	- 0.310720900	- 0.001639142	0.023432740
C5	- 4.3893 32000	0.064433370	- 0.000895550	- 0.032792550
C6	7.910625000	0.543413000	0.003834512	0.149084700
C7	0.016168570	- 0.002064642	- 0.000017815	0.000182424
C8	- 0.010601010	0.002249506	0.000017343	0.000169021
C9	0.005200759	0.001074376	0.000008195	0.000067663
C10	- 0.021876740	- 0.001776723	- 0.000011864	- 0.000437768

Table 6: Sensors specifications and placements for cooling capacity measurement.

Sl no.	Sensors	Numbers	Location	Purpose
1	Temp sensor (20' cable Sensor TMC20-HD)	1	Before Evaporator	To measure air temperature entering through evaporator.
2	Temp sensor (20' cable Sensor	1	After Evaporator	To measure air temperature existing evaporator.

	TMC20-HD)			
3	Data logger (HOBO U12 4-Channel External Data Logger - U12-006)	1	Close to Evaporator	For data acquisition, collected by temperature sensors.
4	Air velocity sensor (Hot wire anemometer T-DCI-F900-L-O)	1	Before evaporator	To measure air velocity passing through the evaporator.

(a): Temp sensor: 20' cable Sensor TMC20-HD

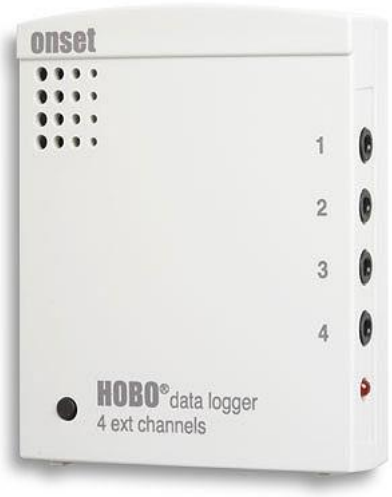

(b): HOBO U12 4-Channel External Data Logger - U12-006

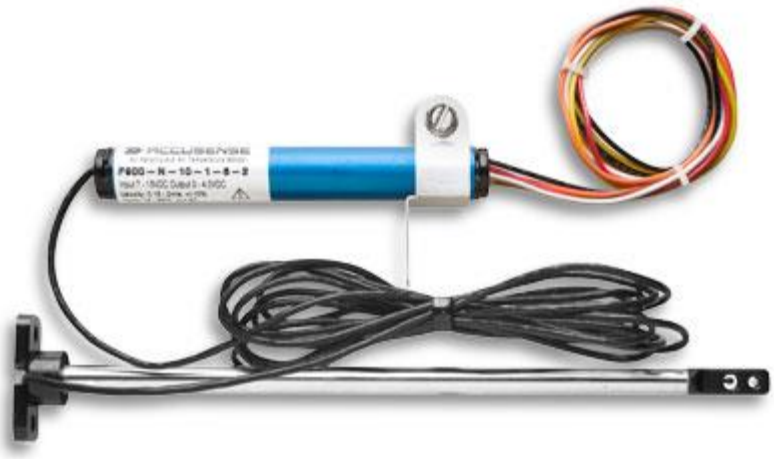

(c): Air velocity sensor: Hot wire anemometer T-DCI-F900-L-O

Figure 48: Sensor and data loggers used in measuring cooling capacity.

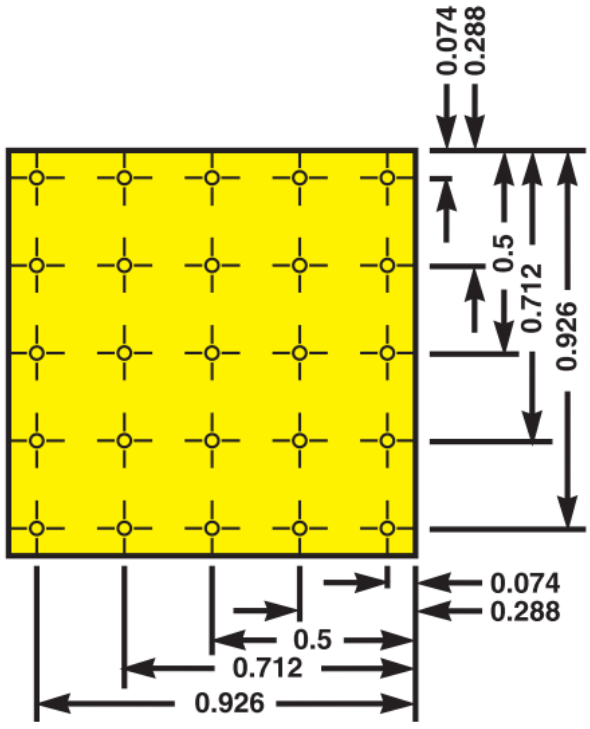

Figure 49: Air flow measurement in rectangular duct.

Table 7: Air velocity measurement using Hotwire Anemometer (measurement range is 0 - 4 volt for .15 m/sec to 10 m/sec).

Velocity Meas.(volt)					
Locations	1	2	3	4	5
1	0.782	0.791	0.742	0.765	0.678
2	0.671	0.659	0.636	0.669	0.598
3	0.669	0.589	0.615	0.636	0.459
4	0.683	0.577	0.589	0.643	0.495
5	0.683	0.586	0.589	0.676	0.655
average (V)	0.698	0.640	0.634	0.678	0.577
average reading (v)	*0.6454*				

Avg. Velocity (10-.15)*.6454/(4-0)=1.589 *m/sec*

Table 8: Temperature and air flow values.

Temp. across Evaporator		
Entry	Exit	
78	35	*F*
25.56	1.67	*C*
Del T	23.89	*C*

Area	0.18	*sq. m*
Flow rate, q	0.29	*Cub. m/min*
Air density, row	1.2	*kg/cub.m*
Air mass flow rate, m_dot	0.35	*kg/sec*
Sp. Heat capacity, Cp	1.005	*KJ/kg-K*
Cooling Cap.	8459.64	*W*
	2.41	*Ton*

Table 9: Sensors and Data loggers for house thermal model identification.

Item	Description	**No.**
Temperature sensor and data logger	HOBO® Temperature Data Logger - U10-001	2
Solar data Logger (Outdoor)	HOBO® Micro Station Data Logger - H21-002	1
Solar sensor(Outdoor)	Solar Radiation Sensor (Silicon Pyranometer) Sensor - S-LIB-M003	1

(a): HOBO® Temperature Data Logger U10-001

(b): Solar Radiation Sensor (Silicon Pyranometer) Sensor - S-LIB-M003

(c): HOBO® Micro Station Data Logger - H21-002

Figure 50: Sensors and data loggers for house thermal model identification.

(a) Experimental site: Trailer house, King's Mountain, NC

(b) Ambient temperature sensor place outside.

(c) Zone temperature sensor placed inside trailer over thermostat.

(d) Solar sensor place outside.

Figure 51: Sensors and data loggers installations on experimental site for thermal model identification.

APPENDIX C: PROGRAMMING

Program: 1

```
% Reading data from files
Indoor = xlsread ('72011indoor.csv');
Outdoor = xlsread ('72011outdoor.csv');
Solar = xlsread ('72011solar.csv');
Current = xlsread ('snapshot-20110720.xlsx');
CurrentA = xlsread ('snapshot-20110720A.xlsx');
Tz = indoor(:,3);To=outdoor(:,3);S=solar(:,3);Qest=current(:,2);Q=currentA(:,2);
 %Savitzky-Golay Smoothing
span=0.002;
Tzs = smooth (Tz, span, 'sgolay', 4);
Tos = smooth (To, span, 'sgolay', 4);
Ss=smooth(S, span, 'sgolay', 4);
figure(1); plot(Tzs); hold on; plot(Tz,'k'); hold off;
figure(2);plot(Ss);hold on;plot(S,'k');hold off;
figure(3);plot(Tos);hold on;plot(To,'k');hold off;
% Defining Cooling Capacity
number= find(Qest > 5);
cool(1:length(Qest))=0;
cool(number)=8460;
number= find(Q > 5);
coolA(1:length(Q))=0;
```

```
coolA(number)=8460;
 %Control oriented model identification with smoothing
data = iddata(Tzs(2044:7742),[-cool(1502:7200)' Tos(2044:7742) Ss(2044:7742)]);
model = pem(data,4,'Focus','simulation');
Y = sim(model,data);
figure(4); plot(Y); hold on; plot(Tz(2044:7742),'r'); hold off;
%Check for Observability, Controllability and Stability
A=model. A; B=model.B; C=model.C; D=model.D;
 Ob = obsv(A,C);rank (Ob)
 Co = ctrb(A,B);rank(co)
 eig(A)
%Control oriented model identification without smoothing
data = iddata(Tz(2044:7742),[-cool(1502:7200)' To(2044:7742) S(2044:7742)]);
model = pem(data,4,'Focus','simulation');
Y= sim(model,data);
figure(5); plot(Y); hold on; plot(Tz(2044:7742),'r'); hold off;
%Energy performance oriented model identification
 data = iddata(-cumsum(cool(1502:7200)'),[Tzs(2044:7742) Tos(2044:7742)
Ss(2044:7742)]);
model = pem(data,4,'Focus','simulation');
Y=sim(model,data);
figure(6);plot(Y.y*60/3600000);hold on;plot(-
cumsum(cool(1502:7200)*60/3600000),'r');hold off;
```

```
clear Y;
X0=model.X0; X{1}=X0;
m=7;
for k=1:m
for i=1:1440
   X{i+1}=A*X{i}+B*[Tz(7742+(k-1)*1440+i);To(7742+(k-1)*1440+i);
S(7742+(k-1)*1440+i)];
   Y(k,i)=C*X{i};
 end
 figure(7);subplot(3,3,k);plot(60*Y(k,:)/3600000);hold on;
plot(-(60/3600000)*cumsum(coolA(1+(k-1)*1440:(k)*1440)),'.');hold off;
end
 % Calculation of errors, i.e. deviation from the filed data
for k=1:m
   a(k)=Y(k,1440)*60/3600000;
   b(k)=-(60/3600000)*sum(coolA(1+(k-1)*1440:(k)*1440));
   c(k)=100*(a(k)-b(k))/b(k);
end
a
b
c
 X0=model.X0; X{1}=X0;
for k=1:m
```

```
for i=1:1440
       X{i+1}=A*X{i}+B*[-coolA((k-1)*1440+i);To(7742+(k-1)*1440+i);
S(7742+(k-1)*1440+i)];
    Y(k,i)=C*X{i};
    end
 figure(8);
subplot(3,3,k);plot(Y(k,:));hold on;plot(Tz(7743+(k-1)*1440:7742+k*1440),'r');hold off;
 end
 %%%%%%%%%%%%%%%%%%%%%%%%%%%%%%%%%%%%%5
Program :2
%Energy Performance Oriented model recursive state estimation
 data=iddata(-cumsum(cool(1502:7200)'),[Tzs(2044:7742) Tos(2044:7742)
Ss(2044:7742)]);
model=pem(data,4,'Focus','simulation');
Y=sim(model,data);
figure(1);plot(Y.y*60/3600000);hold on;plot(-
cumsum(cool(1502:7200)*60/3600000),'r');hold off;
 A=model.A;B=model.B;C=model.C;D=model.D;
 % PEM based recursive initial states updation
 clear Y out;
 Z=0;  Y=[];  out=[];
 X0=model.X0; X{1}=X0;
 r=1440*6; m=24;  n=60;
```

```
 for k=1:m
 for i=1:n
        X{i+1}=A*X{i}+B*[Tz(7742+r+(k-1)*n+i);To(7742+r+(k-1)*n+i);S(7742+r+(k-
1)*n+i)];
   out(i)=C*X{i};
   end
  temp=iddata(-cumsum(coolA(r+(k-1)*n+1:r+(k-1)*n+n))'+Z,[Tzs(7742+r+(k-
1)*n+1:7742+r+(k-1)*n+n) Tos(7742+r+(k-1)*n+1:7742+r+(k-1)*n+n) Ss(7742+r+(k-
1)*n+1:7742+r+(k-1)*n+n)]);
 X{1}=findstates(model,temp);
  for i=1:n
      X{i+1}=A*X{i}+B*[Tz(7742+r+(k-1)*n+i);To(7742+r+(k-1)*n+i);S(7742+r+(k-
1)*n+i)];
 end
  X{1}=X{n+1};
  Z=-sum(coolA(r+1:r+(k-1)*n+n));
  Y=[Y out];
  end
 figure(2);plot(Y*60/3600000);hold on;
plot(-cumsum(coolA(1+r:1440+r)*60/3600000),'r');hold off;
  (-Y(length(Y))*60/3600000-
sum(coolA(1+r:1440+r)*60/3600000))*100/sum(coolA(1+r:1440+r)*60/3600000)
  plot(Y)-Tz(7743:7742+7*1440)');
```

```
 %State estimation space with Kalman filter
 G=model.K; H=1;
QN=model.NoiseVariance;RN=0;NN=0;
sys=ss(A,[B G],C,[D H],1);
[kest,L,P,M] = kalman(sys,QN,RN,NN);
Af=kest.a;Bf=kest.b;Cf=kest.c;Df=kest.d;
 clear Y;
Z=0;Y=[];
X0=model.X0; X{1}=X0;
r=1440*6; m=1; n=1440;
 for k=1:m
for i=1:n
    X{(k-1)*n+i+1}=A*X{(k-1)*n+i}+B*[Tzs(7742+(k-1)*n+i+r);Tos(7742+(k-
1)*n+i+r);Ss(7742+(k-1)*n+i+r)]+L*(-cumsum(coolA((k-1)*n+i)+r)+Z-C*X{(k-
1)*n+i});
   X{(k-1)*n+i}=X{(k-1)*n+i}+M*(-cumsum(coolA((k-1)*n+i)+r)+Z-C*X{(k-1)*n+i});
   temp(i)=C*X{(k-1)*n+i};
   Z=-sum(coolA(r+1:r+(k-1)*n+i));
   end
   Y=[Y temp];
 end
 figure(3);
plot(Y*60/3600000);hold on;plot(-cumsum(coolA(1+r:r+1440)*60/3600000),'r');
```

```
hold off;
%%%%%%%%%%%%%%%%%%%%%%%%5
Program :3
%Kalman state estimation for the Control Oriented Model
data=iddata(Tzs(2044:7742),[-cool(1502:7200)' Tos(2044:7742) Ss(2044:7742)]);
model=pem(data,4,'Focus','simulation');
Y=sim(model,data);
figure(1);plot(Y);hold on;plot(Tz(2044:7742),'r');hold off;
 A=model.A;B=model.B;C=model.C;D=model.D;
 % Kalman filter approach
G=model.K; H=1;
QN=model.NoiseVariance;RN=0;NN=0;
sys=ss(A,[B G],C,[D H],1);
[kest,L,P,M] = kalman(sys,QN,RN,NN);
 Af=kest.a;Bf=kest.b;Cf=kest.c;Df=kest.d;


 clear Y;
Y=[];
X0=model.X0; X{1}=X0;
m=7; n1=600; n=1440;
 for k=1:m
for i=1:n
```

```
    X{(k-1)*n+i+1}=A*X{(k-1)*n+i}+B*[-coolA((k-1)*n+i);Tos(7742+(k-
1)*n+i);Ss(7742+(k-1)*n+i)]+L*(Tzs(7742+(k-1)*n+i)-C*X{(k-1)*n+i});
   X{(k-1)*n+i}=X{(k-1)*n+i}+M*(Tzs(7742+(k-1)*n+i)-C*X{(k-1)*n+i});
   temp(i)=C*X{(k-1)*n+i};
 end
Y=[Y temp];
 end
  figure(2); plot(Y);hold on;
plot(Tzs(7744:7743+1440*7),'r');
hold off;
% PEM based recursive initial states updation
clear Y out;
Y=[];out=[];
X0=model.X0; X{1}=X0;
m=672; n=15;
for k=1:m
for i=1:n
      X{i+1}=A*X{i}+B*[-coolA((k-1)*n+i);To(7742+(k-1)*n+i);S(7742+(k-1)*n+i)];
   out(i)=C*X{i};
   end
 temp=iddata(Tzs(7742+(k-1)*n+1:7742+(k-1)*n+n),[-coolA((k-1)*n+1:(k-1)*n+n)'
Tos(7742+(k-1)*n+1:7742+(k-1)*n+n) Ss(7742+(k-1)*n+1:7742+(k-1)*n+n)]);
X{1}=findstates(model,temp);
```

```
 for i=1:n
      X{i+1}=A*X{i}+B*[-coolA((k-1)*n+i);To(7742+(k-1)*n+i);S(7742+(k-1)*n+i)];
end
 X{1}=X{n+1};
 Y=[Y out];
 end
figure(3);
 plot(Y);hold on;plot(Tz(7743:7742+7*1440),'r');hold off;
```